

**Dissertation zur Erlangung des Doktorgrades  
der Fakultät für Chemie und Pharmazie  
der Ludwig-Maximilians-Universität München**

**Improving gene transfer into skeletal muscle through genetic retargeting of  
adenoviral vectors**

**Christian Thirion**

**aus**

**Konstanz**

**2004**

## **Erklärung**

Diese Dissertation wurde im Sinne von § 13 Abs. 3 bzw. 4 der Promotionsordnung vom 29. Januar 1998 von Prof. Dr. Ernst-Ludwig Winnacker betreut.

## **Ehrenwörtliche Versicherung**

Diese Dissertation wurde selbständig, ohne unerlaubte Hilfe erarbeitet.

München, 4. Juni 2004

Christian Thirion

Dissertation zur Beurteilung eingereicht am 2. Juli 2004

1. Gutachter: Prof. Dr. Ernst-Ludwig Winnacker
2. Gutachter: Prof. Dr. Hanns Lochmüller

Tag der mündlichen Prüfung: 8. Juli 2004

## Scientific publications

Die vorliegende Arbeit wurde in der Zeit von September 1998 bis Dezember 2003 im Labor von Prof. Dr. Hanns Lochmüller am Genzentrum der Ludwig-Maximilians-Universität München angefertigt.

Im Verlauf dieser Arbeit wurden Teile der Arbeit in den folgenden Fachzeitschriften veröffentlicht:

1. **Thirion C.**, Larochelle N., Volpers C., Dunant P., Stucka R., Holland P., Nalbantoglu J., Kochanek S., Lochmüller H. Strategies for muscle-specific targeting of adenoviral gene transfer vectors. *Neuromuscul. Disord.* **12**, S30-S39 (2002).

2. **Thirion C\***, Volpers C\*, Biermann V., Hussmann S., Kewes H., Dunant P., von der Mark H., Herrmann A., Kochanek S., Lochmüller H. Antibody-mediated targeting of an adenovirus vector modified to contain a synthetic immunoglobulin G-binding domain in the capsid. *J. Virol.* **77**, 2093-2104 (2003).

3. Dunant P., Larochelle N., **Thirion C.**, Stucka R., Ursu D., Petrof B.J., Wolf E., Lochmüller H. Expression of dystrophin driven by the 1.35-kb MCK promoter ameliorates muscular dystrophy in fast, but not in slow muscles of transgenic *mdx* mice. *Mol. Ther.* **8**, 80-89 (2003).

4. **Thirion C.**, Volpers C., Ruzsics Z., Boelhaue M., Stucka R., Thedieck C., König C., Kutik S., Kochanek S., Burgert H., Lochmüller H. Characterization of a novel adenovirus serotype 19a vector showing enhanced human muscle cell infection and high potential for human gene therapy. Manuscript in preparation.

### **Weitere wissenschaftliche Veröffentlichungen:**

5. **Thirion C\***, Stucka R\*, Mendel B., Gruhler A., Jaksch M., Nowak K.J., Binz N., Laing N.G., Lochmüller H. Characterization of human muscle type cofilin (CFL2) in normal and regenerating muscle. *J. Eur. Biochem.* **268**, 3473-3482 (2001).

6. Jaksch M., Paret C., Stucka R., Horn N., Müller-Höcker J., Horvath R., Trebesch N., Stecker G., Freisinger P., **Thirion C**, Müller J., Lunchwitz R., Rödel G., Shoubridge E.A., Lochmüller H. Cytochrome *c* oxidase deficiency due to mutations in *SCO2*, encoding a mitochondrial copper-binding protein, is rescued by copper in human myoblasts. *Hum. Mol. Genet.* **26**, 3025-3035 (2002).

7. Walter M.C., Braun C., Vorgerd M., Poppe M., **Thirion C.**, Schmidt C., Schreiber H., Knirsch U.I., Brummer D., Müller-Felber W., Pongratz D., Müller-Höcker J, Huebner A., Lochmüller H. Variable reduction of caveolin-3 in patients with LGMD2B/MM. *J. Neurol.* **250**, 1431-1438 (2003).

\* Authors contributed equally

### **Vorträge und Auszeichnungen:**

1. Oral presentation at the 10<sup>th</sup> international meeting of basal membranes (ISBM) 2001 in Salzburg, Austria. Title: Strategies for muscle-specific gene therapy using adenoviral vectors.

2. 3<sup>rd</sup> Poster prize at the annual meeting of the European Society of Gene Therapy (ESGT) Antibes, France (2002). Title: Gene transfer to differentiated muscle cells with a versatile system for antibody-mediated targeting of adenoviral vectors.

## **Danksagung**

Ich möchte mich bei allen Menschen bedanken, die mich während der Doktorarbeit begleitet und gefördert haben. Allen voran danke ich meinem Doktorvater, Herrn Professor Dr. Hanns Lochmüller, dafür, dass er mir die Möglichkeit gegeben hat, in seiner Arbeitsgruppe ein ebenso anspruchsvolles wie interessantes Thema zu bearbeiten, für sein mir entgegengebrachtes Vertrauen und die Möglichkeit mich wissenschaftlich zu entfalten ohne die gemeinsame Zielsetzung aus den Augen zu verlieren. Meine besondere Hochachtung möchte ich den Eltern der „aktion benni & co“ aussprechen, welche durch ihren persönlichen Einsatz Forschungsgelder für die Therapieforschung für Duchenne Muskeldystrophie sammeln und Arbeitsgruppen weltweit zur Verfügung stellen. Dieses Engagement, ohne dass Teile dieser Arbeit nicht hätten realisiert werden können, war mir stets Verpflichtung und Motivation zugleich. Ich hoffe, mit der hier vorliegenden Arbeit einen Beitrag geleistet zu haben, welcher in Zukunft zur Entwicklung einer Therapie für Muskeldystrophie Duchenne führen möge. Besonders möchte ich Herrn Professor Dr. Ernst-Ludwig Winnacker dafür danken, diese Doktorarbeit als Mitglied der Fakultät für Biochemie offiziell zu betreuen. Hervorheben möchte ich die besondere, interdisziplinäre Forschungsumgebung, welche ich im Genzentrum vorfand, und ohne welche eine solch vielschichtige Herangehensweise an die Aufgabenstellung nicht möglich gewesen wäre. Weiter möchte ich denjenigen Personen danken, welche am Gelingen der Arbeit maßgeblich beteiligt waren. Ich danke der Arbeitsgruppe von Herrn Priv-Doz. Dr. Stefan Kochanek, insbesondere dessen Mitarbeiter Dr. Christoph Volpers, für die konstruktive und effiziente Zusammenarbeit bei der genetischen Modifizierung von Adenoviren. Weiter möchte ich Herrn Professor Hans Burgert und Herrn Dr. Szolt Ruzicks für ihre Unterstützung bei der Charakterisierung des neuen Adenovirus 19a-basierten Serotypvektors danken. Meinen Kollegen, Dr. Patrick Dunant, Dr. Angela Abicht, Dr. Rolf Stucka, Dr. Sabine Krause, Juliane Müller und Ursula Klutzny möchte ich für die vielen schönen zusammen verbrachten Tage und die vielen fruchtbaren wissenschaftlichen Gespräche danken. Zudem möchte ich meinen drei Praktikanten aus Tübingen, Cornelia Thedieck, Cornelia König und Stephan Kutik für ihren erbrachten Einsatz danken. Ganz besonders möchte ich meinen Eltern und meiner Familie danken, die mich während der gesamten Zeit begleitet und unterstützt haben. Doch allen voran möchte ich dir, Diemuth, für deine Liebe, deine Geduld und deine Stärke danken.

## Table of content

<b>Scientific publications</b>	<b>3</b>
<b>Danksagung</b>	<b>5</b>
<b>Summary</b>	<b>8</b>
<b>Abbreviations</b>	<b>11</b>
<b>Introduction</b>	<b>13</b>
<b>1.1 Molecular events involved in cell binding and entry of adenovirus serotype 5</b>	<b>13</b>
1.1.1 Primary receptors involved in adenovirus binding	13
1.1.2 Adenovirus internalization and clathrin-mediated endocytosis	15
1.1.3 Release of adenoviral particles from endosomal vesicles and intracellular transport	16
<b>1.2 Gene therapeutic approaches to treat Duchenne muscular dystrophy (DMD)</b>	<b>17</b>
1.2.1 Molecular pathology of Duchenne muscular dystrophy (DMD)	17
1.2.2 Learning about the pathology of muscular dystrophies from mutated proteins of the DGC and extracellular matrix	19
1.2.3 Molecular and gene therapy approaches to treat muscular dystrophies.	20
1.2.4 Vectors for gene therapy	22
<b>1.3 Adenoviral vectors for gene therapy</b>	<b>24</b>
1.3.1 Immunological barriers to adenovirus gene therapy	25
1.3.2 Maturation-dependent decrease in adenovirus transduction of skeletal muscle	26
1.3.3 Expression level of CAR is crucial for transduction of skeletal muscle by adenovirus in vivo	26
1.3.4 The extracellular matrix may act as a physical barrier to adenovirus in vivo	27
<b>1.4 Targeting of viral vectors for gene therapy</b>	<b>28</b>
1.4.1 Ablation of the native tropism	29
1.4.2 Genetic modifications of the adenovirus fiber protein	31
1.4.3 Compound targeting vectors	32
<b>2. Material and methods</b>	<b>34</b>
<b>2.1 Primary cells and cell lines</b>	<b>34</b>
2.1.1 Culture conditions for established cell lines	34
2.1.2 Culture conditions for primary cells	34
2.1.3 Enrichment of myoblasts with magnetic cell sorting MACS	35
2.1.4 Isolation and differentiation of primary monocyte-derived dendritic cells	35
2.1.5 Growth conditions for hybridoma cells, adaptation to serum-free conditions, and purification of monoclonal antibodies	36
2.1.6 Differentiation of myoblasts into myotubes	36
<b>2.2 Viral vectors</b>	<b>36</b>
2.2.1 Propagation and purification of adenoviral vectors	36
2.2.2 Construction of AdFZ33 $\beta$ Gal	37
2.2.3 Titration of adenoviral vectors	38
<b>2.3 Retargeting of AdFZ33<math>\beta</math>Gal</b>	<b>38</b>
2.3.1 Monoclonal and polyclonal antibodies	38
2.3.2 Complex formation between AdFZ33 $\beta$ Gal and antibodies	39
<b>2.4 Adenovirus transduction and competition assays</b>	<b>39</b>
2.4.1 Adenoviral transduction and competition assays for AdFZ33 $\beta$ Gal	39
2.4.2 Virus transduction assay	40
2.4.3 Virus transduction competition assay	40
2.4.4 Quantification of transgene expression	40

2.4.5 Flow cytometry (FACS)	41
2.4.6 Confocal laser immunofluorescence and immunofluorescent staining of human muscle cells	41
2.4.7 Visualization of transgene expression (X-Gal) and fluorescence microscopy	42
<b>2.5 Expression and purification of viral proteins</b>	<b>42</b>
2.5.1 Cloning, expression and purification of recombinant fiber proteins in E.coli	42
2.5.2 Cloning, expression and purification of fiber proteins in SF9 cells	43
2.5.3 Cloning, expression and purification of fiber proteins using recombinant vaccinia virus	44
2.5.4 Detection of trimeric fiber proteins in vaccinia virus-infected cells by means of semi-native polyacrylamid gel electrophoresis	46
<b>3. Results</b>	<b>47</b>
<b>3.1 Molecular mechanism of adenovirus serotype 5 for binding and entry into primary human muscle cells.</b>	<b>47</b>
3.1.1 Attachment of Ad5 to human muscle cells involves more than one receptor	47
<b>3.2 Antibody-mediated targeting of an adenoviral vector, modified to contain a synthetic IgG-binding domain in the capsid</b>	<b>50</b>
3.2.1 Incorporation of the antibody-binding Z33-domain into the Ad5 HI-loop	50
3.2.2 Functionality of mutant fiber genes expressed in CV-1 cells	51
3.2.3 The Fc-binding Z33-domain retains its antibody-binding activity within the Ad5 fiber HI-loop	54
3.2.4 Rescue and functional analysis of AdFZ33βGal	55
3.2.5 Muscle-specific retargeting of AdFZ33βGal to NCAM and $\alpha_7\beta_1$ integrin	56
3.2.5 Specificity of antibody-mediated retargeting of AdFZ33βGal	62
<b>3.3 Enhanced human muscle cell transduction by subgroup D adenovirus Ad19a</b>	<b>63</b>
3.3.1 Attachment of Ad19aEGFP to primary human myoblasts (FHM) depends on a sialic acid-containing receptor.	63
3.3.2 Comparing Ad5 and Ad19a for their ability to infect muscle cells	66
3.3.3 Ad19a is a human muscle cell tropic virus.	66
3.3.4 Differential muscle cell transduction efficiencies of Ad5EGFP and Ad19aEGFP evaluated by quantitative real time PCR	69
3.3.5 Lack of maturation-dependent decrease for transfection of myotubes	72
3.3.6 Transduction of primary human cells by Ad19aEGFP	73
<b>4. Discussion</b>	<b>75</b>
<b>4.1 Overcoming the hurdles in adenovirus-mediated gene delivery <i>in vivo</i></b>	<b>75</b>
4.1.1 Development of low-immunogenic adenovirus gene therapy vectors	75
4.1.2 Long-term transgene expression and site-specific gene integration into human chromosomes	76
4.1.3 Retargeting or detargeting?	77
4.1.4 Genetic retargeting of adenovirus using the protein A-derived antibody-binding domain Z33	77
4.1.5 Genetic retargeting of adenoviral vectors and the choice of the targeting ligand and insertion site	79
4.1.6 Methods to increase high-affinity binding of targeting ligands to targeted molecules	80
4.1.7 Perspective for muscle-specific targeting of adenoviral vectors	81
<b>4.2 Exploiting the natural adenovirus serotype pool.</b>	<b>82</b>
4.2.1 Infectious pathway of adenovirus serotypes 5 and 19a in primary human muscle cells	82
4.2.2 Tropism of Ad19a-based recombinant vector	84
4.2.3 Inter-species differences for viral transduction	85
<b>4.3 Outlook - Finding new molecular targets to treat muscular dystrophy</b>	<b>87</b>
<b>References</b>	<b>90</b>
<b>Curriculum vitae</b>	<b>118</b>

## Summary

The extraordinary evolutionary adaptation of viruses to different hosts and environments, though often hostile, makes them valuable tools for gene therapy. Gene therapy seeks to cure a disease by “correcting” the underlying cause of the illness, defective or mutated genes, through transfer of functional or curative gene constructs into affected cells or tissues. Duchenne muscular dystrophy (DMD) is the most common X-linked lethal disorder, occurring in approximately 1 in 3500 male births. Affected children are generally confined to a wheelchair by their early teens due to limb muscle weakness, and death eventually occurs during the third decade of life as a result of either respiratory or cardiac muscle failure. Deficiency of the 427kDa protein dystrophin is the causative molecular event leading to DMD. Due to the large size of dystrophin cDNA (14kb), the choice of suitable vectors for gene therapy is currently limited to non-viral DNA and adenovirus vectors. However, adenovirus-mediated gene transfer into skeletal muscle is hampered by low efficiency. The inefficient transduction of adult skeletal muscle by adenovirus may be linked to the lack of primary (coxsackie-adenovirus receptor CAR) and secondary ( $\alpha_v$  integrins) virus attachment receptors. Therefore, the molecular events involved in attachment and internalization of adenovirus were evaluated on the level of primary human muscle cells. Adenovirus attachment to primary human muscle cells involved initial binding of two receptors: CAR and heparansulfate proteoglycans. In agreement with the proposed two-step model for adenovirus infection, internalization of adenovirus was dependent on interaction with  $\alpha_v\beta_3$  integrin. It was shown previously that CAR expression on skeletal muscle decreases with age. Therefore, we aimed to modify adenoviral vectors by redirecting them to abundant muscle-specific receptors. The goal was to simultaneously increase the transduction specificity and efficiency for skeletal muscle by means of retargeting adenovirus vectors. Finding the appropriate muscle-cell specific receptors necessitated the development of a targeting platform. Since molecular and structural data were available for Ad5 virus-receptor interaction, and insertion of small targeting ligands into the HI loop of adenovirus knob protein had already been demonstrated, the HI loop was chosen as the site for insertion of a 33-amino-acid long antibody-binding domain derived from staphylococcus protein A. Functional insertion of this domain allowed us to screen potential receptors by simply interchanging the retargeting monoclonal antibody before Ad-mediated transduction. Indeed, we were able to show that the

HI loop was flexible enough to accommodate larger targeting ligands and, moreover, that the 33-amino-acid long Fc-binding domain retained full functionality within the context of the HI loop and bound antibodies with high affinity. Screening with antibody-retargeted vectors led to the identification of two muscle-specific candidate target receptors: neuronal cell adhesion molecule (NCAM) and  $\alpha_7\beta_1$  integrin. Retargeting of adenovirus to these receptors enhanced transduction of myoblasts and myotubes in a specific way. Binding of antibody-retargeted adenoviruses to muscle cells was independent of binding to CAR, the natural cellular receptor of Ad5. Further experiments are underway to test this new strategy *in vivo*. In the second part of this work, the effectiveness of a different adenovirus serotype vector, based on Ad19a, for efficient transduction of muscle cells was explored. To date, 51 human serotypes with distinct tropisms have been described. Most adenovirus vectors used for gene therapy are based on serotypes 2 and 5 (Ad2; Ad5). The ability of the EGFP-expressing Ad19a-based vector (Ad19aEGFP) to transduce primary cells, including differentiated human myotubes that are otherwise difficult to transduce with Ad5, was explored. Transduction of a panel of myoblasts originating from different species revealed a human-cell-specific infection profile for the Ad19a-based vector. Unlike Ad5EGFP, attachment of Ad19aEGFP to human myoblasts was mainly dependent on  $\alpha(2-3)$ -linked sialic-acid-containing receptors. Transgene expression after Ad19aEGFP-mediated gene transfer was increased 10-fold in smooth muscle cells, up to 78-fold in human myoblasts, and 19-fold in human myotubes as compared to Ad5. Determination of viral particle numbers by means of real-time PCR in transduced myoblasts of different species revealed two putative transductional barriers for Ad5EGFP and Ad19aEGFP vectors. A post-internalization block in pig and ape myoblasts was observed for Ad19aEGFP, where high numbers of intracellular particles accumulated without expressing EGFP. Second, an early block probably occurred at the level of virus attachment and internalization in primary mouse and rat L6 myoblasts, where low numbers of intracellular Ad5EGFP and Ad19aEGFP particles could be detected. Moreover, Ad19aEGFP transduced monocyte-derived dendritic cells significantly better than Ad5. In summary, this work demonstrates that the HI-loop of Ad5 can be used for the insertion of large functional ligands like the antibody-binding domain Z33. Moreover, the developed antibody-based retargeting strategy for Ad5 proved useful for screening and identification of alternative attachment receptors on primary human muscle cells, and may therefore be extended to other cell lines and target tissues. Retargeting of Z33-modified adenovirus vector (AdFZ33 $\beta$ Gal) to NCAM

and  $\alpha_7$  integrin increased the transduction efficiency of differentiated human muscle cells (myotubes) by 67- and 77-fold, respectively. Since myotubes are a good *in vitro* model for adenovirus transduction of skeletal muscle, the ability of NCAM and  $\alpha_7$ -integrin-retargeted adenovirus to transduce skeletal muscle *in vivo* shall be explored in the future. Attempts to transfer the enhanced muscle-cell-transduction capability of Ad19a to Ad5 are the subject of ongoing research. The Ad19a fiber protein shall be transferred to Ad5 and a chimeric virus generated. Despite recent advances in the field of gene therapy and vector development major hurdles still have to be overcome until gene therapy will be a safe clinical option to treat hereditary diseases. The development of safe adenovirus vectors for gene therapy, which do not integrate into the host genome, is essential if large cDNAs like dystrophin have to be transferred. Retargeting of adenovirus vectors to muscle-specific receptors, as demonstrated in this work, led to transduction of muscle cells in a specific way while using less vector particles, and may contribute to an improvement in safety and efficacy of adenovirus vectors in muscle-directed gene therapy applications.

## Abbreviations

aa	amino acid
AAV	adeno-associated virus
AAV-5	adeno-associated virus serotype 5
AAT-1	alpha-antitrypsin 1
AdV	adenovirus
Ad5 / Ad19a	adenovirus serotype 5 / adenovirus serotype 19a
Ad5.FX	pseudotyped Ad5 vector carrying a fiber molecule from another adenovirus serotype X (X=16, 19a,35, and 50)
AdF $\beta$ Gal	first generation Ad5-based vector expressing $\beta$ -galactosidase
AdFZ33 $\beta$ Gal	first generation ad5-based vector expressing $\beta$ -galactosidase with incorporated immunoglobuline-binding domain Z33 into the fiber protein
AdFK7	first generation Ad5-based vector expressing $\beta$ -galactosidase carrying a C-terminally-modified fiber gene with 7 lysine residues added.
<i>attP</i> / <i>attB</i>	phage attachment site ( <i>attP</i> ) / bacterial attachment site ( <i>attB</i> )
BFU	blue forming unit: number of $\beta$ -galactosidase expressing cells obtained after titration of adenovirus on 293 cells
BMD	Becker muscular dystrophy
bp	base pair
CAR	coxsackie adenovirus receptor
CAR-Tg	transgenic mouse line expressing CAR under the control of the muscle-specific MCK promoter
CC	coiled-coiled domain
cDNA	complementary (to mRNA) DNA
CMV	cytomegalovirus promoter
CV-1	African green monkey kidney fibroblast cell line
DAPs	dystrophin-associated proteins
DC	dendritic cell
DGC	dystrophin-glycoprotein complex
DMD	Duchenne muscular dystrophy
DNA	deoxyribonucleic acid
ds	double stranded
E1, E2, E4	early region 1, 2, and 4 genes of adenovirus
EBNA-1	Epstein-Barr virus nuclear antigen 1
<i>E. coli</i>	<i>Escherichia coli</i>
EDTA	ethylenediaminetetraacetic acid
EGFP	enhanced green fluorescent protein
EGFR	epidermal growth factor receptor
FITC	fluoresceineisothiocyanate
FACS	flow cytometry (Fluorescence Activated Cell Sorter, FACS)
FGF / bFGF	fibroblast growth factor / basic fibroblast growth factor
FHM	fetal human myoblasts
hc-Ad	high-capacity adenovirus
HeLa	cervical carcinoma cell line derived from the name-giving person "Henrietta Lacks"
HIV-1	human immunodeficiency virus type 1

HUVEC	human umbilical vein endothelial cells
HSPG/HSG	heparansulfate proteoglycan / heparansulfate glucosaminoglycans
HSV-1	herpes simplex virus type 1
Ig	immunoglobulin
IL1	interleukin 1
ITR	inverted terminal repeat
kb	kilobase
kDa	kilodalton
L6	rat myoblast cell line L6
L6 <sup>CAR</sup>	L6 myoblast cell line stably expressing CAR
<i>lacZ</i>	$\beta$ -galactosidase gene
LMO2	LIM domain only-2, a cysteine-rich (LIM) finger protein involved in hematopoiesis.
MACS	magnetic cell sorting
MB	myoblasts
MCK	muscle creatine kinase
MHCI	major histocompatibility complex class I
MLV / MoMuLV	Moloney murine leukaemia virus
MOI	multiplicity of infection
MPA	mycophenolic acid
MT	myotubes
NCAM	neural cell adhesion molecule
Neu5Ac	5-N-acetylneuramic acid (sialic acid)
Neu5Gc	5-N-glycolylneuramic acid
NF- $\kappa$ B	nuclear factor kappa B
nt	nucleotide
PAGE	polyacrylamide gel electrophoresis
PBMCs	peripheral blood mononuclear cells
PBLs	peripheral blood lymphocytes
PCR	polymerase chain reaction
PEG	polyethyleneglycol
PH	pleckstrin homology domain
PHPMA	poly-N-(2-hydroxypropyl)-methacrylate
RLU	relative light unit
RNA	ribonucleic acid
SD	standard deviation
SDS	sodium dodecyl sulfate
TA	tibialis anterior
TK	thymidine kinase
WGA	wheat germ agglutinin: lectin binding to N-acetyl- $\beta$ -(1,4)-D-glucosamine
WT	wild type
XGPT	xanthine-guanine phosphoribosyltransferase
X-Gal	5-bromo-4-chloro-3-indolyl-beta-D-galactopyranoside. Chromogenic substrate for $\beta$ -galactosidase, that hydrolyzes X-Gal and forms an intense blue precipitate.

# Introduction

## *From basic interaction of adenovirus with the cell surface to gene therapy of muscular dystrophies*

### 1.1 Molecular events involved in cell binding and entry of adenovirus serotype 5

The infectious pathway of adenovirus serotype 5 involves attachment to the cell membrane, very efficient virus uptake upon receptor-mediated endocytosis, directed intracellular transport, and nuclear uptake of adenovirus DNA. During this process adenovirus particles are dismantled stepwise and the infectious DNA is liberated from the protecting capsid (Fig.1). The molecules involved in each distinct step are discussed below.

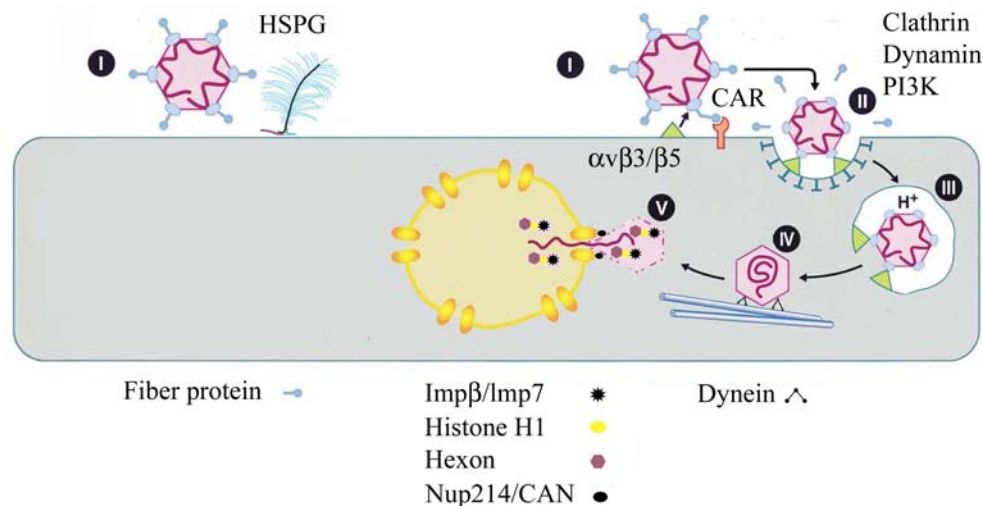


**Fig.1 Infectious pathway of subgroup C adenoviruses.** Subgroup C adenoviruses bind to the cellular receptor CAR and to alternative attachment receptors like heparansulfate-containing proteoglycans (HSPGs) (I). Uptake of viral particles occurs through receptor-mediated endocytosis upon interaction of the adenovirus penton base protein with cellular  $\alpha_v$  integrins (I+II). Signaling through  $\beta_3$  integrins results in PI3K kinase activation, which in turn induces dynamin-dependent endocytosis in clathrin-coated vesicles and leads to activation of small Rho GTPases Rac1 and Cdc42. Loss of fiber proteins and partial uncoating of adenovirus particles occurs in early endosomes. Acid-dependent virus escape from early endosomes (III) is followed by dynein-dependent transport on microtubules towards the center of the cell (IV). Complete disassembly of viral particles and nuclear import of viral DNA occurs at the nuclear pore complex (NPC) where adenovirus hexon protein directly interacts with nuclear pore complex filament protein Nup214/CAN. At the NPC, hexon associates with histone H1, which in turn is recognized by importin  $\beta$  and mediates the translocation of hexon-histone H1 complexes across the NPC (V).

#### 1.1.1 Primary receptors involved in adenovirus binding

To date 51 human serotypes have been identified and classified into 6 subgroups (A to F)<sup>1</sup>. Subgroup B adenoviruses use CD46 as a cellular attachment receptor<sup>2,3,4</sup>, whereas sialic acid is likely to function as a cellular receptor for subgroup D adenoviruses causing epidermal

conjunctivitis<sup>5,6</sup>. Subgroup C adenoviruses use separate receptors for attachment and entry. While the attachment of the virus to the cell is mediated by high-affinity binding to a 46 kDa receptor, termed coxsackie-adenovirus receptor (CAR)<sup>7,8</sup>, internalization of the virus occurs through endocytosis upon interaction of the penton-base protein with  $\alpha_v$  integrins<sup>9,10</sup>. CAR functions as an attachment receptor for type B coxsackieviruses, as well as for many human adenovirus serotypes from subgroups A, C, D, E, and F, and also for adenoviruses from different species<sup>11,12,13</sup>.

CAR is a member of the immunoglobulin receptor superfamily, forms homodimers between molecules, and is a functional part of the tight junction where it mediates cell-cell contacts<sup>14,15,16</sup>. Due to the presence of a basolateral targeting signal in the cytoplasmic domain of CAR, exclusive basolateral localization of CAR in polarized epithelial cells has been observed<sup>17</sup>. In well-differentiated epithelial airway cells CAR was found below the tight junctions as part of the adherens junction where it colocalizes with  $\beta$ -catenin<sup>18</sup>.

Adenovirus fiber knob binds with high affinity to a region overlapping the CAR:CAR binding interface and competes for CAR-binding on the cell surface<sup>14,19,20</sup>. CAR is sequestered in tight junctions and along the basolateral membrane. How Ad5 infects the polarized respiratory epithelium is still a matter of debate. It is unlikely that incoming Ad bind CAR in tight and adherens junctions. Infection may start in regions with localized CAR expression on the apical surface, as observed in lesions of the epithelium, or might involve other receptors. Instead of serving as an adenovirus attachment receptor, binding to CAR may also facilitate the adenovirus' escape and virus spread from the airway epithelium. It has been proposed that the excess fiber protein produced during viral propagation in addition to the large amount of defective adenoviral particles, which outnumber the functional infectious particles, may together lead to the sequential disruption of cell adherens and tight junctions, enabling adenovirus escape to the apical surface<sup>18,21</sup>.

Various adenovirus serotypes bind to CAR, although the *in vivo* tropism varies considerably<sup>22</sup>. For instance, Ad40 and Ad41 from subgroup F readily infect cells of the gastrointestinal tract and are associated with gastroenteritis. Serotypes Ad8, Ad19a, and Ad37 (subgroup D) are associated with epidemic keratoconjunctivitis, and Ad4 (subgroup E) is associated with pneumonia<sup>22</sup>. Since CAR forms homodimeric complexes between neighboring cells, it may not be accessible to adenovirus in most tissues. It is therefore not surprising that a number of alternative attachment receptors have been described recently for adenovirus serotype 5,

involving heparansulfate proteoglycans (HSPGs)<sup>23,24</sup>, MHC class I  $\alpha 2$  domain<sup>25</sup>, and  $\alpha_3\beta_1$ <sup>26</sup>. Some adenoviruses (*e.g.*, Ad9) use the penton base protein instead of the fiber protein for attachment<sup>27</sup>. The penton base protein from Ad5 might also be involved in direct binding to the cell surface, as demonstrated by binding of Ad5 penton base protein to integrin  $\alpha_M\beta_2$ <sup>28</sup>.

### *1.1.2 Adenovirus internalization and clathrin-mediated endocytosis*

Efficient internalization of adenovirus particles requires a second interaction with internalization-promoting receptors. The Ad5 penton base binds to integrins  $\alpha_v\beta_3$  and  $\alpha_v\beta_5$  through its RGD motif and mediates internalization of Ad5 through receptor-mediated endocytosis in clathrin-coated pits<sup>9,29</sup>. Binding of penton base protein to vitronectin-binding integrins  $\alpha_v\beta_3$  and  $\alpha_v\beta_5$  induces discrete conformational changes that lead to receptor activation and induce signaling events that mediate clathrin-coated pit endocytosis and enhance macropinocytosis<sup>30,31</sup>. Low expression of adenovirus receptor CAR and  $\alpha_v$  integrins in peripheral blood mononuclear cells (PBMCs) correlates with low transduction efficiency of these cells. Relevance of  $\alpha_v$  integrins for efficient transduction by subgroup C adenoviruses was demonstrated upon upregulation of  $\alpha_v$  integrins by specific growth factors (macrophage colony-stimulating factor or granulocyte-macrophage colony-stimulating factor), which increased Ad5-mediated gene delivery to PBMCs<sup>32</sup>. Primary attachment of Ad5 to PBMCs is thought to occur via binding to  $\alpha_m\beta_2$  integrin but still requires binding to integrins  $\alpha_v\beta_3$  and  $\alpha_v\beta_5$  for internalization<sup>28</sup>.

Clathrin-mediated endocytosis involves initial recruitment of the heterotrimeric clathrin adaptor complex AP2 or neuronal accessory clathrin adaptor protein AP180 to the plasma membrane followed by binding of clathrin to the adaptor and assembly of the coat<sup>30,33</sup>. Vesicle constriction and fission requires the GTPase dynamin, which self-assembles at the collar of invaginated coated pits to form a ring-like structure<sup>34</sup>.

Many components involved in clathrin coated vesicle formation interact specifically with PtdIns(4,5)P<sub>2</sub>, which seems to be critically important in the recruitment of AP-2/clathrin coats to membranes<sup>35,36</sup>. The importance of PtdIns(4,5)P<sub>2</sub> for vesicle integrity was demonstrated by the involvement of synaptojanin-1, a phosphatidylinositol-5 phosphatase, in the regulation of clathrin-coated vesicle uncoating<sup>36</sup>.

The interaction of Ad5 penton base with  $\alpha_v$  integrins mediates activation of the p85 subunit of PI3K, which results in PtdIns(3,4)P<sub>2</sub> and PtdIns(3,4,5)P<sub>3</sub> synthesis, activation of protein

kinase C (PKC), and is linked to Ras and Rho signaling cascades<sup>37,38</sup>. Eventually Rho family GTPases Rac1, CDC42, and RhoA are activated and link Ad5 internalization to actin cytoskeleton reorganization, which is required for Ad uptake<sup>38,39</sup>. Activation of macropinocytosis through small Rho family GTPases is another aspect of adenovirus-mediated integrin signaling and represents a second endocytic pathway controlled by Ad5<sup>29</sup>.

### *1.1.3 Release of adenoviral particles from endosomal vesicles and intracellular transport*

The fate of cell surface-bound adenovirus particles was studied in detail. Integrin-mediated internalization of Ad particles occurred rapidly within 5min at 37°C and was followed by vesicle rupture within 15 min post internalization<sup>40</sup>. Fiber proteins are first dissociated from endocytosed virions. Adenovirus endocytosis and penetration in the cytosol are then associated with gradual loss of association between hexon and hexon-associated proteins (proteins IIIA, VIII, and penton base protein). This in spite of electron microscopic analysis that indicates that particles with intact morphology are also released into the cytosol<sup>40</sup>. The internal capsid protein adenovirus cysteine protease p23 plays an important role in the uncoating of adenovirus particles at the nuclear pore complex through the cleavage of protein VI, which links the DNA to hexon<sup>41</sup>. Degradation of protein VI was only observed after interaction of the virus with integrins, though it was dispensable for Ad5 membrane penetration during endosome-cytoplasm transition. Indeed, the cytoplasmic tail of integrin  $\beta_5$  regulates adenovirus-mediated membrane permeabilization and endosomal escape<sup>42,43</sup>. It should be mentioned that  $\alpha_v\beta_5$  interaction with Ad2 penton base alone did not increase membrane permeabilization in endocytic vesicles, and thus other viral /host factors could be involved (see discussion). Confocal microscopy of Ad5-transduced CHO cells stably expressing integrin  $\alpha_v\beta_3$  not only demonstrated enhanced adenovirus endocytosis compared to the wild type CHO cells, but also revealed that the  $\beta_3$  subunit colocalized with Ad5 hexon in large intracellular vesicles during intracellular traffic and eventually accumulated at the nuclear membrane after dissociation from hexon (Fig.2, C.Thirion unpublished results).

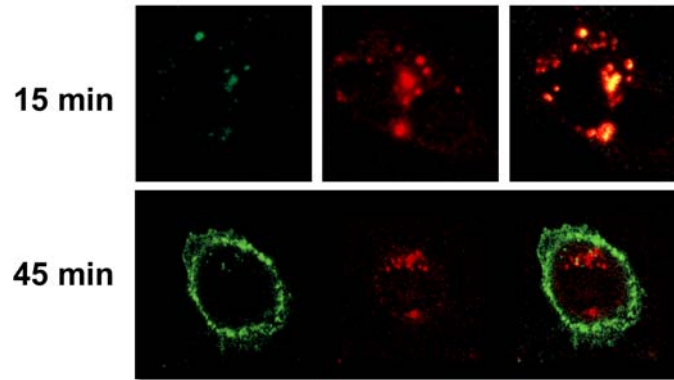


**Fig.2 Colocalization of  $\beta_3$  integrin and hexon protein during intracellular Ad5 transport.**

CHO cells stably expressing  $\alpha_v\beta_3$  integrin were transduced with MOI 1000 Ad5 and stained for  $\beta_3$  integrin and hexon protein 15 or 45 minutes after infection<sup>44</sup>. Confocal microscopy revealed colocalization of hexon and  $\beta_3$  integrin in large cytoplasmic vesicles 15 minutes post infection. After 45 minutes, most of the  $\beta_3$  integrin was localized in proximity to the nuclear membrane, whereas most of the hexon protein was dissociated from  $\beta_3$ .

After endocytosis and release into the cytosol, adenovirus particles move towards the nucleus in a dynein- and microtubule-mediated way<sup>45,46</sup>. Tracking of fluorescent adenovirus particles (Cy3-Ad) in Ad2-transduced A549 cells revealed that more than 80 % of Cy3-Ad overlapped with nuclear DAPI staining within 60 minutes after infection<sup>45</sup>. Nuclear-localized adenoviral particles are further dismantled at the NPC, where they are associated with the nuclear pore filament protein CAN/Nup214<sup>47</sup>. Binding of Ad2 particles to the nuclear envelope occurs in a Ran-independent way. Disassembly of bound adenovirus particles at the NPC involves histone H1 and nuclear import proteins importin- $\beta$  and importin-7<sup>47</sup>.

## **1.2 Gene therapeutic approaches to treat Duchenne muscular dystrophy (DMD)**

### *1.2.1 Molecular pathology of Duchenne muscular dystrophy (DMD)*

Duchenne muscular dystrophy (DMD) is the most common X-linked lethal disorder, occurring in approximately 1 in 3500 male births. Affected children are generally confined to a wheelchair by their early teens due to limb muscle weakness, and death usually occurs during the third decade of life as a result of either respiratory or cardiac muscle failure. Effective treatment is not available. The damage to skeletal and cardiac muscle is caused by a deficiency in an essential membrane-associated cytoskeletal protein called dystrophin. This dystrophy results from various mutations (point mutations, deletions) in the dystrophin gene<sup>48</sup>. Deficiency of dystrophin protein in skeletal muscle as well as in other tissues in which

isoforms of dystrophin are expressed (brain, retina, and smooth muscle) is the likely cause of skeletal muscle wasting, cardiomyopathy, mental retardation, abnormal electroretinograms, and gastrointestinal disturbances in DMD patients. Histological features of dystrophic muscles reveal necrotic or degenerating muscle fibers at all stages of disease progression. Degenerating muscle fibers are often seen in clusters (grouped necrosis) and confined to damaged segments of the muscle. These necrotic fibers are subject to phagocytosis, as revealed by the presence of infiltrating macrophages and CD4+/CD8+ lymphocytes. In early stages of dystrophinopathies active regeneration and replacement of damaged fibers occur. The regenerative capacity of the muscle is eventually lost and muscle fibers are gradually replaced by adipose and fibrous connective tissue, which results in muscle wasting and ultimately muscle weakness<sup>49</sup>.

The most-used animal model for DMD is the dystrophin-deficient *mdx* mouse, which lacks expression of full-length dystrophin due to a point mutation in exon 23 of the DMD gene generating a premature stop codon that leads to disruption of the dystrophin-associated glycoprotein complex (DGC)<sup>50,51</sup>. One hallmark of DMD and *mdx* muscle is an increase in mechanical-stress-induced permeability of the plasma membrane as demonstrated by dye-uptake experiments *in vivo*<sup>52</sup>. This supports the theory that dystrophic muscle fibers may have diminished membrane stability leading to ingress of molecules and ions that are normally excluded from the cytoplasm. Additionally, abnormal activity of a leak Ca<sup>2+</sup> channel in dystrophic muscle fibers was demonstrated, which was activated by calpain protease<sup>53,54,55</sup>. Loss of integrity of the DGC leads to secondary loss of neuronal nitric oxide synthase (nNOS) at the membrane and reduced NO production<sup>56</sup>. Studies in transgenic mice that were either deficient for nNOS or overexpressing nNOS, demonstrated that NO production was required for attenuation of vasoconstriction in exercising muscle and contributed to alleviation of muscle membrane injury by means of an anti-inflammatory mechanism<sup>57,58,59</sup>. Thus, reduced or mislocalized NO production may contribute to DMD pathology through defective reversible vasoconstriction following muscle contraction and lack of anti-inflammatory response to macrophage action. Moreover, infiltrating T lymphocytes are likely to cause progressive fibrosis, as observed in the diaphragm of *mdx* mice<sup>60</sup>. The capacity of muscle regeneration seems to be impaired in *mdx* and DMD muscles and eventually fails to keep pace with muscle fiber necrosis, resulting in muscle atrophy<sup>61,62</sup>. The role of satellite cells in muscle regeneration in muscular dystrophies has recently been investigated<sup>63</sup>. A protective effect due to reexpression of functional  $\alpha$ -DG in regenerating fibers by satellite cells was

observed in patients with mild limb girdle dystrophies caused by a primary defect that results in aberrant glycosylation of  $\alpha$ -DG in mature muscle fibers. This finding implies a differentially regulated  $\alpha$ -DG glycosylation pathway in satellite cells leading to functional  $\alpha$ -DG expression in regenerating muscle fibers. Expression of functional  $\alpha$ -DG in satellite cells of a conditional  $\alpha$ -DG knockout mouse protected muscle fibers from severe damage throughout life<sup>64</sup>. Since ongoing muscle regeneration in very young DMD patients prevents fibrosis, a decrease of the regenerative capacity of satellite cells may be linked to disease progression.

### *1.2.2 Learning about the pathology of muscular dystrophies from mutated proteins of the DGC and extracellular matrix*

The dystrophin-associated glycoprotein complex is composed of three subcomplexes: the dystroglycan complex, the sarcoglycan:sarcospan complex, and the dystrophin-containing complex. Mutations in nearly every member of these complexes are associated with dystrophic phenotypes. Interactions between  $\alpha$ -dystroglycan ( $\alpha$ -DG) and the cytoplasmic globular domains of laminin  $\alpha$ 1 and  $\alpha$ 2 establish the link between the DGC and the extracellular matrix<sup>65,66</sup>. The importance of this link for muscle fiber integrity was demonstrated by loss-of-function mutations that resulted in severe congenital (laminin  $\alpha$ 2-chain) and Duchenne muscular dystrophies (dystrophin). Loss-of-function mutations within  $\alpha$ -DG are lethal due to developmental defects in membrane formation. The lectin-type interaction between laminin alpha-2 chain and  $\alpha$ -DG is affected by altered glycosylation of  $\alpha$ -DG<sup>67</sup>. Accordingly, mutations within glycotransferases that modify  $\alpha$ -DG (Fukutin, Fukutin-related protein, LARGE, POMT1, POMGnT1) lead to abnormal glycosylation, impaired interaction with laminin-2, and are associated with muscular dystrophies<sup>68,69,70</sup>.

Another binding partner of laminin-2 is  $\alpha$ <sub>7</sub> $\beta$ <sub>1</sub> integrin, linking the cortical actin filaments to the basal membrane via  $\alpha$ -actinin<sup>71</sup>. Likewise, mutations in the  $\alpha$ <sub>7</sub> integrin gene are associated with muscular dystrophies in humans<sup>72</sup>. The sarcoglycan protein family is composed of 6 transmembrane glycoproteins ( $\alpha$ , $\beta$ , $\gamma$ , $\delta$ , $\epsilon$ , $\zeta$ ) which form a complex at the plasma membrane. The sarcoglycan complex is tightly bound to  $\beta$ -dystroglycan via  $\delta$ -sarcoglycan<sup>73</sup>. Mutations in sarcoglycan genes are the primary genetic defects in some forms of human autosomal-recessive limb-girdle muscular dystrophy (LGMD2C-F), leading to disruption of the sarcoglycan-sarcospan complex. The  $\alpha$ -sarcoglycan subunit of the sarcoglycan complex is

exclusively expressed in skeletal muscle and is replaced by  $\epsilon$ -SG in other tissues<sup>74</sup>. Knowledge of the existence of  $\epsilon$ -SG-containing sarcoglycan-sarcospan complexes in smooth and heart muscle explains the cardiomyopathic phenotype in  $\beta$ -, and  $\delta$ -SG deficient mice, which is absent in  $\alpha$ -SG knockout mice<sup>75,76</sup>. The syntrophin family of proteins is a component of the DGC binding directly to dystrophin. Syntrophins share similar protein domain structures consisting of a PH domain, PDZ domain, two coiled-coiled (CC) modules and unique syntrophin C-terminal regions. Syntrophins interact with a number of proteins including dystrobrevin, nNOS, ErbB4 receptor tyrosine kinase, voltage-gated Na<sup>+</sup> channel, stress-activated protein kinase-3 (SAPK), and phosphatidylinositol-4,5-bisphosphate (reviewed in<sup>77,78</sup>).

As demonstrated by the role of NO-signaling in reversal of vasoconstriction, signaling through cytosolic DGC-associated proteins may be important for muscle function and survival. Insights into the complex molecular muscle pathology of DMD helped to identify molecular targets for therapy and to design experimental gene therapy approaches.

### *1.2.3 Molecular and gene therapy approaches to treat muscular dystrophies.*

The dystrophin paralog protein, utrophin, shares most of the dystrophin functions, including binding to  $\beta$ -dystroglycan and  $\beta$ -actin and interacting with  $\alpha$ -syntrophin. Despite its similarity to dystrophin, utrophin displays a different localization in normal muscle, where it is confined to the neuromuscular and myotendinous junctions<sup>78</sup>. The hypothesis that utrophin may substitute for dystrophin function in dystrophin-deficiency was tested by generating transgenic lines of *mdx* mice overexpressing utrophin under the control of a muscle-specific muscle creatine kinase (MCK) promoter<sup>79</sup>. Indeed, utrophin expression was observed throughout the sarcolemma and alleviation of muscle pathology, including calcium homeostasis, membrane permeability, correct assembly of DGC at the sarcolemma, and force generation was observed<sup>79,80</sup>.

Permanent gene therapy of DMD by direct dystrophin/utrophin transfer represents the therapy of choice. Due to the large size of dystrophin cDNA (14kb), gene transfer vectors with large packaging capacity must be used *e.g.*, herpes simplex-based vectors, high-capacity adenovirus (hc-Ad), and plasmid DNA vectors). Accordingly, hc-Ad-mediated dystrophin transfer in *mdx* mice resulted in sustained long-term expression of dystrophin and improvement in muscle function one year after the gene transfer<sup>81,82</sup>. Similarly, transfer of the non-immunogenic

utrophin led to mitigation of the dystrophic phenotype and improvement in muscle function<sup>83</sup>. Surprisingly, extrasynaptic utrophin localization with therapeutic effect in *mdx* mice was encountered after muscle-specific overexpression of cytotoxic T-cell N-acetylgalactose transferase (CT-GalNAc)<sup>84</sup>. CT-GalNAc was shown to specifically transfer  $\beta$ -1,4-GalNAc to synaptic  $\alpha$ -DG and has been proposed to influence alternative dystroglycan proteolysis and eventually leading to extrasynaptic accumulation of CT-modified  $\alpha$ -DG and sarcolemmal utrophin association<sup>85</sup>. Alpha 7 integrin was overexpressed in the intention of compensating for the loss of sarcolemma membrane stability via additional  $\alpha_7$  integrin - laminin  $\alpha_2$  chain interactions, and led to a partial amelioration of the dystrophic phenotype in *mdx/utr (-/-)* mice<sup>86</sup>.

Due to the fact that most frame-shift-causing mutations in DMD are located within the spectrin-like rod domain, and partial in-frame deletions of this domain are associated with a milder phenotype in Becker muscular dystrophy (BMD), antisense oligoribonucleotide-based therapy was considered<sup>87,88</sup>. Masking of critical splice sites on pre-mRNA with RNaseH-resistant 2-O-methylated phosphothionated antisense oligoribonucleotides (2OMeAO)<sup>88</sup> led to expression of functional dystrophin in the *mdx* mouse by promoting skipping of the mutated exon<sup>89,90,91,92</sup>. In a recent report Barton-Davis *et al.* used the stop codon read-through activity of aminoglycoside antibiotics to restore dystrophin-expression in *mdx* mice<sup>93</sup>. Although the read-through of stop codons by aminoglycoside antibiotics was successful *in vitro*<sup>94</sup>, the positive effect of gentamycin that was reported in *mdx* mice was neither reproducible in other laboratories nor in humans by other investigators<sup>95,96</sup>.

Overexpression of NO in transgenic *mdx* mice reduced inflammation and membrane damage<sup>59</sup>. This result supports the theory that loss of membrane NOS contributes to muscle pathology in *mdx* mice. Indeed, reduction of inflammation with corticosteroids prednisone and deflazacort increases muscle strengths in some patients and is a partially effective therapy for DMD<sup>97,98</sup>.

In 1989, Partridge *et al.* demonstrated that transplantation of myogenic precursor C2C12 cells into dystrophic muscles of *mdx* mice led to dystrophin expression and phenotypic correction of dystrophin-positive fibers<sup>99</sup>. Unfortunately these results could not be expanded to transplanted myoblasts in DMD patients, which poorly survived and had an impaired proliferative capacity *ex vivo*<sup>100,101</sup>. Recently, bone-marrow-derived stem cells and a specialized class of vessel-associated foetal stem cells termed *mesoangioblasts* were

transplanted into *mdx* mice and led to the restoration of dystrophin and  $\alpha$ -sarcoglycan expression in dystrophic muscles<sup>102,103</sup>. Sampaolesi *et al.*, transferred a copy of  $\alpha$ -SG using a lentiviral vector in autologous mesoangioblasts, expanded these cells *in vitro* and reinjected these cells into the femoral artery of  $\alpha$ -SG null mice. Intra-arterial delivery of corrected mesoangioblasts resulted in morphologic and functional correction of all downstream muscles<sup>103</sup>. Nonetheless correction of autologous stem cells for cell therapy of DMD with full-lengths dystrophin cDNA will require a stably integrating vector with large insertion capacity.

#### 1.2.4 Vectors for gene therapy

Great efforts have been undertaken to develop a gene-replacement therapy by introducing a functional copy of the affected gene back into the target organ. Vectors for gene delivery can be divided into non-viral plasmid-based DNA vectors and viral vectors, including AAV, AdV, HSV-1, Retro- and Lentiviral vectors. Typically,  $10^6$  plasmid copies are needed to transfect a single cell resulting in  $10^2$ - $10^4$  nuclear copies<sup>104,105</sup>, whereas up to 5% of applied adenoviral genomes can be detected in cells 48h post-transfection with only  $10^3$  transducing vector genomes used per cell (see chapter 3.1.4). The low transduction efficiency observed with plasmid DNA vectors is due to the numerous hurdles encountered by naked DNA-based vectors during the transduction process. Degradation by serum and cytosolic nuclease activity, cellular association of DNA complexes, lack of specific internalization, inefficient endosomal escape, or low intracellular diffusion of large DNA molecules has to be overcome for efficient delivery. However, solutions for these problems are currently developed to facilitate gene delivery *in vivo*<sup>106,107,108,109</sup>. One way to overcome these hurdles is to transfer functional properties of viruses to non-viral vectors, and by doing so, exploiting the cellular machinery by an effective gene delivery. DNA polyplexes are comprised of cationic peptides or polymers with DNA-condensing capacity to which functional ligands are covalently attached. These “artificial viruses” have been successfully used *in vivo* for targeted gene transfer, and may be equivalent to virus-based vectors in the future<sup>110</sup>.

Viruses, on the other hand have developed mechanisms to exploit the cellular machinery to gain access and efficiently deliver their genomes into the nucleus. The five main classes of viral vectors can be divided in strictly integrating vectors (oncoretroviruses, lentiviruses) and episomally maintained vectors (AAV, adenoviruses, HSV-1). Most oncoretroviruses are based

on Moloney murine leukaemia virus (MLV) and have recently been used to cure patients suffering from severe immunodeficiency (SCID)-XI disease following transduction of autologous hematopoietic stem cells *ex vivo*<sup>111</sup>. Unfortunately, the inherent risk of insertional mutagenesis that is associated with oncoretroviruses is a serious concern, since two out of the 11 patients treated developed a leukemia-like syndrome that arose from retrovirus insertion into the *LMO2* oncogene region<sup>112</sup>. Besides being potentially oncogenic, MLV-type retroviruses require cell division to gain access to the nucleus, and thus transduction is limited to dividing cells. In contrast to oncoretroviruses, lentivirus vectors are able to penetrate a nuclear membrane and transduce non-dividing cells. Most lentiviral vectors are HIV-derived, though they retain only minimal parts of the parental genome (<5%). Lentiviral vectors are able to generate long-term gene expression without inflammation and have been successfully used for gene therapy of CNS disorders like Parkinson's disease<sup>113,114</sup>. Both oncoretrovirus- and lentivirus-based vectors have an inherent oncogenic potential due to insertional mutagenesis.

Table1

Vector type	Vector Genome	Packaging capacity	Tropism	Acute Inflammation	Genomic ntegration	Application Limitations	Vector advantages
Retrovirus	RNA	8kb	Diving cells only	Low	Integration	1. Transduction limited to diving cells 2. Insertional mutagenesis	Persistent gene expression
Lentivirus	RNA	8kb	Broad	Low	Integration	1. Insertional mutagenesis	Persistent gene expression
HSV-1	dsDNA	40-150kb	Neuronal	High	Episomal	1. Acute inflammation	1. Large packaging capacity 2. Neuronal cell tropism
AAV	ssDNA	4.8kb	Broad	Low	Episomal; Integration (<10%)	1. Small packaging capacity 2. Integration in transcriptionally active genes	1. Non-inflammatory 2. Non-pathogenic
Adenovirus	dsDNA	8kb-36kb*	Broad	High	Episomal	1. Inflammation (capsid-mediated)	1. Efficient transduction 2. High packaging capacity

Table1. Main characteristics of the currently used viral vectors for gene therapy. \*High capacity adenoviral vectors devoid of all viral genes with a maximum packaging capacity of 36kb.

Site-directed integration of vector genomes into the host genome would therefore be a breakthrough in gene therapy and make treatment safer and regulatory approval more probable.

A small proportion of wild type adeno-associated virus 2 (AAV2) is able to integrate into a specific site in HeLa cells on chromosome 19, which is called AAVS1. The majority of AAV2, however, tends to integrate into multiple sites and active genes of hepatocytes *in vivo*<sup>115,116</sup>. One particularly beneficial feature of AAV vectors is the lack of acute inflammatory response after gene transfer and its natural tropism for skeletal muscle, which makes AAV a good candidate for muscle-directed gene therapy<sup>117,118</sup>. Major limitations of AAV vectors are the small packaging capacity of 4.8 kb and conversion of the single-stranded into a double-stranded DNA genome. Solutions for both problems are currently being developed through the construction of ds hairpin AAVs and splitting of expression cassettes, which can be reconstituted by splicing between linear concatemeric AAV genomes<sup>119,120</sup>.

Adenoviruses are the most efficient class of vectors in terms of gene delivery to the nucleus and will be presented in detail in the next chapter. The main features of the currently used viral vectors for gene therapy are summarized in Table 1.

### **1.3 Adenoviral vectors for gene therapy**

Adenoviruses are non-enveloped DNA viruses carrying a linear double-stranded genome. To date 51 human serotypes have been identified and classified into 6 subgroups (A to F)<sup>1</sup>. The history of adenovirus vectors in gene therapy is incontestably marked by the death of Jesse Gelsinger, who took part in a gene therapy trial for ornithine transcarbamylase (OTC) replacement therapy at the University of Pennsylvania in Philadelphia. After receiving the highest dose of vector in the trial ( $3.8 \times 10^{13}$  particles) he developed symptoms of liver injury and disseminated intravascular coagulation, eventually leading to multiorgan failure and death<sup>121</sup>. The fatal course of the treatment was directly related to an acute inflammatory response to the injected adenoviral vector. The vector used in this trial was a first-generation adenovirus with deleted early genes (E1 and E3). Indeed, the initial response to intravascularly administered Ad vectors occurs within minutes and can be attributed to the innate response. A detailed evaluation of risks and side effects following the application of first-generation adenoviruses in clinical human trials was reported in a special issue of Human Gene therapy<sup>122</sup>.

### 1.3.1 Immunological barriers to adenovirus gene therapy

Adenovirus capsid is able to directly activate antigen-presenting cells (e.g., dendritic cells, macrophages), and triggers the release of proinflammatory cytokines<sup>123,124,125</sup>. Adenoviruses have therefore been extensively engineered to reduce their immunogenicity. Second-generation vectors having E1, E2 and E4 gene deletions, as well as third-generation vectors that are devoid of all viral genes, both show reduced immunogenicity. Third generation vectors can accommodate large DNA fragments up to 36 kb, and allow for prolonged transgene expression *in vivo* due to decreased acute and chronic toxicity<sup>126,127,128,129,130</sup>. Despite a strong stimulating action of first-generation vectors on the innate immune system, efficient local application is possible, which may be particularly suited for applications requiring only transient gene expression. The brain is an organ where the innate immune system can be investigated in isolation from the acquired immune system. Infiltration of peripheral T lymphocytes into the brain only occurs if priming of the peripheral immune system has previously taken place and signs of acute brain inflammation related to the same group of antigens are established<sup>131</sup>. The observed immune response to adenovirus-transduced brain cells after peripheral immunization (with adenovirus) is due to an anti-Ad genome immune response, that is partly directed against leakily expressed adenovirus genes and the transgene itself<sup>132</sup>. In agreement with this model, gene transfer in the brain using a third generation adenovirus was not associated with long-term brain inflammation and no loss of transgene expression occurred after peripheral immunization with adenovirus (the vector used for peripheral immunization shared the same Ad backbone but lacked the corresponding transgene expression cassette)<sup>129</sup>. Acute adenovirus-mediated vector cytotoxicity is a dose-dependent phenomenon that contributes to the loss of transgene expression in transduced tissues upon injection of  $>10^8$  infectious particles<sup>133</sup>. One major goal for vector development is therefore to decrease the required vector dose. Preexisting anti-virus immunity is another hurdle for adenovirus gene therapy preventing vector readministration. In humans the extent of the humoral response is dependent upon preexisting antibody titers and the route of administration<sup>134,135</sup>. However, another serious concern is the generation of an antibody-mediated immune response to transgenes, especially if the antigen is to be secreted. In this case generation of humoral anti-transgene response depends upon expression of the transgene in antigen-presenting cells. This can be avoided if tissue-specific promoters are used to limit transgene expression to non-hematopoietic tissues<sup>136,137</sup>. Preexisting humoral immunity can be

evaded by using tropism-modified viral vectors, which are able to circumvent anti-fiber neutralizing antibodies present in ascites fluid<sup>138</sup>. In an alternative strategy used to circumvent neutralizing antibodies, adenoviral particles were coated with a multivalent polymer capable of shielding viral epitopes from neutralizing antibodies and achieving good gene transfer efficiency *in vivo*<sup>139</sup>. In another approach designed to circumvent preexisting anti-Ad5 immunity, non-Ad5-based adenoviral vectors were used to infect cells *in vitro*<sup>140</sup>. Likewise, sequential administration of two different adenovirus serotype vectors “sero-switching“ allowed for repeated transgene expression even if the vectors belonged to the same subgroup<sup>141,142</sup>. Transduction of dendritic cells by adenovirus plays a central role for the induction of anti-adenovirus-directed immunity. Transgene expression in non-target tissues can be avoided by targeting gene expression, either transcriptionally through the use of tissue-specific promoters, or transductionally by redirecting attachment of viral vectors to tissue-specific receptors. Expression of transgenes under control of the muscle creatine kinase promoter (MCK) led to stable long-term expression of transgenes in muscle after adenovirus-mediated gene transfer<sup>143,144,145,146</sup>. Similarly, use of liver-specific promoters allowed for adenovirus-mediated long-term expression of apolipoprotein A-I in hepatocytes of immunocompetent mice<sup>137</sup>.

### *1.3.2 Maturation-dependent decrease in adenovirus transduction of skeletal muscle*

A major hurdle for gene transfer to skeletal muscle was revealed with gene-transfer experiments in animals of different ages. Transduction efficiency was linked to the maturation state of the muscle. Whereas skeletal muscle fibers of newborn mice were efficiently transduced by adenovirus, mature muscle fibers of adult mice were only poorly transduced<sup>147</sup>. This maturation-dependent decrease in transduction of mouse skeletal muscle *in vivo* was mirrored *in vitro* by the decrease in transducibility of cultured human myotubes as compared to myoblasts. In contrast, adenoviral transduction of regenerating and dystrophic muscle fibers of adult dystrophin-deficient *mdx* and merosin-deficient *dy/dy* mice was higher than that of normal muscle fibers, although still considerably lower than in neonate muscle<sup>148,149</sup>.

### *1.3.3 Expression level of CAR is crucial for transduction of skeletal muscle by adenovirus in vivo*

The high adenoviral transduction of newborn myofibers may be partly due to transduction of myoblasts and partly to the higher levels of CAR present in these myofibers<sup>150</sup>. Moreover, in

adult mice, the low expression levels of the primary virus-attachment receptor CAR, in conjunction with the decrease of secondary internalization receptors, integrins  $\alpha_v\beta_3$  and  $\alpha_v\beta_5$ , may account for the low transducibility of skeletal muscle *in vivo*<sup>151,152</sup>. However, CAR expression is upregulated on the surface of regenerating myofibers in *mdx* mouse muscles. A similar increase in CAR levels has been observed in regenerating fibers of human inflammatory and degenerative muscle disorders<sup>153</sup>, suggesting that these fibers may also be susceptible to adenoviral transduction.

Therefore, several strategies based on the augmentation of CAR molecules on the cell surface that enable increased transduction efficiency and adenovirus-mediated gene transfer in adult myofibers have been developed. Sequential administration of hCAR- and EGFP-encoding AdV have allowed for repetitive and efficient transduction of young adult myofibers<sup>154</sup>. In order to evaluate how overexpression of CAR in muscle may affect adenovirus-mediated gene transfer into mature skeletal muscle, transgenic mice expressing the CAR cDNA under control of a muscle-specific creatine kinase (MCK) promoter were generated<sup>155</sup>. In adult CAR transgenic mice (CAR-Tg) the susceptibility of skeletal muscle to adenovirus transduction was significantly higher than in non-transgenic littermates. After a single injection of  $2 \times 10^{10}$  particles adenovirus carrying a  $\beta$ -galactosidase reporter gene in tibialis anterior muscle of adult animals, the transgene was expressed in  $433 \pm 121$  muscle fibers of CAR-Tg mice vs.  $8 \pm 4$  fibers in non-transgenic controls. A single AdV injection may lead to the transduction of the entire tibialis anterior and extensor digitorum longus (EDL) muscle<sup>155</sup>. This study demonstrated that (i) upregulation of the primary adenovirus receptor CAR in myofibers confers a high susceptibility to adenovirus-mediated gene transfer *in vivo*, and (ii) that low expression of CAR in adult skeletal muscle is a major impediment to efficient adenoviral transduction. Recent studies using an experimental histone H3 deacetylase inhibitor FR901228 showed that this compound upregulated CAR and alpha v integrins and enhanced adenovirus gene transfer into CD34+ cells by 10-fold<sup>156</sup>. The use of this compound in adenovirus-mediated gene transfer experiments to skeletal muscle is currently being explored

#### *1.3.4 The extracellular matrix may act as a physical barrier to adenovirus in vivo*

A further explanation for the poor transducibility of adult skeletal muscle may be the presence of the extracellular matrix itself, which may constitute a physical barrier for large viral particles. The average pore size of the extracellular matrix has been estimated to be 40 nm<sup>157</sup>. Indeed, large herpes simplex viral vectors (HSV-1) are unable to penetrate and transduce

mature myofibers when injected directly into skeletal muscle<sup>158</sup>. Since adenovirus particles have a diameter of 60-85 nm, depending on the fiber length of different adenovirus serotypes, a physical inhibition of myofiber transduction by the myofiber basal lamina may not be ruled out completely.

In addition to low efficient AdV-mediated gene transfer to adult skeletal muscle, several obstacles have been encountered in *in vivo* experimentation in different animal models for muscular dystrophy. These limitations, in particular systemic dissemination of the vector and immunologic reactions of the host, need to be overcome before therapeutic use of AdV in human muscular dystrophy can be considered. To prevent major muscle degradation in the *mdx* mouse, 30 to 40 % of the normal level of dystrophin must be expressed in an even distribution throughout the muscle<sup>159,160</sup>. The route of vector administration determines the biodistribution and transduction efficiency of tissues<sup>161</sup>. After intramuscular vector injection, transgene expression is found only within a restricted area near the injection site and in the vicinity of the encoding myonucleus<sup>162,163</sup>. The muscle fascicles as well as the connective tissue may function as barriers for the spread of viral vectors within the muscle after intramuscular injections. Intravascular delivery of plasmid DNA vectors with increased pressure to limbs of monkeys resulted in transgene expression in all limb muscles without notable toxic side effects<sup>164</sup>. Histamine-induced endothelial permeabilization allowed for a similarly widespread expression in hind-limb muscles after intraarterial injection of recombinant adeno-associated virus<sup>118</sup>. Likewise, AdV can egress out of the intravascular compartment if increased hydrostatic and decreased osmotic pressure is applied<sup>165</sup>. Tissue targeting may be even more essential for systemic delivery of gene-transfer vectors than it is for local administration.

#### **1.4 Targeting of viral vectors for gene therapy**

To render the binding properties of the gene-transfer vectors tissue-specific, targeted viral vectors with modified binding properties are currently being developed. As discussed above, targeted viral vectors are likely to be less immunogenic, less toxic and safer, and may eventually allow a systemic application of the vector. Retargeting of viral vectors has been achieved for several viruses including retrovirus, adenovirus, and adeno-associated virus<sup>166,167,168,169</sup>. Targeting adenovirus requires a two step approach involving (i) ablation of the native tropism, and (ii) introduction of a novel targeting moiety. Several strategies based on

the augmentation of CAR molecules on the cell surface, direct targeting of adenoviral particles through genetic engineering of the fiber and capsid proteins, and compound-mediated retargeting of AdV have been developed to enhance gene delivery to target tissues (Fig.3).

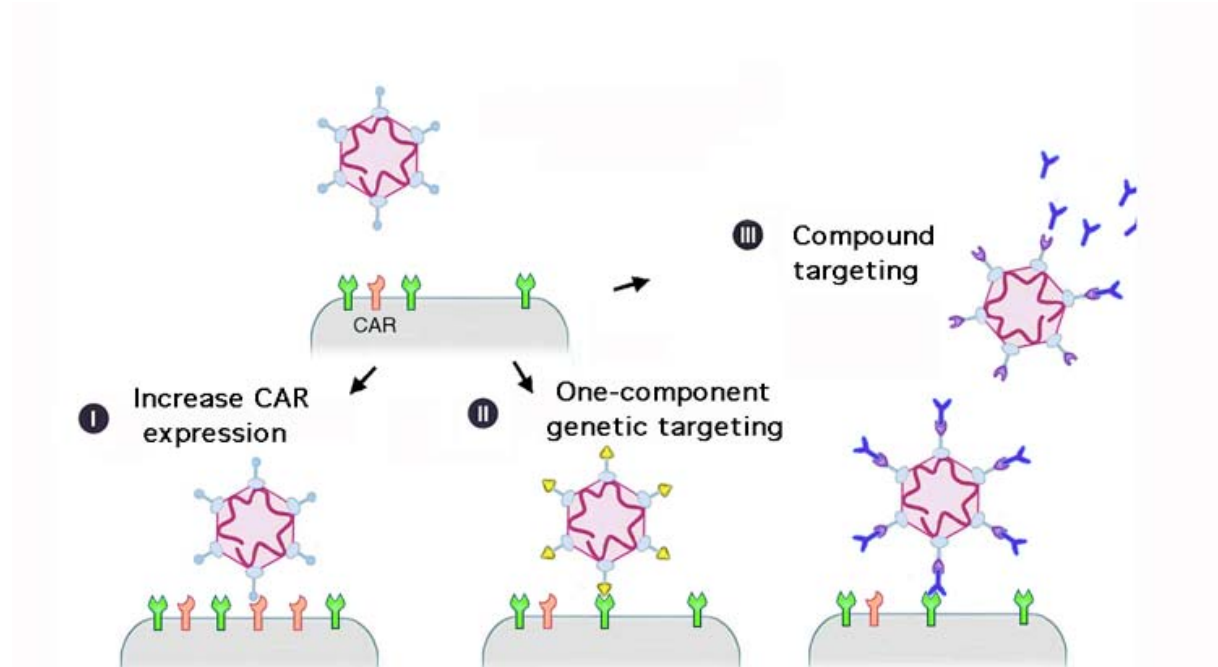


**Fig.3 Strategies for adenovirus targeting and enhanced gene delivery into the targeted tissues.**

Increase of CAR expression on the target tissue surface (I), direct targeting of adenoviral particles through genetic engineering, including insertion of targeting ligand into the HI-loop, addition of C-terminal targeting ligands, fiber-swap between Ad-serotypes, or genetic engineering of the capsid proteins (II) and compound-mediated retargeting of AdV through attachment of bispecific protein- or antibody-adaptors (III) are currently being tested for adenovirus retargeting.

#### 1.4.1 Ablation of the native tropism

The development of a tissue-specific viral vector for gene therapy necessitates an understanding of the molecular process and the ability to manipulation virus-cell interactions. The solved crystal structure of adenovirus type 12 fiber knob and its cellular receptor CAR was the first step towards a rational design of retargeted vectors. The CAR-binding interface of Ad12 knob is formed by four loop regions of Ad12 knob that interact with a single face on the N-terminal domain of human CAR (CAR-D1) (Fig.4).



**Fig.4 Ribbon diagram of the Ad12 knob-CAR D1 complex viewed down the viral fiber.**

The core of each knob monomer is composed of an eight-stranded antiparallel beta sandwich. The V sheet is colored purple and the R sheet including the HI loop are blue. The AB loop is highlighted in yellow, and all other regions are grey. The CAR D1 domain is colored in turquoise. In Ad12 knob the interfacial residues are D415, P415, P418, I426 (AB loop), V450, K451 (CD loop), and Q487, Q494, S497, and V498 (E and F strands) for one knob monomer and P517, P519, N520, and E523 (FG loop) for the adjacent knob molecule. The figure was kindly provided by Paul Freimuth and John Flanagan with reprint permission from Science magazine<sup>19</sup>.

The interacting region is constituted by the AB loop, the C-terminus of the DE loop, the short F strand, and the FG loop on the adjacent knob monomer (Fig.4)<sup>170</sup>. Sequence analysis of the fiber knobs of different Ad serotypes led to the identification of residues critical for CAR-Ad5 knob interaction<sup>171,172</sup>. The point mutations S408E, K417G (AB loop), K420A (B sheet), L485K (beta strand F), and Y477A (DE loop) have been found to be very effective in ablating CAR-knob interactions<sup>171,172,173</sup>. Likewise, introduction of the double K417I + K420I double point mutations effectively ablated CAR binding<sup>174</sup>.

However, the *in vivo* tissue-distribution of systemically applied CAR-ablated viruses was unchanged after intravenous AdV administration, in contrast to detargeting mutations in the putative HSG-binding motif contained within the Ad5 shaft, which reduced the hepatic gene transfer *in vivo*<sup>175,176</sup>. The investigation of the blood clearance rate of adenovirus demonstrated that 99.9 % of the circulating virus was removed within the first hour with a half life of less than 2 minutes<sup>177</sup>. Tissue macrophages like liver Kupffer cells are likely to

sequester adenovirus via a CAR-independent entry mechanism, which may involve opsonizing serum factors and occur directly through integrins of the  $\alpha_v$  or  $\alpha_M\beta_2$  type<sup>178,179</sup>. Indeed, depletion of Kupffer cells led to increased gene transfer of AAT-1 to liver without generating an anti-AAT1 humoral immune response<sup>180</sup>. Likewise, since monocyte-derived dendritic cells (DC) do not express CAR, ablation of binding to CAR is not likely to influence DC transduction, and hence adenoviruses defective for CAR-binding may not reduce the DC-mediated immune-response after AdV gene transfer<sup>181</sup>. It was further shown that efficient ablation of the native tropism required simultaneous removal of CAR and integrin interactions<sup>182</sup>.

#### 1.4.2 Genetic modifications of the adenovirus fiber protein

Modification of the adenovirus tropism can be achieved through genetic modification of the fiber protein by the addition of targeting ligands to the C-terminus<sup>183,184,185,186</sup>. Limited enhancement of the transduction of myofibers and glioma cells was achieved *in vivo* using an extended tropism vector with a C-terminal poly-lysine modification (20 residues added)<sup>187</sup>. However, C-terminal additions to the fiber seem to be restricted to small ligands, since the addition of 27 amino acids prevented trimerization of the fiber protein<sup>184,185,188</sup>.

The HI-loop of the fiber protein seems better suited as an insertion site for targeting ligands. Proof-of-principle was demonstrated upon insertion of a FLAG octapeptide<sup>189</sup>. Similarly, the insertion of poly-lysine and RGD-peptides into the HI-loop led to increased transduction of cell lines *in vitro*<sup>190</sup>. Insertion of small targeting peptides into the HI loop, *e.g.*, selected by phage display, is an effective way to retarget adenovirus. Nicklin *et al.* combined CAR-ablation with insertion of a cell-specific ligand selected by phage display and achieved selective transduction of endothelial cells<sup>191</sup>.

Since hc-Ad vectors display an enhanced safety profile and reduced toxicity, retargeting of hc-Ad constitutes a logical step towards a clinical application of AdVs. Retargeting of hc-Ad by incorporating RGD-4C peptides into the HI loop was reported<sup>192</sup>.

The generation of fiber chimeras, which transfer parts of the Ad serotype-specific tropism from one virus to the other, represents another possibility to genetically alter the adenovirus tropism<sup>193,194,195</sup>. Multitudes of serotype-specific tropisms provide a considerable natural reservoir for tissue-specific retargeting of Ad5. The chimeric vector Ad5.F35, which contains the Ad35 fiber in the Ad5 capsid, efficiently transduced CD34+ cells in an  $\alpha_v$ -integrin independent manner<sup>196</sup>. Likewise, transduction of smooth muscle cells was enhanced with

Ad5.F16 fiber-chimeric adenovirus<sup>303</sup>. Removal of the entire fiber knob represents a more drastic modification to retarget adenovirus. Targeting ligands are added as C-terminal extensions to trimerization-promoting domains derived from T4 phage protein fibrin, MoMuLV envelope glycoprotein, or neck region peptide of human lung surfactant protein D, which are fused to 7 fiber shaft repeats<sup>197,198,199</sup>. Gene transfer into CAR-negative, but  $\alpha_v\beta_{3/5}$  integrin-positive human embryonal rhabdomyosarcoma (RD) cells with knobless retargeted adenovirus resulted in a 10-fold higher transduction with the modified vector as compared to with unmodified Ad5<sup>198</sup>. Attempts to fuse the immunoglobulin-binding triple-helix bundle scaffold Z, which is derived from domain B of Staphylococcal protein A, to knobless adenovirus particles failed<sup>200</sup>. However, other ligands that fold independently from disulfide bridge-formation have been successfully fused to knobless adenovirus particles<sup>201,202</sup>. In addition to genetic retargeting via modifications of the Ad fiber protein, targeting ligands have been successfully added to adenovirus hexon, penton base, and protein IX<sup>203,204,205</sup>. Protein IX fusions can be of considerable length, as demonstrated by the rescue of adenovirus that displays a protein IX-EGFP C-terminal fusion protein<sup>206</sup>.

#### 1.4.3 Compound targeting vectors

Adaptor-mediated retargeting entails the conjugation of an anti-adenovirus antibody with a targeting ligand. Redirecting AdV to the folate receptor validated this concept<sup>207</sup>. Using similar approaches, AdV has been targeted to multiple receptors including  $\alpha_v$  integrin, FGF2, EGFR, CD105, CD3, E-selectin, CD40, and  $\beta_1$ -integrin. These retargeted adenoviruses significantly enhanced the specificity of viral infection *in vitro*<sup>208,209,210,211,212,213</sup>. Moreover, these results clearly demonstrate that cell lines refractory to infection may efficiently be transduced with retargeted AdV, and internalization of Ad vectors by cells that lack  $\alpha_v$  integrins can be achieved through targeting cytokine/growth factor receptors<sup>214</sup>. Studies *in vivo* indicate that adenovirus-conjugate complexes are stable and provide for increased target cell transduction and decreased liver toxicity<sup>215</sup>. Markedly increased transduction of target tissues, longer residence time in the circulatory system, lower systemic toxicity with absence of liver necrosis, and *in vivo* therapeutic benefit have been observed<sup>216,217,218</sup>. Although these results are encouraging, after systemic administration most AdV particles are still found in the liver and the secondary target organs (lung, heart, spleen). When administered locally, fibroblast growth factor receptor-retargeted Ad5 is able to transduce tumor cells more

efficiently than non-targeted vectors<sup>216</sup>. EGFR-targeted adenoviruses are particularly useful for transduction of tissues with low expression of alpha v integrins, since the internalization of EGFR-bound Ads occurs via internalization of the EGF receptor<sup>211</sup>. Reynolds *et al.* reported a highly efficient double-targeting approach in which a tissue-specific promoter controlled transgene expression, ‘transcriptional targeting’, and was combined with antibody-mediated retargeting of adenovirus to a pulmonary endothelial marker, ‘transductional targeting’<sup>219</sup>. In this case, 30 times more transgene expression was detected in the targeted tissue after systemic vector administration (compared to liver), which was equivalent to a 10000-fold reduced transgene expression in the liver as compared to a conventional non-targeted vector.

## 2. Material and methods

### 2.1 Primary cells and cell lines

#### 2.1.1 Culture conditions for established cell lines

293A cells, CV-1 cells, and rat L6 myoblasts were grown in Dulbecco's modified Eagle medium (DMEM) supplemented with 10% fetal calf serum (FCS) (Invitrogen Life Technologies, Karlsruhe, Germany) in a humidified atmosphere with 5% CO<sub>2</sub> at 37°C. N52.E6 cells<sup>221</sup> were grown in alpha MEM (Invitrogen Life Technologies, Karlsruhe, Germany) containing 10 % FCS in a humidified atmosphere with 5% CO<sub>2</sub> at 37°C. CHO cells expressing integrin alpha v beta 3 (CHO $\alpha_v\beta_3$ ) were kindly provided by Dr. Gawaz (Medizinische Klinik, Klinikum rechts der Isar und Deutsches Herzzentrum, Technische Universität München, Germany). CHO $\alpha_v\beta_3$  cells were cultured in Ham's F10 medium (Invitrogen Life Technologies, Karlsruhe, Germany) containing 10 % FCS in a humidified atmosphere with 5% CO<sub>2</sub> at 37°C.

#### 2.1.2 Culture conditions for primary cells

Primary human, ape, pig and mouse myoblasts were obtained from the Muscle Tissue Culture Collection, Friedrich-Baur-Institut (Munich, Germany). Primary human, ape and pig cells were grown in skeletal muscle cell growth medium supplemented with 5% FBS in a humidified chamber with 5% CO<sub>2</sub> at 37°C (Promocell, Heidelberg, Germany). Primary mouse myoblasts were grown in Quantum 212 medium (PAA laboratories, Pasching, Austria) in a humidified atmosphere with 5% CO<sub>2</sub> at 37°C. Human umbilical vein endothelial cells (HUVEC) were kindly provided by A. Herrmann (Cardion AG, Erkrath, Germany) and were grown in M199 medium with 60 mg/l ECGS (epidermal cell growth substrate), 100 mg/l Heparin (both from Sigma, Deisenhofen, Germany), 20% FBS and penicillin-streptomycin. HUVECs were used at passage 3 and 4.

Specimens of human saphenous vein were obtained from patients undergoing aortocoronary bypass surgery with approval by the local ethics committee and informed consent of the patients, and vascular smooth muscle cells isolated using the explant technique<sup>220</sup>. Cells were grown in DMEM supplemented with 15% fetal calf serum, 100  $\mu$ g/ml streptomycin, 100 U/ml penicillin, 1.9 mmol/L L-glutamine, 9.6 mmol/L sodium pyruvate and non-essential amino acids (all reagents were purchased from Invitrogen Life Technologies, Karlsruhe, Germany)

in a humidified atmosphere with 5% CO<sub>2</sub> at 37°C. For transfection experiments subconfluent cells in 24-well-plates were used.

### *2.1.3 Enrichment of myoblasts with magnetic cell sorting MACS*

Primary human myoblasts were separated from co-purified fibroblasts by means of MACS. Myoblasts ( $1 \times 10^6$  cells) were cultured in a 10cm cell culture dish and detached by trypsination (treatment with 0.25% trypsin and 1mM EDTA (reagents from Sigma, Deisenhofen, Germany) for a maximum of 2 min at 37°C followed by centrifugation (200 x g, 5 min). Cells were resuspended in 1ml MACS buffer (PBS supplemented with 0.5% BSA) and incubated for 45min on ice with purified 3µg/ml anti-NCAM antibody 5.1H11. Cells were washed 3 times, resuspended in 80µl MACS buffer, and 20µl of rat anti-mouse IgG1 micro beads added, and incubated for 30 min on ice (Miltenyi Biotech GmbH, Bergisch Gladbach, Germany). Cells were washed again in MACS buffer, resuspended in 0.5ml MACS buffer and loaded onto the pre-equilibrated MACS column placed in the magnetic column holder. Non-labeled cells passed the column and were discarded. Bound cells were eluted directly in SGM medium from the column outside the column holder in 1ml MACS buffer.

### *2.1.4 Isolation and differentiation of primary monocyte-derived dendritic cells*

Monocyte-derived dendritic cells were obtained by differentiation of monocytes isolated from primary peripheral blood lymphocytes (PBLs) by MACS enrichment of CD14<sup>+</sup> cells. Heparinated blood (Heparin from Sigma) was collected and 20 ml Ficoll (Pancoll human, density 1.077g/ml from Pan Biotech GmbH, Aidenbach, Germany) overlaid with 30ml blood per Falcon (50ml). Following centrifugation (2000rpm, 30min, RT, without brake) the interphase containing PBLs was removed and transferred into a new falcon and mixed 1:1 with PBS. After centrifugation (1900 rpm, 10 min, RT) the cell pellet was resuspended in 50 ml PBS and once again centrifuged (1900 rpm, 10 min, RT). Next, the cell pellet was resuspended in MACS buffer (80µl per  $1 \times 10^7$  cells) and 15µl anti-CD14 magnet beads added per  $1 \times 10^7$  cells. MACS separation was done as described above and cells grown in dendritic cell differentiation medium (DC medium). Monocytes were cultured for 7 days in DC medium and immature DCs characterized by FACS for surface expression of DC-specific markers CD11c, DC-SIGN, and CD86. DC medium contained X-Vivo 15 growth medium (2ml per  $3 \times 10^6$  cells) supplemented with GM-CSF 800U/ml and IL4 800U/ml cells (BioWhittaker, Walkersville, USA).

### *2.1.5 Growth conditions for hybridoma cells, adaptation to serum-free conditions, and purification of monoclonal antibodies*

5.1H11 hybridoma cells were cultured in DMEM supplemented with 10% FCS, 2mM glutamine, 0.1mM non-essential amino acids, and 1mM sodium pyruvate. Production of hybridoma supernatant in serum-free Hybridoma-SFM (Invitrogen Life Technologies, Karlsruhe, Germany) was done by direct adaptation of 5.1H11 cells to hybridoma-SFM medium. Serum-containing medium was removed from 5.1H11 cells and only semi-adherent cells, which are 100% viable, overlaid with hybridoma-SFM medium. Supernatant was collected after 48h and antibodies affinity-purified with protein G. Briefly, supernatant was diluted 1:4 in equilibration buffer (20mM sodium phosphate pH 7.0) and passed through a protein G column (Roche Diagnostics GmbH, Mannheim, Germany). Unbound material was washed from the column with 50ml washing buffer (washing buffer: 20mM sodium phosphate pH 7.0, 150mM NaCl, 2mM EDTA) and the protein eluted with elution buffer (elution buffer: 100mM glycine pH 2.7). Eluted protein was neutralized with 20% 1M sodium carbonate pH 9.0 and concentrated with Vivapin column cut off 10kDa (Vivascience AG, Hannover, Germany). Antibody was directly used for retargeting of AdFZ33βGal or stored at -20°C in elution buffer supplemented with 50% glycerin and 0.02% sodium azide until use.

### *2.1.6 Differentiation of myoblasts into myotubes*

Fusion and differentiation of myoblasts into myotubes was induced by replacing the growth medium by DMEM containing 2% horse serum (Invitrogen Life Technologies, Karlsruhe, Germany). Cells were cultured for a minimum of 5 days until multinucleated myotubes had formed.

## **2.2 Viral vectors**

### *2.2.1 Propagation and purification of adenoviral vectors*

The viral vector AdEGFP was a kind gift from Dr. Christoph Volpers and generated by insertion of a blunted *AfIII/AfIII* fragment from pEGFP-N1 (Clontech, Heidelberg, Germany) into the *PacI* site of pGS66<sup>221</sup> after removal of overhanging ends with T4 DNA polymerase. The plasmid pAdEGFP contains an EGFP open reading frame under control of the CMV promoter and an SV40 polyA region at the 3' end in a left-to-right orientation (identical to the Ad19aEGFP) in the E1 region of the Ad5 genome between the left ITR and the E2

transcription unit. Rescue and propagation of Ad vectors: The EGFP reporter vector AdEGFP which was used as a control vector (unmodified Ad5 capsid) and was rescued by transfection of 10µg of *SwaI*-cut pAdGFP DNA into N52.E6 cells<sup>221</sup> by the calcium phosphate method. Plaques were picked after eight days from the agarose overlay of the culture plate, the vector was amplified by serial propagation on N52.E6 cells and purified by CsCl equilibrium density gradient centrifugation as previously described<sup>222</sup>.

The first generation vector Ad19aEGFP was provided by Dr. Ruzsics. Ad19aEGFP contains the E1-deleted adenovirus 19a backbone with an EGFP open reading frame under control of the CMV promoter and an SV40 polyA region at the 3' end in a left-to-right orientation.

### 2.2.2 Construction of AdFZ33βGal

Dr. Volker Biermann constructed the vector AdFZ33βGal by insertion of the nucleotide sequence encoding the Z33-peptide into the fiber HI loop region of pVB6. Three pairs of 5'-phosphorylated oligonucleotides:

5'-TAAGTTTAAACATGCAGCAGCAGCGCCGCTTTTAC-3' and 5'-CGGCGCTGCTGCTGCATGTTAAACTTAAT-3', 5'-GAGGCCCTGCACGACCCCAACCTGAACGAGGAGCAG-3' and 5'-CTCGTTCAGGTTGGGGTCGTGCAGGGCCTCGTAAAA-3', as well as 5'-CGCAACGCCAAGATTAAGAGCATTTCGCGACGACAT-3' and 5'-CGATGTCGTCGCGAATGCTCTTAATCTTGGCGTTGCGCTGCTC-3',

were annealed and ligated to the *PacI/ClaI*-cleaved expression plasmid pVB6<sup>192</sup>. The infectious adenovirus plasmid pVB6 contains the genome of a first-generation Ad vector with a CMV promoter/*lacZ* expression cassette replacing the E1 region and unique *PacI* and *ClaI* restriction sites at Ad5 nucleotide position 32,670 in the HI loop region of the fiber gene. The correct sequence and position of the insert was confirmed by cycle sequencing.

Rescue and propagation of AdFβGal, and AdFZ33βGal. 10 µg of pVB6 and pVB44 DNA, respectively, were cleaved with *SwaI*, followed by phenol extraction and ethanol precipitation. The DNA was transfected into N52.E6 cells by the calcium phosphate method and the cells harvested after 14 days when they showed cytopathic effect (CPE). After three cycles of freeze/thawing to release vector particles N52.E6 cells were infected with half of the cell lysate, and the cell monolayer was overlaid with 0.5% agarose mix. After plaque purification, the Ad vectors were propagated in N52.E6 cells as previously described<sup>222</sup>. Following CsCl

equilibrium density gradient centrifugation, the infectious titer of AdF $\beta$ Gal and AdFZ33 $\beta$ Gal, respectively, was determined by standard  $\beta$ -galactosidase assay on 293 cells<sup>223</sup>.

### *2.2.3 Titration of adenoviral vectors*

The virus titer was expressed either in viral genomes per ml (vg/ml) as determined with real time PCR, or in gene transfer units [GTU] as previously described<sup>223,224</sup>. Quantification of adenoviral genomes was performed by means of quantitative PCR. Genomic titers of CsCl gradient-purified virus preparations were determined using real-time fluorescence detection ABI Prism 7000 Sequence Detector (Applied Biosystems, Foster City, USA) and SybrGreen as a double-stranded DNA-specific fluorescent dye (Applied Biosystems, Foster City, USA). Serial dilutions of plasmid pEGFP-N1 (Clontech, Palo Alto, USA) were used to obtain a standard calibration curve and fluorescence threshold values (Ct) plotted against plasmid copy numbers. The primers EGFPf214 (5'GCAGTGCTTCAGCCGCTAC3'), and EGFPPr309 (5'AAGAAGATGGTGCCTCCTG 3') were designed with the software Primer Express (Applied Biosystems, Foster City, USA) and their working concentration optimized according to the manufacturer's guidelines.

Capsid-free viral DNA was used as template and prepared as previously reported<sup>224</sup>. The PCR amplification was preceded by Uracil-N-glycosidase (Applied Biosystems, Foster City, USA) treatment for 2 min at 50°C and followed by a denaturation step of 10 min at 94°C and 40 cycles of 15 s at 95 °C, 30 s at 60°C, and 30 s at 72°C.

## **2.3 Retargeting of AdFZ33 $\beta$ Gal**

### *2.3.1 Monoclonal and polyclonal antibodies*

the following antibodies were used for adenovirus retargeting: Mouse IgG2a type monoclonal anti-human EGFR antibody (mAb) LA22 (Upstate Biotechnology, Lake Placid, USA), anti-human CD3 mAb HIT3a (Pharmingen BD, Hamburg, Germany), anti-human p53 mAb DO-1 (Santa Cruz Biotechnology, Santa Cruz, USA), monoclonal antibody 2A6 specific for adenovirus trimeric fiber protein (NeoMarkers, Westinghouse, USA), and polyclonal anti Ad5 hexon antibody (Biotrend, Köln, Germany). Antibody mAb-15 against integrin beta 3 was kindly provided by Dr. Gawaz (Medizinische Klinik, Klinikum rechts der Isar, und Deutsches Herzzentrum, Technische Universität München, Germany). The mAbs 3C12 and 6A11 against mouse  $\alpha_7$ -integrin were obtained from Prof. Dr. Helga von der Mark (University of

Erlangen, Germany)<sup>225,226</sup>. The anti-human NCAM mAb 5.1H11<sup>227</sup> was a kind gift by Dr. Shoubridge (Montreal Neurological Institute, McGill University, Canada). Anti-NCAM and anti- $\alpha_7$  integrin antibodies were affinity-purified from hybridoma cell culture supernatant with protein G-agarose (Roche Diagnostics, Mannheim, Germany). The purity of antibody preparations was higher than 90%, as assessed by polyacrylamide gel electrophoresis followed by silver staining<sup>250</sup>. Protein concentrations of purified antibody preparations were determined with a colorimetric bicinchoninic acid (BCA)-based protein detection and quantitation assay (Pierce, Rockford, USA). A polyclonal antibody against the Ad5 fiber knob was raised in rabbits by immunization with recombinant purified knob protein (Charles River Deutschland, Kiblegg, Germany). Anti-MHC class I antibody W6/32 was kindly provided by Dr. Ruzsics (Max-von-Pettenkofer Institut, München, Germany).

### *2.3.2 Complex formation between AdFZ33 $\beta$ Gal and antibodies*

In order to form antibody-virus complexes, AdFZ33 $\beta$ Gal vector (MOI=10) was preincubated with retargeting mAbs at different concentrations in serum-reduced Opti-MEM medium (Invitrogen Life Technologies, Karlsruhe, Germany) for one hour at room temperature. The cell culture media was replaced with Opti-MEM (Invitrogen Life Technologies, Karlsruhe, Germany) supplemented with 2% fetal bovine serum containing ultra low IgG amounts (Invitrogen Life Technologies, Karlsruhe, Germany), and 4  $\mu$ l of the preincubated AdFZ33 $\beta$ Gal vector antibody complexes added to the cells for 1h on ice. Cells were washed twice with Opti-MEM and further incubated with 10% FBS-containing growth medium for 48 hours at 37°C until the transgene expression was quantified.

## **2.4 Adenovirus transduction and competition assays**

### *2.4.1 Adenoviral transduction and competition assays for AdFZ33 $\beta$ Gal*

One day prior to transduction fetal human myoblasts (FHM) were seeded in 96-well ( $1 \times 10^4$  cells per well) flat-bottom tissue culture plates (Corning Glass Works, Corning, USA).

For competition experiments the Ad vector was preincubated with mAb as described and transduction done in the presence of 20 $\mu$ g/ml recombinant Knob protein, 20 $\mu$ g/ml KnobZ33 protein, or 10 $\mu$ g/ml staphylococcal protein A fragment, respectively. Cells were washed twice with Opti-MEM and further incubated with 10% FBS-containing growth medium for 48 hours

at 37°C until the transgene expression was quantified. Transduction efficiencies were evaluated by luminometric quantification of  $\beta$ -galactosidase activity or X-Gal staining.

#### *2.4.2 Virus transduction assay*

One day prior transduction fetal human myoblasts (FHM) were seeded in 48-well ( $1 \times 10^4$  cells per well) flat-bottom tissue culture plates (Corning Glass Works, Corning, USA) and transduced over night (16h) in Opti-MEM medium (Invitrogen Life Technologies, Karlsruhe, Germany) supplemented with 2% FBS with 1250, 2500, and 12500 viral genomes per cell (vg/cell). Cells were washed twice with Opti-MEM and further incubated with 10% FBS-containing growth medium for 48 hours at 37°C until the transgene expression was quantified.

#### *2.4.3 Virus transduction competition assay*

One day prior transduction fetal human myoblasts (FHM) were seeded in 48-well ( $1 \times 10^4$  cells per well) flat-bottom tissue culture plates (Corning Glass Works, Corning, USA).

For competition experiments Ad5EGFP and Ad19aEGFP vectors were preincubated with 10 $\mu$ g/ml Ad19a fiber protein, purified knob proteins (Ad19a knob: 10 $\mu$ g/ml and 100 $\mu$ g/ml; Ad5 knob: 10 $\mu$ g/ml), 2mM GRGDS peptide (Sigma), 10  $\mu$ g/ml heparin (Sigma), 50 $\mu$ g/ml wheat germ agglutinin (Sigma),  $\alpha$ (2-3) neuraminidase (New England Biolabs, Beverly, USA) alone, or combinations thereof, respectively, in Opti-MEM supplemented with 2%FBS. Incubation with competing substances was done for 1h on ice prior to vector addition. Cells were transduced with Ad5EGFP and Ad19aEGFP (MOI=20) for 1h on ice. Then the cells were washed twice with Opti-MEM and further incubated with 10% FBS-containing growth medium for 48 hours at 37°C until the transgene expression was quantified.

Virus internalization-competition assay: Cells were incubated with inhibiting substances for 1h on ice as described above, and transduced with virus (MOI=20) for 1h at 37°C. Then the cells were washed twice with Opti-MEM and further incubated with 10% FBS-containing growth medium for 48 hours at 37°C until the transgene expression was quantified.

#### *2.4.4 Quantification of transgene expression*

Transgene expression in cells transduced with EGFP-expressing vectors (Ad5EGFP, Ad19aEGFP) was evaluated using a fluorescence multi-well plate reader (Perseptive Biosystems, Framingham, USA). Fluorescence was stimulated by excitation of EGFP at

488nm and emitted fluorescence measured at 508nm. Transgene expression of cells transduced with vectors expressing  $\beta$ -galactosidase (Ad5 $\beta$ Gal, AdFZ33 $\beta$ Gal) was evaluated by luminometric quantitation of  $\beta$ -galactosidase activity. For luminometric quantitation of  $\beta$ -galactosidase activity equal amounts of protein were incubated with Galacto-Star reagent (PE Biosystems, Weiterstadt, Germany) according to the manufacturer's instructions and light emission measured in a Berthold plate luminometer (Berthold, Bad Wildbad, Germany). Total amount of cell protein was determined with micro BCA protein assay (Pierce, Rockford, USA).

#### 2.4.5 Flow cytometry (FACS)

For CD11c surface staining of monocyte-derived dendritic cells  $5 \times 10^5$  cells were labeled with PE-conjugated primary anti-CD11c antibody (50 $\mu$ g/ml) (DakoCytomation, Glostrup, Denmark) for 30min at RT in 500 $\mu$ l FACS buffer (PBS containing 1%FBS). Cells were washed 3 times with PBS and fixed with PBS containing 1% paraformaldehyde (PFA) for 30 min at RT. Next, cells were washed once with PBS and resuspended in 500 $\mu$ l FACS buffer supplemented with 0,01% NaN<sub>3</sub> for analysis on a FACScan (Becton Dickinson Bioscience, Heidelberg, Germany). A total of 10000 cells per experiment were analyzed.

#### 2.4.6 Confocal laser immunofluorescence and immunofluorescent staining of human muscle cells

The protocol for detection of surface NCAM expression on fetal human myoblast-derived myotubes by immunofluorescence was adapted from Walsh *et al.*<sup>228</sup>. Human myoblasts and myotubes were grown on laminin-1 coated glass cover slips and incubated with 5.1H11 hybridoma supernatant diluted 1:100 in PBS for 45min at RT. Cells were washed thoroughly with PBS and incubated with Cy3-conjugated sheep-anti mouse secondary antibody (DakoCytomation, Glostrup, Denmark) diluted 1:200 in PBS supplemented with 10% FBS for 45 min at RT. Cells were washed twice with PBS and fixed with 2% PFA/PBS for 5 min at RT. For confocal laser microscopy of virus-infected cells CHO $\alpha_v\beta_3$  cells were cultured on cover slips (Menzel Gläser, Braunschweig, Germany). Internalization of Ad5 vector into CHO $\alpha_v\beta_3$  cells was analysed at 2 time points (15min and 45 min). Ad5 $\beta$ Gal vector (MOI=1000) was added to CHO $\alpha_v\beta_3$  cells for 1h on ice. Internalization was induced by incubating the cells at 37°C for the indicated times followed by immediate fixation with 2%

PFA/PBS for 20 min on ice. For staining, coverslips were blocked for 1h at RT with 10%FBS/PBS and co-stained with anti-hexon antiserum and anti- $\beta_3$  integrin mAb Ab-15 (both 50 $\mu$ g/ml) diluted in PBS containing 0.2% Triton X-100 (Sigma). TRITC-conjugated rat anti-goat and fluorescein isothiocyanate (FITC)-conjugated rabbit anti-mouse secondary antibodies (50 $\mu$ g/ml) were used as secondary antibodies (DakoCytomation, Glostrup, Denmark). Immunofluorescence analysis was performed on a Leica confocal laser microscope with TCS software program.

#### 2.4.7 Visualization of transgene expression (*X-Gal*) and fluorescence microscopy

$\beta$ -galactosidase expression in transduced cells was visualized by means of X-Gal staining according to a standard protocol<sup>229</sup>. Pictures of fluorescent cells were recorded with AxioCam HRC (Zeiss, Jena, Germany) on a Leica DMRBE epifluorescence microscope and analyzed with AxioVision 3.1 software (Zeiss, Jena, Germany).

## 2.5 Expression and purification of viral proteins

### 2.5.1 Cloning, expression and purification of recombinant fiber proteins in *E. coli*

The bacterial expression plasmid pTrcK19a was generated by PCR-amplification of the fiber gene region encoding knob domain amino acids (aa) 187 to 365 by use of forward and reverse primers containing non-hybridizing *EcoRI* and *BamHI* restriction site sequences, respectively. The PCR product was purified, cut with *EcoRI* and *BamHI*, and ligated to *EcoRI/BamHI*-cleaved pTrcHisB (Invitrogen Life Technologies, Karlsruhe, Germany). Primer sequences for Ad19a knob PCR are: Knob19aF (5'ATATGGATCCAGTAAGAGCAAGAGAAGG3'), and Fiber19aR (5'TTATGAATTCTGGTCTTTCATTCTTGGGC3'). The bacterial expression plasmid pTrcK5 was generated by PCR-amplification of the fiber gene region encoding knob domain amino acids (aa) 387 to 581 by use of forward and reverse primers containing non-hybridizing *EcoRI* and *BclI* restriction site sequences, respectively. The PCR product was purified, cut with *EcoRI* and *PstI*, and ligated to *EcoRI/BclI*-cleaved pTrcHisB (Invitrogen Life Technologies, Karlsruhe, Germany). Primer sequences for Ad5 knob PCR are: Knob5F (5'CAATGATCATGGCCTAGAATTTGAT3'), and Knob5R (5'ATAGAATTCCTATTCTTGGGCAATGTATG3'). The Ad19a fiber transfer plasmid pTrcFib19a was generated by cloning the *EcoRI/BamHI* restricted PCR-fragment encoding Ad19a fiber into *EcoRI* and *BamHI* sites of the bacterial expression vector pTrcHisB (Invitrogen Life Technologies,

Karlsruhe, Germany). Amplification by PCR of the Ad19a fiber gene was done using Ad19a fiber-specific primers containing non-hybridizing *EcoRI* and *BamHI* restriction sites. Primer used for Ad19a fiber PCR are: Fiber19aF (5' ATATGGATCCAATGTCAAAGAG GCTCCG3'), and Fiber19aR (see above). For recombinant expression of knob proteins *E.coli* strain BL21 (Stratagene, La Jolla, CA, USA) was transformed with plasmids pTrcK5 and pTrcK19a, respectively, and protein expression induced with 0.1mM isopropyl- $\beta$ -D-thiogalactopyranoside (Sigma, Deisenhofen, Germany). Knob proteins were affinity-purified with Ni-NTA Agarose (Qiagen, Hilden, Germany) according to standard protocols.

### 2.5.2 Cloning, expression and purification of fiber proteins in Sf9 cells

The baculovirus transfer plasmid pFB-Knob was generated by PCR-amplification of the fiber gene region encoding knob domain amino acids (aa) 387 to 581 by use of forward and reverse primers containing non-hybridizing *EcoRI* and *PstI* restriction site sequences, respectively, and adding a 6xHis-tag encoding sequence to the 5'-end. The PCR product was purified, cut with *EcoRI* and *PstI*, and ligated to *EcoRI/PstI*-cleaved pFastBac1 (Invitrogen Life Technologies, Karlsruhe, Germany). The plasmid pFB-KnobZ33 was constructed in the same way, using pVB45 as a template for PCR. The transfer plasmid pFB-CAR was obtained by PCR-amplification of the extracellular CAR region encoding aa 1-236 with primers containing *BamHI* and *XbaI* restriction site sequences. After cloning into *BamHI/XbaI*-cut pFastBac1, oligonucleotides encoding a Flag-tag and a subsequent stop codon were annealed and inserted into the *XbaI* site.

The transfer plasmids pFB-Knob, pFB-KnobZ33 and pFB-CAR were used to rescue recombinant baculoviruses according to the Bac-to-Bac-protocol (Invitrogen Life Technologies, Karlsruhe, Germany). Cell culture medium supernatants from transfected insect cells were harvested and recombinant baculoviruses propagated by two rounds of amplification. For expression of Knob protein and KnobZ33 protein, respectively, baculovirus-infected Sf9 cells were harvested 72 hours p.i., washed with phosphate-buffered saline, and resuspended in 5 ml dounce buffer (10 mM sodium phosphate buffer pH 8.0, 10 mM NaCl, 1.5 mM MgCl<sub>2</sub>) per  $1.8 \times 10^8$  cells. After incubation on ice for 10 min, cells were lysed by 50 strokes in a tight-pistill glass/teflon homogenizer. The lysate was cleared by centrifugation at 5000 x g for 15 min and adjusted to equilibration buffer (50 mM sodium phosphate buffer, 300 mM NaCl, 10 mM Imidazole). His-tagged recombinant proteins were purified from the lysate in a batch procedure by incubation with Ni-NTA agarose beads

(Qiagen, Hilden, Germany) for 2 hours at 8°C. After washing the beads three times for 10min with equilibration medium the protein was eluted in one bead volume of elution buffer (equilibration buffer with 250 mM Imidazole) and dialysed against phosphate-buffered saline. For expression of soluble CAR (sCAR) protein, Hi-Five cells in serum-free media were infected with the recombinant baculovirus, and the Flag-tagged sCAR protein was purified from the cell culture supernatant by affinity chromatography on anti-Flag agarose (Sigma, Deisenhofen, Germany).

For construction of the baculovirus transfer plasmid pFB-Fiber19a, the 1.2-kb fragment containing the complete fiber open reading frame of Ad19a was cut out of plasmid pTrcFib19a with *Bam*HI and *Eco*RI and inserted into pFastBacHTa (Invitrogen Life Technologies, Karlsruhe, Germany) (*Bam*HI/*Eco*RI). The transfer plasmid pFB-Fiber19a was used to rescue a recombinant baculovirus according to the Bac-to-Bac protocol (Invitrogen Life Technologies, Karlsruhe, Germany). Cell culture medium supernatant from transfected Sf9 insect cells was harvested and recombinant baculovirus propagated with three rounds of amplification. Expression of full-length Ad19a fiber protein carrying a 6xHis tag at the N-terminus in insect cells and purification by Ni-NTA affinity chromatography was performed according to the manufacture's recommendations.

### *2.5.3 Cloning, expression and purification of fiber proteins using recombinant vaccinia virus*

For construction of the vaccinia virus shuttle plasmid pTkgFZ33, a fragment encoding 10.5 fiber shaft repeats and the Z33 knob domain was amplified by PCR from plasmid pVB44 using the primers 10.5*Not*IHis<sub>6</sub> (5' ATAGAATTCTGCGGCCGCTTATTAATGATGATGATGATGTTCTTGGGCAATGTATG 3'), and 10.5*Hind*III (5' ATATTAAAGCTTGCCACCATGGACCTAAACACTTTGACC3'). Primer 10.5*Not*IHis<sub>6</sub> contains a non-hybridizing *Not*I restriction site followed by a hexa-His encoding sequence. Purified PCR fragments were cut with *Not*I and *Hind*III and ligated to *Not*I/*Hind*III-digested vaccinia virus expression plasmid pTkg<sup>230</sup>, yielding pTkgFZ33.

### *Generation of pTkgFZ34C vaccinia virus shuttle plasmid*

For construction of the vaccinia virus shuttle plasmid pTkgFZ34C, a nucleotide sequence encoding for Z34C-peptide was inserted into the *Pac*I/*Cla*I digested pTkgFZ33. The nucleotide sequence encoding for Z34C was obtained by ligation of annealed pairs of 5'-

phosphorylated oligonucleotides (A1, A2, B1, and B2) to the *PacI/ClaI*-digested expression plasmid pFZ33. A1 (5'TAAAAGCAAAAGCAAAAGCAAAAGCAAATT CAACATGCAGTGCCAGAGAAGATTCTACGAAGCTCTCCACGACCCTAACCTGAAC GAAGAA3'); A2 (5'CAGAGAAACGCTAAAATCAAAAGCATCAGAGACGACTGCA AAAGCAAAAGCAAAAGCAAAAGCAAAAT3'); B1 (5'GAGAGCTTCGTAGAATCT TCTCTGGCACTGCATGTTGAATTTGCTTTTGCTTTTGCTTTTGCTTTTAAT3'); B2 (5'CGATTTTGCTTTTGCTTTTGCTTTTGCTTTTGCTTTTGCTTTTGCTTTTGATT TTGACGTTTCTCTGTTCTTCGTTTCAGGTTAGGGTTCGTG3').

#### *Generation of recombinant vaccinia virus*

Vaccinia virus transfer plasmids were transfected in CV-1 cells using the calcium phosphate method and recombined with wild-type vaccinia virus (WR strain) *in vivo*. Recombinant vaccinia viruses were selected with mycophenolic acid as previously described<sup>230</sup>. Briefly,  $1 \times 10^6$  confluent CV-1 cells were infected with MOI=5 wild type vaccinia virus and subsequently transfected with vaccinia virus shuttle plasmids. Insertion of the transgene occurs via homologous recombination within the thymidine kinase (TK) gene. The resulting recombinant vaccinia viruses are deficient for thymidine kinase (TK<sup>-</sup>) and carry *E. coli* xanthine-guanine phosphoribosyltransferase (XGPR) as second selection marker. Selection of recombinant vaccinia viruses was done with mycophenolic acid (MPA), which inhibits inosinemonophosphate dehydrogenase (IMPDH), an enzyme that is essential for guaninemonophosphate (GMP) biosynthesis. Rescue of recombinant vaccinia viruses carrying the XGPR selection marker was done by addition of xanthine to the MPA-containing selection medium (DMEM supplemented with 2.5% FBS, containing 25 $\mu$ g/ml MPA; 250 $\mu$ g/ml xanthine, and 15 $\mu$ g/ml hypoxanthine). *E. coli* xanthine-guanine phosphoribosyltransferase is able to convert Xanthine into xanthinemonophosphate (XMP), which can be further processed to guaninemonophosphate (GMP). Recombinant viruses were subjected to 3 rounds of plaque-purification. Selected recombinant vaccinia viruses were amplified in CV-1 cells. Recombinant viral stocks were generated by infection of  $1 \times 10^8$  CV-1 cells with recombinant vaccinia virus (MOI=1). Cells showing complete CPE were harvested, resuspended in 5ml PBS, and subjected to 3 rounds of freeze/thawing. Virus stocks were stored at  $-80^\circ\text{C}$  until use. Contamination of recombinant vaccinia virus stocks was excluded by means of a sensitive PCR-based detection method. Briefly, genomic DNA from virus-infected CV-1 cells was isolated using the genomic DNA preparation blood kit (Qiagen,

Hilden, Germany). Contaminating wild type vaccinia virus was detected by amplification of a 619bp long fragment from the thymidine kinase gene spanning the integration site. The primers used for amplification are the following: TKFor (5' ATCCTCGTCGCAATATCGC 3') and TkRev (5' ATTATGAGTCGATGTAAC 3'). Amplification protocol was 94°C, 3min; 27x [94°C, 30s; 55°C, 1min; 72°C, 90s]; 72°C, 7min; hold 4°C.

#### *2.5.4 Detection of trimeric fiber proteins in vaccinia virus-infected cells by means of semi-native polyacrylamid gel electrophoresis*

CV-1 cells ( $3 \times 10^7$ ) were infected with recombinant vaccinia virus (MOI=10) expressing FZ33 and FZ34Z proteins, respectively. Cells were harvested after 16h and lysates from vaccinia-infected CV-1 cells prepared as previously described<sup>231</sup>. Proteins were separated on a 7.5% SDS-PAA gel. Western blot analysis: Recombinant proteins were incubated in sample buffer, boiled for 5 min, and subjected to 10% sodium dodecylsulphate-polyacrylamide gel electrophoresis (SDS-PAGE)<sup>232</sup>. For semi-native electrophoresis, protein lysates were not boiled and sample buffer without  $\beta$ -mercaptoethanol used. Proteins were separated on a 7.5% SDS-PAGE gel and subsequently blotted onto a nitrocellulose membrane. The blots were developed using the trimeric fiber-specific monoclonal antibody 2A6 (1:1,000 in TBST 5% skimmed milk) and a peroxidase-coupled goat anti-mouse secondary antibody diluted 1:5000 in TBST 5% skimmed milk (Jackson ImmunoResearch, Dianova, Hamburg).

## 3. Results

### 3.1 Molecular mechanism of adenovirus serotype 5 for binding and entry into primary human muscle cells.

In order to determine the molecular mechanism which is used by Ad5 to infect muscle cells, experiments aimed to identify receptors involved in virus binding and uptake to myoblasts and differentiated myotubes were undertaken. Virus binding and internalization can be experimentally dissociated from each other at low temperature (0-4°C), where only virus attachment occurs, whereas endocytosis of viral particles takes place at higher temperatures<sup>9,40</sup>.

#### *3.1.1 Attachment of Ad5 to human muscle cells involves more than one receptor*

In order to identify receptors involved in virus attachment to primary human muscle cells (FHMs), cells were treated with substances known to interfere with binding of Ad5 to cellular virus attachment and internalization receptors. Cells were treated either with recombinant Ad5 knob protein, GRGDS peptide, and heparin alone, or combinations thereof. To test the bioactivity of recombinant Ad5 knob protein, the CAR overexpressing rat muscle cell line (L6CAR) was transduced with Ad5 (MOI 50) using competing amounts of *wt*Knob protein and non-CAR binding mutated knob protein (*MUT*Knob) during the infection<sup>174</sup>. Infection of L6CAR cells by adenovirus was efficiently (>90%) inhibited using less than 1µg/ml recombinant Ad5 knob protein, whereas no inhibition occurred with *MUT*Knob even at higher concentrations. Therefore it was concluded that, Ad5 knob protein binds to CAR and infection of L6CAR cells depended almost exclusively on interaction of Ad5 with CAR (Fig.5).

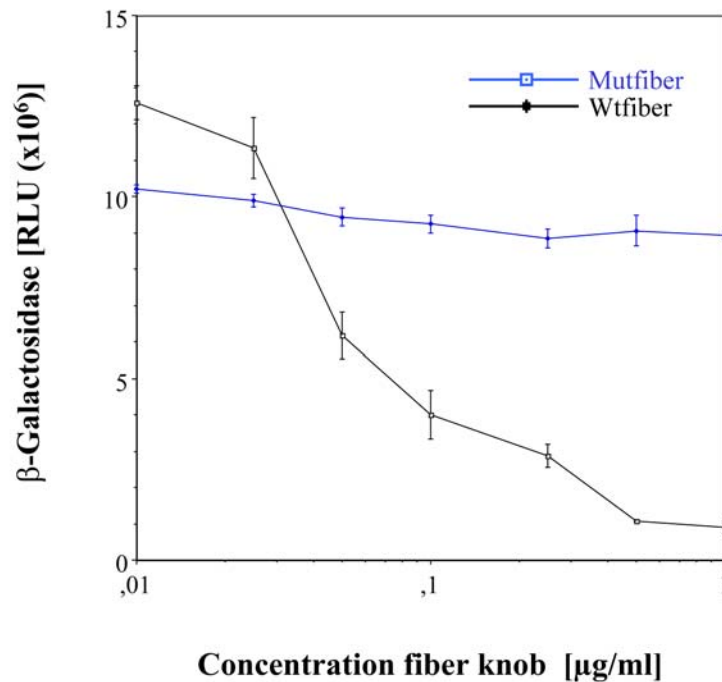


**Fig.5 Introduction of two point mutations into Ad5 fiber knob (K417I+K420I) prevents binding of the Ad5 fiber knob to its cellular receptor CAR.** L6CAR cells were transduced for 2h at 37°C with  $\beta$ -galactosidase expressing adenovirus (Ad5 $\beta$ Gal) in the presence of increasing amounts of wt-Ad5 knob protein (Wtfiber) or mutant Ad5 knob protein (Mutfiber). Addition of 1 $\mu$ g/ml wt knob protein to the infection medium inhibited the transduction of FHM by (>90%), whereas addition of mutated knob protein had no influence on transfection.  $\beta$ -galactosidase activity in relative light units [RLU] was quantified after 48h. Data shown represent the means  $\pm$  SD of three independent experiments.

Interaction of Ad5 with its secondary receptors  $\alpha_v\beta_3$  and  $\alpha_v\beta_5$  can be inhibited with soluble GRGDS peptide<sup>9</sup>, whereas heparin can be used to compete with Ad5 for binding to heparan sulfate glucoseaminoglycans (HSGs)<sup>23,24</sup>. First the optimal working concentrations were determined for each substance. Maximal inhibitory activity for attachment of Ad5 (MOI=10) to FHM occurred at 10 $\mu$ g/ml heparin, 2mM GRGDS peptide, and 10 $\mu$ g/ml knob protein, respectively (data not shown). Incubation of FHM with competing substances partially decreased binding of Ad5 to FHM. Additive effects were observed when heparin was combined with knob protein and virus attachment reduced by  $80 \pm 2\%$  (Fig.6A). In order to investigate Ad5 internalization, cells were preincubated for 1h at 4°C with competing substances and vector added for 1h at 37°C. Preincubation with knob protein led to  $40 \pm 1,6\%$  reduction of transgene expression, pre-incubation with heparin decreased transgene expression by  $39 \pm 4,3\%$ , competition with GRGDS peptide decreased transgene expression by  $25 \pm 2,4\%$ , whereas additive effects were observed when GRGDS was combined with knob protein and heparin, respectively. GRGDS combined with Ad5 knob protein decreased

transgene expression by  $66\pm 5,2\%$ , and GRGDS combined with Heparin reduced expression by  $60\pm 8,3\%$ , respectively (Fig.6B).

Additive inhibitory effects of GRGDS peptide and Ad5 knob, and GRGDS and heparin have only been observed at  $37^{\circ}\text{C}$ , but not at  $4^{\circ}\text{C}$ , a temperature non-permissive for virus internalization. These results are in agreement with the proposed two-step model for Ad5 infection<sup>7,9</sup>, and support recent findings, stating a role for heparansulfate glucosaminoglycans (HSGs) in Ad5 transduction *in vitro*<sup>23,24</sup>. Myotubes behaved similarly as myoblasts. Binding of Ad5 to myotubes was sensitive to knob protein and heparin, but not to RGD peptide, whereas internalization was sensitive to knob protein and soluble GRGDS peptide (data not shown).

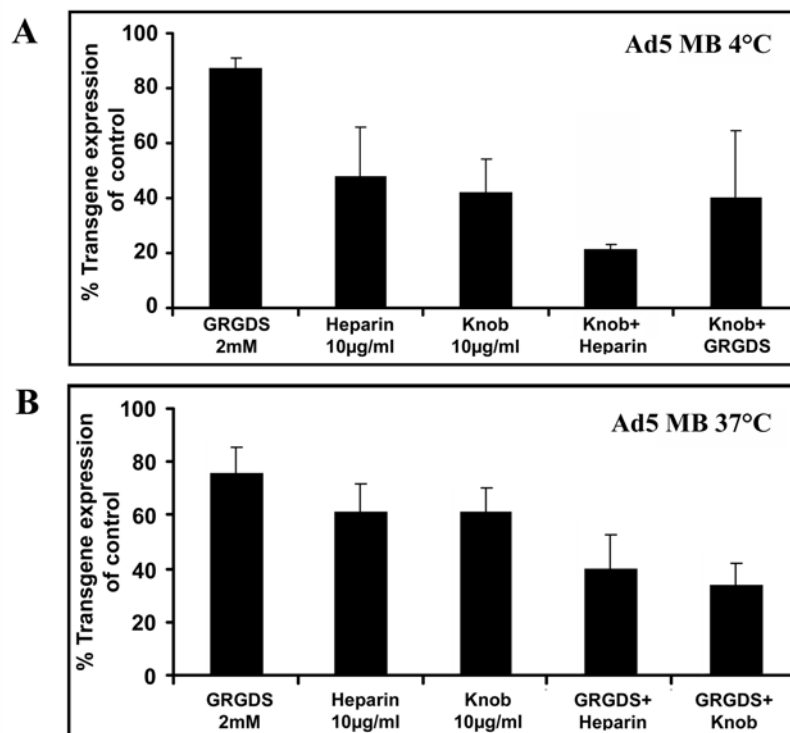


**Fig.6 Attachment and internalization of Ad5 to human primary myoblasts.** Myoblasts (MB) were pretreated for 1h on ice with 2mM GRGDS peptide, 10mM heparin, 10µg/ml recombinant Ad5 knob or combinations thereof, and virus (MOI=10) added for 1h on ice (A). Cells were preincubated with inhibiting substances as indicated for 1h at  $4^{\circ}\text{C}$ , and then virus (MOI=10) added for 1h at  $37^{\circ}\text{C}$  (B). The data represent the mean percentage of transgene expression per 1µg total protein  $\pm$  SD from three independent experiments normalized to FHMs transduced with AdFβGal (control=100%).

## **3.2 Antibody-mediated targeting of an adenoviral vector, modified to contain a synthetic IgG-binding domain in the capsid**

### *3.2.1 Incorporation of the antibody-binding Z33-domain into the Ad5 HI-loop*

Acute adenovirus-mediated vector cytotoxicity is a dose-dependent process leading to loss of transgene expression in transduced cells<sup>233</sup>. Transduction of non-target cells, especially antigen-presenting cells, is known to mediate anti-virus and anti-transgene immune responses. Consequently, the major goals for adenovirus vector development are to simultaneously decrease the vector dose needed for efficient transduction, and second, to increase the specificity of virus infection. Therefore, we decided to design a versatile retargeting system, which would allow us to screen new adenovirus entry receptors, simply by exchanging the monoclonal antibodies bound to Ad vector particles.

A stable variant of the immunoglobulin (Ig)-binding B-domain of the staphylococcal protein A<sup>234</sup>, the so-called Z-domain, is a triple alpha-helical 59-amino-acid peptide that binds to the Fc portion of IgG with high affinity<sup>235,236</sup>. The entire Z-domain or derivatives thereof have been incorporated into capsid proteins of baculovirus<sup>237,238</sup>, sindbis virus<sup>239,240</sup>, and recently into the capsid of adeno-associated virus (AAV2)<sup>241</sup>.

In this work a fiber-modified Ad vector was generated (AdFZ33βGal), displaying a short modified version of the Z-domain (Z33) on its capsid<sup>242, 243</sup>. The HI-loop was chosen as insertion site because it protrudes from the knob structure without contacting other knob residues (Fig.7).

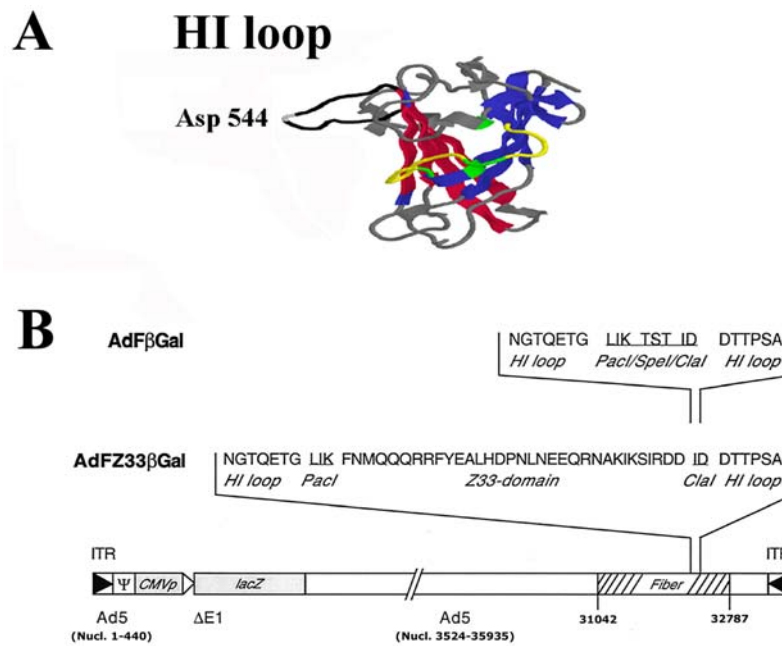


**Fig.7 Insertion of the functional Z33 ligand into the Ad5 HI loop.** The HI loop (black) does not overlap with CAR binding AB loop (yellow) and was chosen as insertion site for the Z33 ligand. In order to insert ligands a cloning site containing *PacI*, *SpeI* and *ClaI* restriction enzyme recognition sites was introduced into the Ad5 HI loop at its most distant site (Asp 544) (A). Genomic organization of the Ad5-based, fiber-modified vector AdFZ33βGal, containing the Z33-peptide inserted into *PacI/ClaI* restriction sites in the HI-loop, and the control vector AdFβGal containing only the *PacI/ClaI* restriction site sequence in the HI-loop. Numbers refer to nucleotide positions in the Ad5 genome (B).

### 3.2.2 Functionality of mutant fiber genes expressed in CV-1 cells

The recombinant fiber molecule containing the Z33-insertion had to retain basic features for functionality: trimerization of the fiber protein, which is essential for proper virus assembly, and Fc-binding activity of the Z33-domain, which would allow for the complexation with targeting antibodies.

These essential activities were first assessed at the molecular level of recombinant proteins and baculoviral and vaccinia expression vectors constructed. Recombinant vaccinia viruses expressing a truncated (10.5 fiber shaft repeats) Ad5 fiber with Z33 (FZ33), and Z34C-modified (FZ34C) HI-loops, respectively, were constructed. FZ34C is based on an improved minimized domain of the immunoglobulin (Ig)-binding B-domain of the staphylococcal protein A, and contains two N- and C-terminal cysteine residues forming a disulfide bond, conferring supplemental structural stability and higher affinity to IgG<sup>244</sup>.

### *Selection of recombinant vaccinia virus*

The selection of recombinant vaccinia virus is based on the integration of the transgene together with a selection marker gene *E. coli* xanthine-guanine phosphoribosyltransferase (XGPRT) into the thymidine kinase gene of vaccinia virus.

A PCR-based protocol was set up to screen for contaminating wild type vaccinia virus in recombinant stocks. A primer pair flanking the integration site within the thymidine kinase gene (TkFor x TkRev) was chosen to discriminate between recombined and *wt* Vaccinia virus. A small fragment of 619 bp length is amplified from *wt* Vaccinia virus DNA, whereas much larger fragments > 4kb are amplified from recombinant vaccinia virus DNA (Fig.8A). After selection of recombinant vaccinia viruses and infection of CV-1 cells with 10 infectious particles per cell<sup>230</sup>, expression of proteins was analysed by Western blot under semi-native and denaturing conditions (Fig. 8B). Two bands migrating at approximately 130-140kDa were detected under semi-native conditions with the trimer-specific antibody 2A6<sup>245</sup>, corresponding to the trimeric FZ33 and FZ34C fiber mutants, respectively. As expected, under denaturing conditions, the bands disappeared. This result demonstrated that insertion of Z33 and Z34C ligands into the HI loop did not compromise the trimerization of fiber protein, and thus would not interfere with rescue of recombinant adenoviruses.

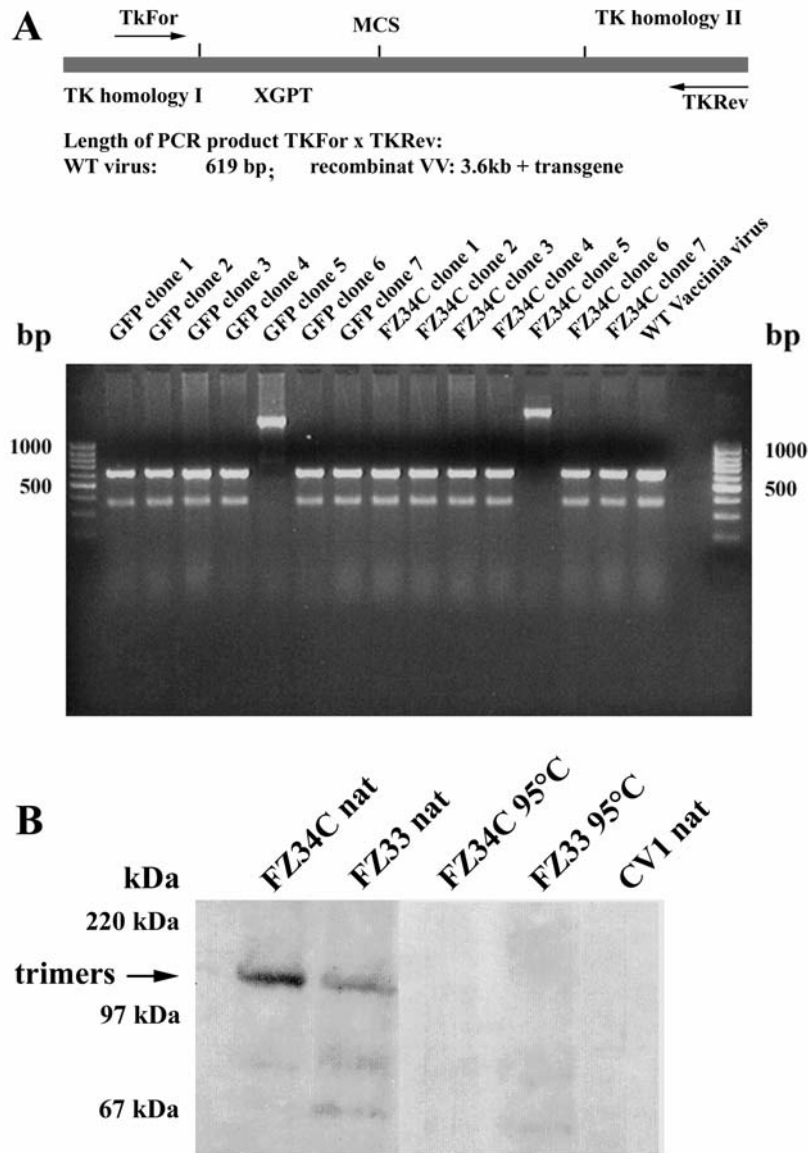


**Fig.8 Generation of recombinant vaccinia virus expressing Z33- and Z34C-modified fiber proteins.** Schematic representation of pTk vector with multiple cloning site (MCS) flanked by thymidine kinase homology regions I and II. The plasmid pTk contains the selection marker gene *E.coli* xanthine-guaninephosphoribosyltransferase (XGPT). PCR-based detection of contaminating wild type vaccinia virus (VacciniaWT) results in the generation of a small 619bp long PCR product, whereas long PCR-products are detected in wild type-free stocks of recombinant vaccinia viruses. PCR products were separated on a 0.8% agarose gel and ethidiumbromide used to visualize the bands under UV light. Large PCR products corresponding to wild-type-free recombinant GFP-expressing vaccinia virus (GFP clone 5), and wild-type-free recombinant FZ34C vaccinia virus stock (FZ34C clone 5), respectively, were amplified (A). Trimerization of fiber proteins FZ33 and FZ34C. Western blot of protein lysates (20µg/lane) from CV-1 cells infected with vaccinia virus expressing fiber mutants under semi-native (FZ33nat and FZ34Cnat) and denaturing conditions (FZ3395°C, and FZ34C95°C). Trimeric fiber proteins were detected using the Ad5 trimeric fiber-specific monoclonal antibody 2A6. The trimeric FZ33 and FZ34C bands disappeared after heat-denaturation of the lysate (95°C) (FZ3395°C and FZ34C95°C). Lysate from CV1 cells infected with GFP-expressing vaccinia virus was used as a negative control (CV-1 nat) and analysed under semi-native conditions (B).

### 3.2.3 The Fc-binding Z33-domain retains its antibody-binding activity within the Ad5 fiber HI-loop

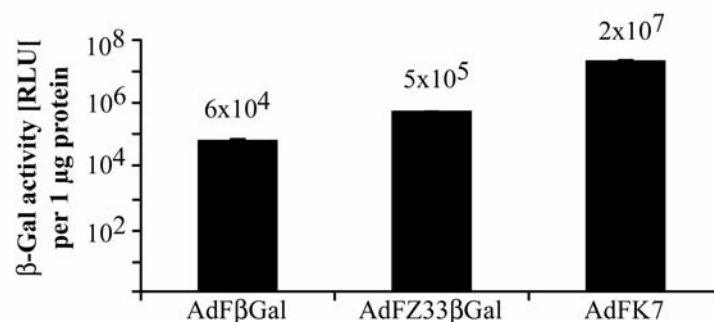
The Fc-binding activity of knobZ33 was quantitatively assessed by surface plasmon resonance measurements. The data was kindly provided by Dr. Helmut Kewes (ZMMK, University of Cologne, Germany). The mouse monoclonal antibody (MAb) against human epidermal growth factor receptor (EGFR; MAb LA22) was immobilized on the surface of a BIAcore CM5 sensor chip and recombinant Knob and KnobZ33 protein were tested as analytes for binding, respectively. Binding constants calculated from primary data using a simple 1:1 model for interaction led to an average dissociation constant ( $K_D$ ) of 2.4 nM (Table 2), which was consistent with the  $K_D$  calculated from the equilibrium data using a Scatchard plot ( $K_D = 5.7$  nM). Expectedly, the wild-type knob protein did not bind to anti-EGFR MAb even at higher concentrations (25 and 307 nM). To further investigate whether the interaction with CAR, another function of the fiber knob domain, was affected by incorporation of the Z33-domain, we coupled Knob and KnobZ33 protein, respectively, on the surface of sensor chips and tested for binding of a purified recombinant soluble CAR (sCAR) protein. When various concentrations of sCAR (9 to 244 nM) were injected over a surface containing 1050 RU of immobilized KnobZ33 and 1180 RU of Knob (not shown), respectively, both KnobZ33 as well as wild-type Knob protein bound to sCAR protein with comparable affinity ( $K_D(\text{KnobZ33}) = 494$  nM;  $K_D(\text{Knob}) = 409$  nM). Thus, insertion of the Z33-peptide into the knob domain obviously had no influence on its binding to CAR. The affinity data are summarized in table 2.

Table 2

Ligand	Analyte	$k_a$ (1/MS)	$k_d$ (1/s)	Kd (nM)
Anti-EGFR MAb LA22	KnobZ33	7.5 X 10e5	1,8 X 10e-3	2.4
Anti-EGFR MAb LA22	Knob	No binding	No binding	No binding
Anti-EGFR MAb LA22	protein A	1.9 X 10e6	3.7 X 10e-3	2.0
KnobZ33	sCAR	1.1 X 10e5	5.3 X 10e-2	494
Knob	sCAR	1.6 X10e5	6.6 X10e-2	409

### 3.2.4 Rescue and functional analysis of AdFZ33βGal

Based on a helper virus plasmid for generation of fiber knob HI-loop-modified high-capacity Ad vectors<sup>292</sup> an infectious first-generation Ad vector plasmid (pAdFβGal) was constructed to contain a LacZ reporter gene under control of a CMV promoter in the deleted E1 region. In addition, pAdFβGal carries unique *PacI* and *ClaI* restriction sites at nucleotide position 32,670 of the Ad5 genome for insertion of peptide ligands into the HI-loop of the knob domain. The infectious adenovirus plasmid pAdFZ33βGal was obtained after insertion of a Z33-domain encoding sequence via annealed oligonucleotides into the *PacI/ClaI* restriction sites of pAdFβGal. Both constructs were released from the plasmid backbone by *SwaI* digestion. Following transfection into N52.E6 producer cells<sup>246</sup> the Ad vectors AdFβGal (control vector) and AdFZ33βGal (Z33-modified) were rescued (Fig.7B). The infectious titers of the CsCl gradient-purified Ad vectors were comparable (AdFβGal:  $4 \times 10^8$  BFU/ml, AdFZ33βGal:  $5 \times 10^8$  BFU/ml). To assess the functionality of AdFZ33βgal, we compared its ability to mediate gene transfer to FHM and compared it to AdFβGal and AdFK7. AdFK7 is a heparansulfate-retargeted adenovirus that was modified to carry 7 lysine residues in the HI loop<sup>184</sup>. AdFZ33βgal transduced primary human myoblasts 8-fold better than the unmodified vector AdFβGal. The poly-lysine retargeted vector AdFK7 transduced FHM 330-fold better than AdFZ33βGal (Fig.9).



**Fig.9 Transfection of FHM with retargeted adenovirus vectors.** Comparison of gene transfer efficiency to FHM cells with Z33-modified adenovirus (AdFZ33βgal), poly-lysine K7-modified (AdFK7) vector, and unmodified control vector (AdFβGal). FHM cells were transduced with 10 BFU (blue forming units) per cell and β-galactosidase activity determined after 48h. β-Galactosidase activity was determined with Galactolight® assay and expressed as relative light units [RLU] per 1μg protein. Values represent means ± SD from 3 independent experiments.

Unlike other vectors (*e.g.* AAV), where incorporation of a targeting ligand reduce the biologic activity compared to the unmodified vector<sup>241</sup>, AdFZ33 $\beta$ Gal showed enhanced gene delivery to FHM.

### 3.2.5 Muscle-specific retargeting of AdFZ33 $\beta$ Gal to NCAM and $\alpha_7\beta_1$ integrin

The development of muscle-specific gene transfer vectors is highly desirable for gene therapy. Only few muscle-specific receptors are known to be sufficiently expressed on dystrophic muscles and accessible to retargeted adenovirus. The capacity of AdFZ33 $\beta$ Gal to transduce primary human myoblast when retargeted to muscle-specific candidate receptors like neuronal cell adhesion molecule (NCAM) and  $\alpha_7\beta_1$  integrin was explored.

Since we believe, that the low expression of primary attachment and secondary internalization receptors on mature muscle fibers is responsible for the inefficient transduction of skeletal muscle, two abundant muscle specific cell surface antigens were selected for retargeting of AdFZ33 $\beta$ Gal to skeletal muscle cells: integrin  $\alpha_7\beta_1$ , a laminin receptor that is almost exclusively expressed on myoblasts and myofibers and overexpressed in dystrophic muscles<sup>247,285</sup>, and neural cell adhesion molecule (NCAM), which mediates intercellular contacts and is expressed in activated satellite cells and myogenic precursor cells during regeneration<sup>248,249,289</sup>.

In an initial experiment, we tested several anti-NCAM antibodies for their ability retargeted AdFZ33 $\beta$ Gal. Two hybridoma-derived and one polyclonal anti-NCAM antibody were used for vector retargeting (anti-human NCAM MAb clone UJ13A, anti-human NCAM MAb clone 5.1H11 and polyclonal anti-human NCAM (C20)). When crude, antibody preparations were used to retarget AdFZ33 $\beta$ Gal, the transduction efficiency was only moderately enhanced for all antibodies tested (Fig.10A).

Since hybridoma supernatant was directly used, the antibody concentration might have been low, and furthermore, serum IgGs might have competed for antibody-binding sites on AdFZ33 $\beta$ Gal. Therefore, we decided to adapt the hybridoma cells to serum free growth conditions and purified the antibody from supernatant by means of protein G affinity chromatography. Antibody produced by this method was >90% pure, as estimated on a silver stained gel after SDS-PAGE (Fig.10B).

Subsequently the pure NCAM-specific MAb 5.1H11 was used to redirect AdFZ33 $\beta$ Gal to FHM. Whereas preincubation of the vector with MAb concentrations of 0.5 and 1  $\mu$ g/ml had no significant effect on transduction efficiency, concentrations of 5  $\mu$ g/ml

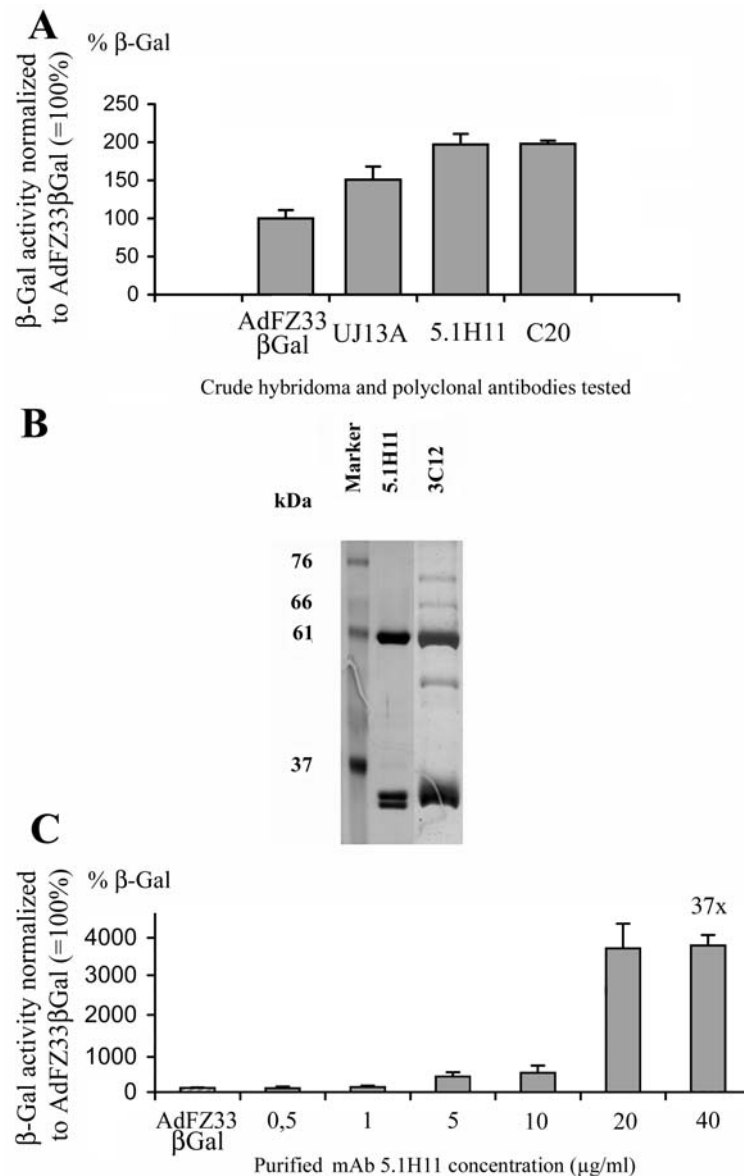


**Fig.10 Retargeting AdFZ33 $\beta$ Gal to NCAM.** Moderate enhancement of gene transfer efficiency to FHM was achieved upon retargeting AdFZ33 $\beta$ Gal to NCAM using crude hybridoma supernatants UJ13A and 5.1H11, and commercially available polyclonal anti-NCAM antiserum C20 (A). The monoclonal antibodies anti-NCAM, clone 5.1H11, and anti- $\alpha$ 7 integrin MAb 3C12 were produced under serum free conditions and further affinity-purified with protein G. Aliquots of the purified antibodies were analysed by SDS-PAGE and the protein bands visualized by silver staining. Heavy and light chains of the purified antibodies were detected (B). Concentration-dependent increase of gene transfer efficiency using purified 5.1H11 anti-NCAM antibody. FHMs were transduced with 10 BFU/cell AdFZ33 $\beta$ Gal retargeted with 5.1H11 and  $\beta$ -Gal activity determined after 48h.  $\beta$ -Gal activity was determined with Galactolight® assay as relative light units [RLU] per 1 $\mu$ g protein. Values were normalized to non-retargeted AdFZ33 $\beta$ Gal (=100%), and represent means  $\pm$  SD from 3 independent experiments (C).

and higher improved reporter gene transfer in a dose-dependent manner (Fig.10C). Transgene expression levels were assessed with a luminometric  $\beta$ -galactosidase assay 48h post-transduction. Transgene expression was enhanced 37-fold when the vector was pretreated with 40  $\mu$ g/ml MAb 5.1H11 (Fig.10C). As expected, no targeting effect was obtained when AdF $\beta$ Gal was pretreated with Mabs (data not shown).

Next, the ability of NCAM- and  $\alpha_7$  integrin-retargeted AdFZ33 $\beta$ Gal to increase the gene transfer to primary fetal human myoblasts (FHM) was compared (Fig.11). AdFZ33 $\beta$ Gal was preincubated with increasing concentrations of MAb 3C12, 5.1H11, or control antibody directed against p53. A 24-fold increase of  $\beta$ -galactosidase expression was observed after preincubation of AdFZ33 $\beta$ Gal with 40 $\mu$ g/ml 3C12, whereas NCAM-retargeted viruses proved superior, with 37-fold increased  $\beta$ -Gal activity at the same concentration (Fig.11A). In contrast, incubation of AdFZ33 $\beta$ Gal with anti-p53 control antibody did only minimally (2.5-fold increase at 40 $\mu$ g/ml MAb anti-p53) increase the gene transfer efficiency (Fig.11A). In agreement with the quantitative data X-Gal staining of FHMs transduced with NCAM- and integrin  $\alpha_7$ - retargeted vector demonstrated a dose-dependent increase of  $\beta$ -Gal positive cells with antibody-retargeted viruses (Fig. 11B).

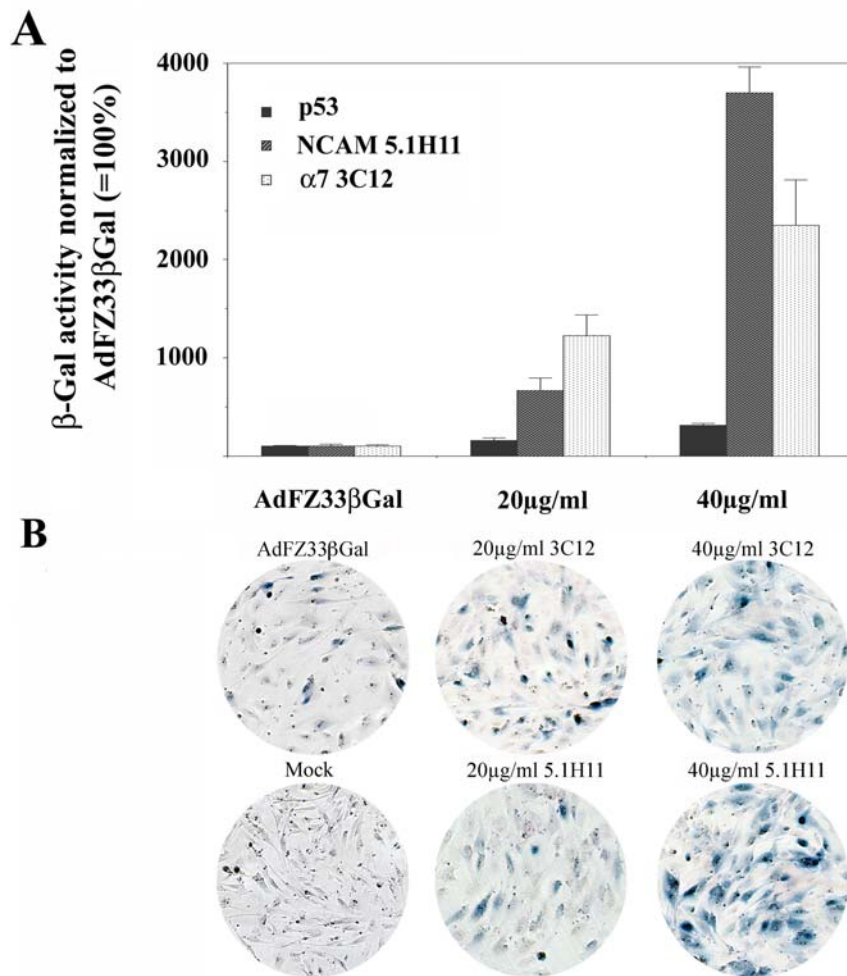


**Fig.11 Transduction of FHM with NCAM and  $\alpha_7$  integrin retargeted AdFZ33 $\beta$ Gal.** Cells were transduced with AdFZ33 $\beta$ Gal vector (MOI=10) preincubated with increasing concentrations of anti-integrin  $\alpha_7$  MAb 3C12, anti-NCAM MAb 5.1H11, and anti-p53 antibody (control), respectively.  $\beta$ -Galactosidase activity was determined as relative light units (RLU) per 1  $\mu$ g protein and normalized to FHMs transduced with AdFZ33 $\beta$ Gal alone (AdFZ33 $\beta$ Gal=100%). Each value represents the means of three independent infections  $\pm$  SD (A). X-Gal staining of transduced FHM cells. Cells were mock-transduced (mock), transduced with AdFZ33 $\beta$ Gal alone (AdFZ33 $\beta$ Gal), and transduced with retargeted AdFZ33 $\beta$ Gal against integrin  $\alpha_7$  (MAb 3C12) or NCAM (MAb 5.1H11). For retargeting, AdFZ33 $\beta$ Gal was preincubated with 20, and 40  $\mu$ g/ml of the corresponding MABs, respectively.  $\beta$ -Galactosidase expression was visualized with chromogenic X-Gal reagent after 48 hours (B).

Myotubes differentiated in cell culture are even less susceptible to infection by subgroup C adenoviruses than are myoblasts. Myotubes express higher amounts of NCAM and have a rudimentary extracellular matrix that more closely resembles the situation *in vivo* (Fig.12A). The ability of NCAM- and  $\alpha_7$  integrin- retargeted AdFZ33 $\beta$ Gal to increase the gene transfer efficiency to human myotubes was tested. Expression of  $\beta$ -galactosidase in myotubes with

retargeted AdFZ33 $\beta$ Gal (40  $\mu$ g/ml 3C12 or 5.1H11) was 68-fold and 77-fold higher, respectively, than with untreated vector (Fig.12B).

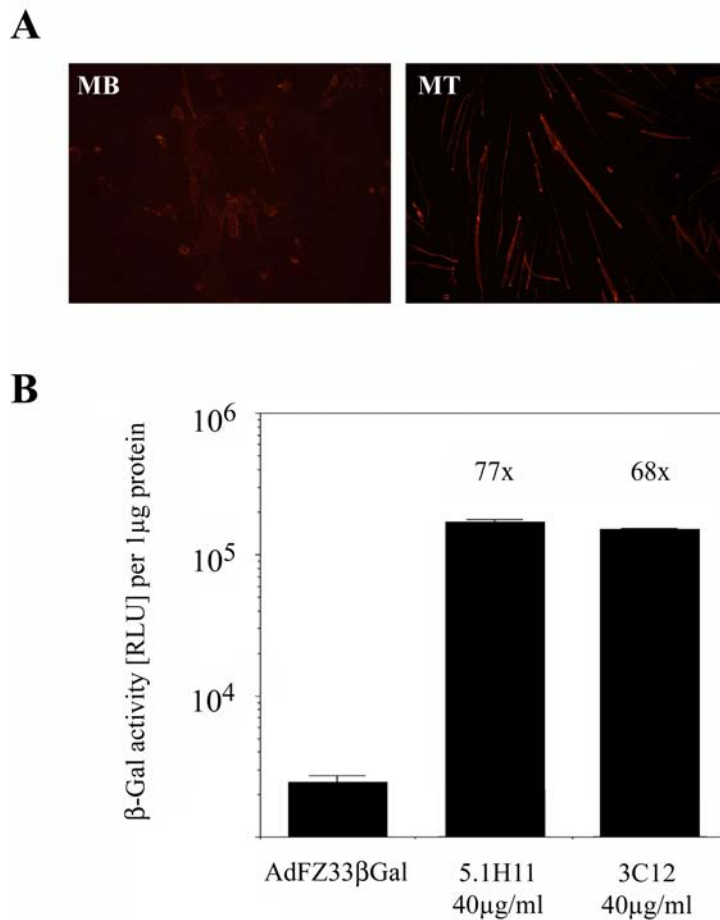


**Fig.12 Transduction of human myotubes with NCAM- and  $\alpha_7$  integrin retargeted AdFZ33 $\beta$ Gal.** NCAM expression on primary human myoblasts and myotubes was visualized by immunofluorescence with anti-NCAM MAb 5.1H11 (A). Antibody-mediated transduction of human myotubes. Differentiated, multinucleated myotubes were transduced with AdFZ33 $\beta$ Gal (MOI=10), and with retargeted AdFZ33 $\beta$ Gal, using 40  $\mu$ g/ml anti-integrin  $\alpha_7$  MAb 3C12, and anti-NCAM MAb 5.1H11, respectively.  $\beta$ -Galactosidase activity was determined as relative light units (RLU) per  $1\mu$ g total cellular protein. Each value represents the means of three parallel infections  $\pm$  SD (B).

These result demonstrates that retargeting of AdFZ33 $\beta$ Gal to integrin  $\alpha_7$ - and NCAM surface proteins can be efficiently used to enhance transduction of differentiated human skeletal muscle cells.

### *Targeting mouse C2C12 cells.*

Since the *mdx* mouse is an extensively used animal model for DMD, retargeting of AdFZ33 $\beta$ Gal to murine muscle cells was assessed. We used the myogenic C2C12 cell line as model for retargeting of AdFZ33 $\beta$ Gal. AdFZ33 $\beta$ Gal was retargeted to  $\alpha_7$  integrin using 40  $\mu$ g/ml of purified anti-mouse  $\alpha_7$  integrin MAb 6A11. The gene transfer efficiency to C2C12 myoblasts was enhanced eight-fold (data not shown). X-Gal staining of C2C12 myoblasts (Fig.13A) and mixed C2C12 myoblast/myotubes (Fig.13C) after infection with integrin  $\alpha_7$ -retargeted virus demonstrated an increase of  $\beta$ -Gal positive cells.

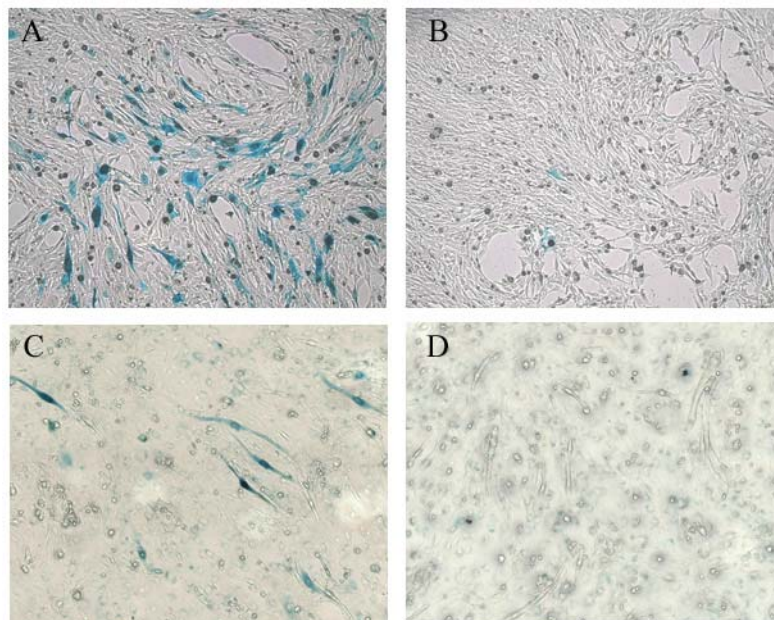


**Fig.13 Retargeting of AdFZ33 $\beta$ Gal to murine integrin  $\alpha_7$ .** C2C12 myoblasts (A+B) and a mixed culture containing both, myoblasts and myotubes (C+D) were transduced with MOI10 of AdFZ33 $\beta$ Gal (B+D), and retargeted AdFZ33 $\beta$ Gal complexed with 40 $\mu$ g/ml anti-mouse integrin  $\alpha_7$  MAb 6A11 (A+C).  $\beta$ -galactosidase activity in cells was visualized with chromogenic X-Gal substrate after 48 hours. Fig. 14C shows a mixed population of C2C12 myotubes and myoblasts with preferentially transduced myotubes (C).

One particularly interesting finding was the selective transduction of C2C12 myotubes in the mixed myoblast/myotubes culture by integrin  $\alpha_7$ -retargeted AdFZ33 $\beta$ Gal. Due to the inhomogeneity of the mixed cell culture,  $\beta$ -galactosidase activity was not quantitatively determined in this case. Moreover, we investigated the ability of retargeted AdFZ33 $\beta$ Gal to a variety of human carcinoma cell lines, including A431, HeLa, and Jurkat cells. A summary of the obtained results is given in table 3.

Table3: Summary of results obtained with retargeted AdFZ33βGal

Cell line	Receptor targeted	Antibody clone	Targeting effect	% transduced (10 BFU /cell)
Lung carcinoma A431	EGFR	LA22*	18 x	20 %
Primary human myoblasts (FHM)	α7 integrin	3C12	24 x	80 %
FHM	NCAM	5.1H11	37 x	85 %
C2C12	α7 integrin	6A11	8 x	ND
HeLa	CD3	HIT3a*	2 x	ND
Jurkat	MHCI	W6/32	no	ND

\*For details and references the reader is referred to Thirion *et al.*<sup>242</sup>.

### 3.2.5 Specificity of antibody-mediated retargeting of AdFZ33βGal

In order to confirm that the MAb-mediated transduction of human myoblasts cells by AdFZ33βGal actually required the specific binding of the MAb to the vector, and occurred via a CAR-independent cell entry pathway, a competitive infection assay was performed. In this experiment AdFZ33βGal was either preincubated with or without anti-NCAM MAb 5.1H11 and the subsequent transduction of myoblasts cells done in the presence of 20 μg/ml recombinant Ad5 knob protein (KnobWT), 10μg/ml mutated (K417I, K420I) knob protein (KnobMUT), or 10μg/ml protein A (Protein A) (Fig.14).

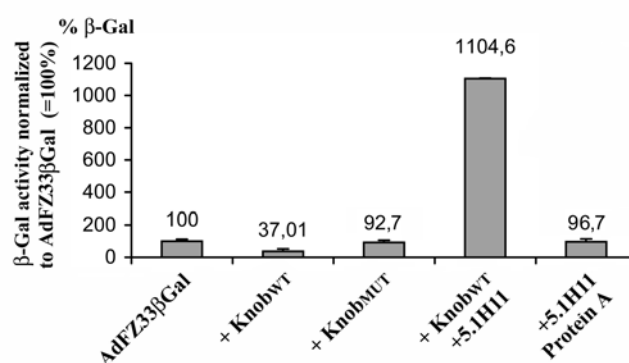


**Fig.14 CAR-independent transduction of primary human myoblasts.** Cells were either preincubated with 10μg/ml Ad5 WT-knob protein (KnobWT) or 10μg/ml Ad5 MUT-knob protein without CAR binding activity (KnobMUT) and transduced with (MOI 10) Z33-modified vector AdFZ33βGal alone (AdFZ33βGal), or with AdFZ33βGal retargeted with anti-NCAM MAb 5.1H11 in the presence of Ad5 knob protein (KnobWT + 5.1H11) and 20μg/ml protein A (5.1H11+Protein A), respectively. β-Galactosidase activity was determined as relative light units (RLU) per 1μg protein and normalized to FHMs transduced with AdFZ33βGal alone (AdFZ33βGal =100%). Each value represents the means of three independent infections ± SD.

KnobWT protein largely reduced the gene transfer efficiency of the non-retargeted vector to FHMs, but did not inhibit the enhanced transduction efficiency of the NCAM-retargeted vector (KnobWT+5.1H11), indicating that infection was largely mediated by a receptor different from CAR. Transduction of antibody-retargeted vector was reduced to the level of non-retargeted vector by competition with 20µg/ml soluble protein A. As expected, KnobMut protein was unable to inhibit transfection by AdFZ33βGal vector (Fig.14).

### **3.3 Enhanced human muscle cell transduction by subgroup D adenovirus Ad19a**

#### *3.3.1 Attachment of Ad19aEGFP to primary human myoblasts (FHM) depends on a sialic acid-containing receptor.*

First, the nature of cellular receptors involved in attachment of Ad19aEGFP vector to primary human myoblasts was investigated. Cells were pre-treated for 1h on ice with competing substances, then the vector was added and allowed to attach to the cells for 1h on ice. Thereafter, unbound virus was aspirated, the cells thoroughly washed, and transduction medium replaced by growth medium. EGFP expression was quantified after 48h by means of fluorescence measurement. Attachment of Ad19aEGFP to FHM was strongly inhibited (>95%) by neuraminidase and wheat germ agglutinin (WGA) (Fig.16A). Wheat germ agglutinin binds specifically to N-acetyl-β-(1,4)-D-glucosamine carbohydrate substrates, which may be a part of the carbohydrate binding epitope recognized by Ad19a. Neuraminidase and WGA did not affect attachment of Ad5 to FHM (data not shown). Binding of Ad19aEGFP was neither affected by heparin nor GRGDS. Recombinant Ad19a knob protein expressed in *E. coli*, did not affect binding of Ad19aEGFP to FHM at concentrations below 10µg/ml, but inhibited attachment of Ad19aEGFP >80% at higher protein concentrations (100µg/ml).

To rule out any non-functionality of Ad19a knob protein expressed in *E. coli*, Ad19a knob protein was tested for its ability to trimerize under non-denaturing conditions (Fig.15A). Recombinant Ad19a knob protein was separated on a 10% polyacrylamide gel under denaturing (K19a den) and semi-native conditions (K19a nat). Proteins were visualized by silver staining. Interestingly, Ad19a knob protein, which contained 1.5 fiber shaft repeats, formed trimers, whereas the corresponding Ad5 knob protein only formed dimers under

similar conditions (data not shown). The purity of Ad19a knob protein preparations was estimated to be >90% (Fig. 15A). To further test the receptor-binding activity of Ad19a fiber protein, N-terminal His<sub>6</sub>-tagged full-length Ad19a fiber protein was expressed with baculovirus in insect cells and affinity-purified on a Ni<sup>2+</sup>-NTA agarose column. Full-length Ad19a fiber proteins were separated on a 10% polyacrylamide gel under denaturing (F19a den) and semi-native conditions (F19a nat) and blotted on a nitrocellulose membrane. Ad19a fiber protein crossreacted with anti-Ad5 knob polyclonal antiserum. Fiber trimers were predominantly detected under semi-native PAGE (Fig.15B).

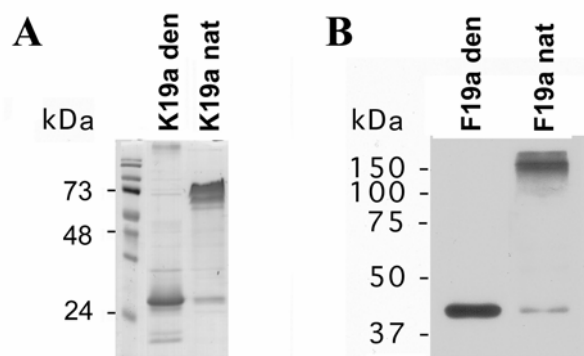


**Fig.15 Purification of recombinant Ad19a knob and Ad19a fiber protein.** N-His<sub>6</sub>-tagged Ad19a knob protein was produced in *E. coli* strain BL21 (Startagene) and affinity-purified with Ni-NTA Agarose (Qiagen) according to standard protocols. Purified proteins were separated on a 10% polyacrylamide gel under semi-native (K19a nat) and denaturing conditions (K19a den). Protein bands were visualized by silver staining<sup>250</sup> (A). Expression of full-length Ad19a fiber protein in insect cells. His<sub>6</sub>-tagged Ad19a fiber protein was purified by means of affinity chromatography. Purified full-length Ad19a fiber protein was separated on a 10% polyacrylamide gel under semi-native (F19a nat) and denaturing conditions (F19a den). Fiber proteins were transferred to a nitrocellulose membrane and detected with anti-Ad5 knob polyclonal antiserum (B).

To test if the receptor-binding activity was located on Ad19a fiber, FHM were preincubation for 1h on ice with 10μg/ml purified Ad19a fiber protein and transduced with Ad19aEGFP (MOI=20). Ad19a full-length fiber protein efficiently decreased virus attachment by 79±2 % at 10μg/ml (Fig. 16A), and was able to block virus attachment completely (97±2 %) at higher concentrations (50μg/ml) (data not shown). This result demonstrates that the Ad19a fiber protein mediates binding to the cellular receptor. Therefore, it may be possible to transfer the receptor-binding activity from Ad19a to the better-characterized Ad5 serotype by swapping the fiber molecules.

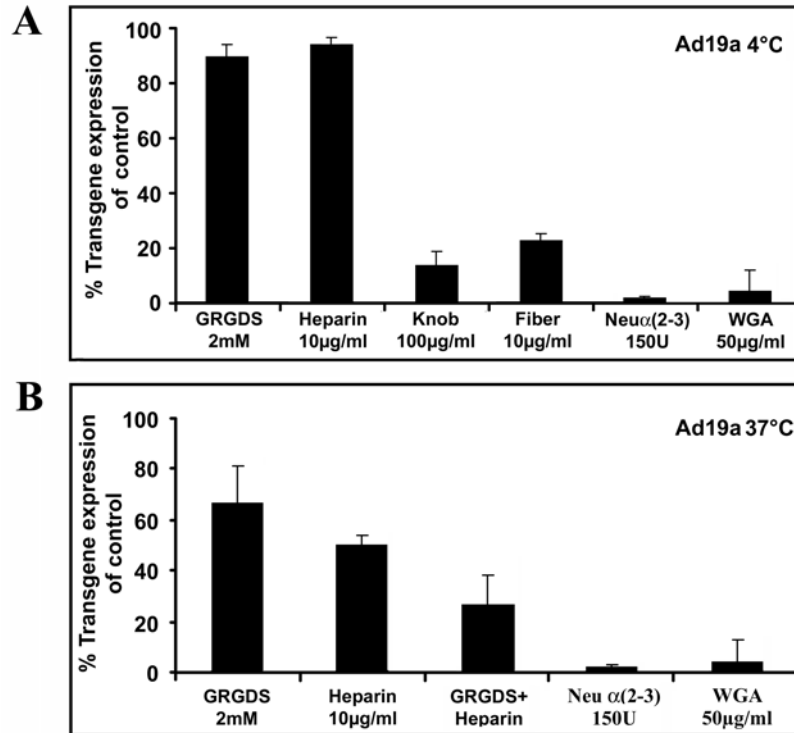


**Fig.16 Receptors involved in attachment and uptake of Ad19aEGFP vector.** Primary human myoblasts were preincubated for 1h on ice with 10µg/ml Ad19a fiber protein, 100µg/ml Ad19a knob protein, 2mM GRGDS peptide, 10 µg/ml heparin, 50µg/ml wheat germ agglutinin, and 150 U /well α(2-3)-specific neuraminidase, respectively, and then transduced with 20 infectious viral particles per cell (20FFU added per cell) at 4°C (Ad19a 4°C), or 37°C (Ad19a 37°C). Transgene expression was quantified at 48 h with a fluorescence multi-well plate reader (A). Virus uptake-competition study: Cells were incubated with inhibiting reagents for 1h on ice and transduced with virus (MOI=20) for 1h at 37°C (B). Transgene expression was quantified at 48 h with a fluorescence multi-well plate reader and normalized to cells transduced with Ad19aEGFP alone (Ad19aEGFP=100%). Each value represents the means of three independent experiments ± SD.

Next, we investigated which factors were involved in virus uptake. FHM were preincubated with competing substances for 1h at 4°C and vector added for 1h at 37°C (Fig.16B). Interestingly, some substances like heparin, which did not interfere with virus binding at 4°C, showed inhibiting activity at 37°C. Preincubation with heparin decreased transgene expression by 50±4.1 %. To clarify the role of α<sub>v</sub> integrins in Ad19a internalization, FHM were transduced with Ad19a in the presence of 2mM GRGDS peptide, resulting in a 34±4,7 % reduction of transgene expression. Transgene expression was reduced by 74±8,9 % when GRGDS was combined with Heparin. In addition, transduction of myoblasts at 37°C still was highly sensitive to WGA and neuraminidase pretreatment (>95% inhibition) (Fig.16B). Binding of Ad19aEGFP to myotubes and myoblasts was very much alike. Transduction of

FHM-derived myotubes with Ad19aEGFP vector was completely abolished upon neuraminidase and WGA treatment (data not shown).

### 3.3.2 Comparing Ad5 and Ad19a for their ability to infect muscle cells

Comparison of two different adenovirus serotypes poses the problem of how to quantify both vectors in a comparable manner. Since the transduction efficiency of one cell type (e.g., 293 cell line, which is commonly used for titration) is likely to differ between the two serotypes, vector genomes were determined by means of quantitative PCR<sup>223,224</sup>. We took advantage of the fact, that both vectors shared identical CMVEGFP expression cassettes replacing the E1 region, and therefore amplified a 96bp amplicon from the EGFP coding region for quantitative PCR as previously described<sup>224,251</sup> (Fig. 17).

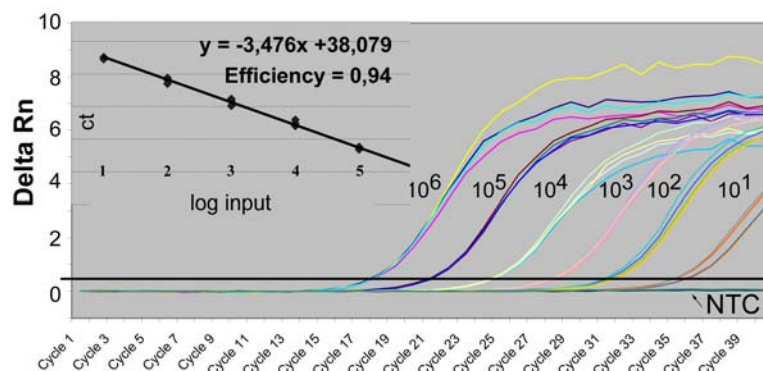


**Fig.17 Efficiency of real time PCR for Ad vector titration.** Serial dilutions of linearized plasmid pEGFP-N1 ( $10^1$  to  $10^6$  copies) were used to obtain a standard calibration curve displaying Ct values vs. copy number. Genomic titers of CsCl-purified virus preparations were determined using real-time fluorescence detection ABI Prism 7000 Sequence Detector and SybrGreen as a double-strand DNA-specific fluorescent dye.

### 3.3.3 Ad19a is a human muscle cell tropic virus.

Myoblasts of different origin, including primary mouse myoblasts, primary fetal pig myoblasts, primary ape myoblasts, primary fetal human myoblasts, and rat L6 myoblasts, were compared for their transducibility by Ad19aEGFP and Ad5EGFP, respectively. Cells were transduced with vector in serum-reduced infection medium over night with 1250, 2500, and 12500 viral genomes per cell (vg/cell), respectively, and EGFP expression quantified after

48h. Cells expressing EGFP (EGFP+) were counted by means of flow cytometry (table 4). Due to the fast proliferation of rat L6 myoblasts no FACS data was collected for this cell line.

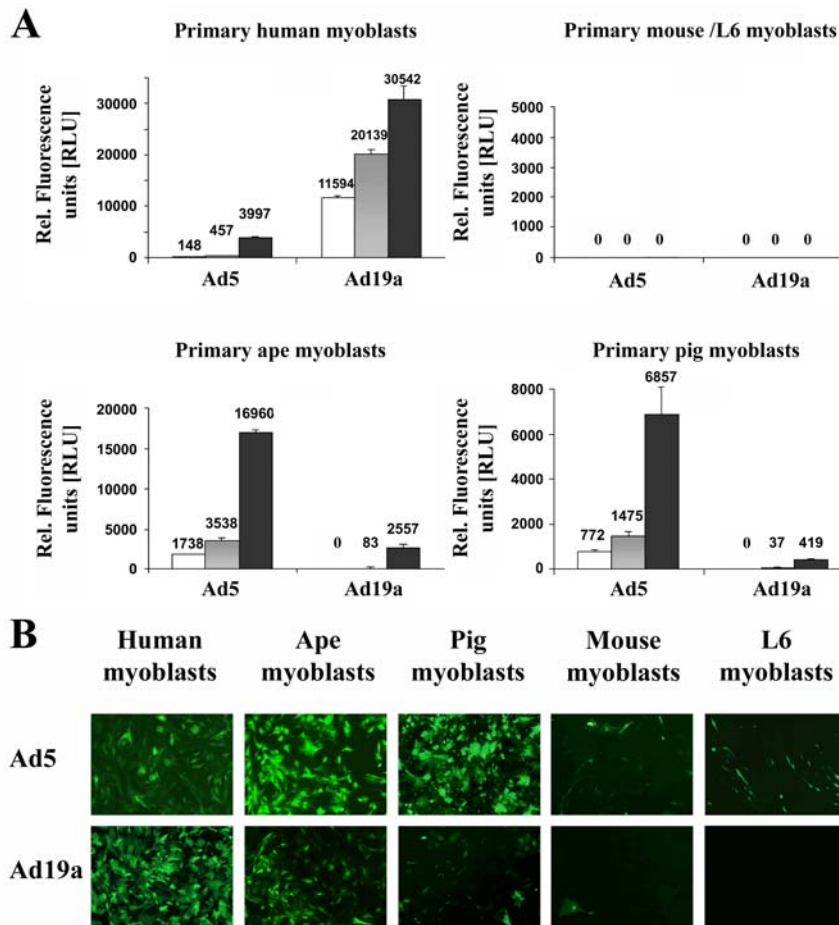
Table4

Transduction efficiency in % of EGFP-expressing cells, as determined by FACS of transduced myoblasts

	Human myoblasts	Ape myoblasts	Pig myoblasts	Mouse myoblasts
Ad5EGFP 1250vg/cell	43.2 %	70.7 %	29.2 %	7.6 %
Ad5EGFP 2500 vg/cell	59.8 %	84.6 %	42.9 %	14 %
Ad5EGFP 12500 vg/cell	88.7 %	99.1 %	86.1 %	39.8 %
Ad19aEGFP 1250 vg/cell	93.4 %	13.5 %	2.5 %	3.5 %
Ad19aEGFP 2500 vg/cell	94 %	23.3 %	4.3 %	2.8 %
Ad19aEGFP 12500 vg/cell	97 %	80 %	17.8 %	5.8 %

The mean percentage of EGFP+ cells from 3 independent transduction experiments are listed.

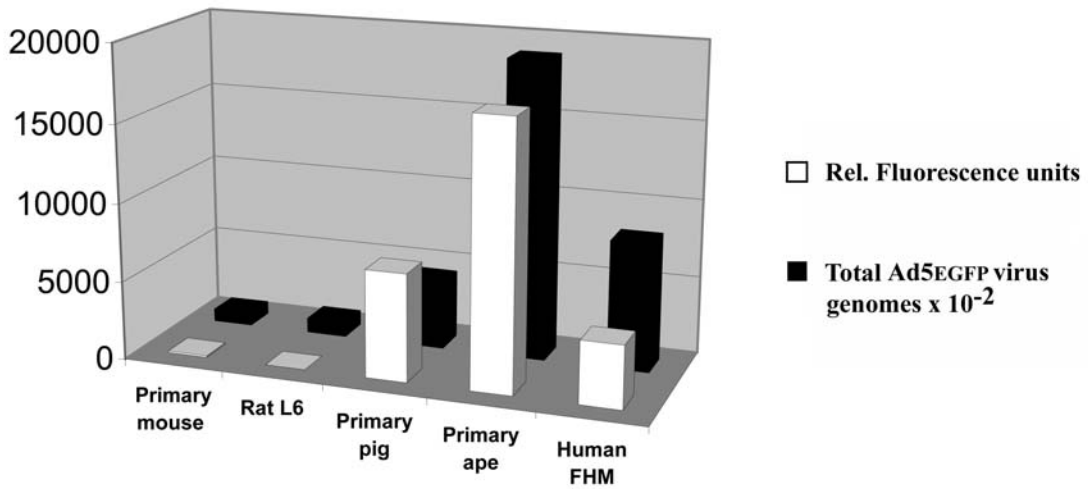
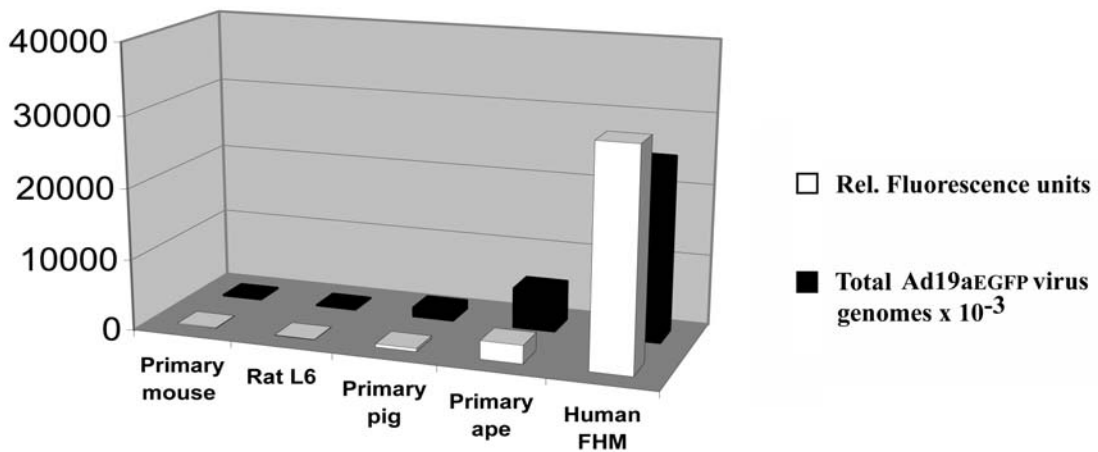
Strikingly, even with the 2 lower Ad19aEGFP titers used, >90% of human myoblasts were EGFP+, and transgene expression was 27 and 30-fold higher if compared to Ad5EGFP, (Fig. 18A). The highest transgene expression of Ad5EGFP-transduced cells was observed in ape myoblasts, followed by, in decreasing order, pig, human, mouse, and L6 myoblasts (Fig.18A). Ad5EGFP transduced ape myoblasts better than Ad19a: 99% of ape myoblasts were EGFP+ cells when transduced with 12500 vg/cell Ad5EGFP, compared to 75 % of EGFP+ ape myoblasts in the case of Ad19aEGFP. Average transgene expression was 6.6-fold higher in Ad5EGFP-transduced ape myoblasts than in Ad19aEGFP-transduced cells (12500 vg/cell). In contrast to ape and human cells, only 39.8 % of primary mouse myoblasts expressed EGFP at the highest vector dose used, and correspondingly, only 5.75 % of mouse myoblasts expressed EGFP+ when transduced with 12500 vg/cell of Ad19aEGFP. Transgene expression in primary mouse myoblasts was too low to be quantified with a fluorescence reader. For all titers used, Ad5EGFP transduced pig myoblasts better than Ad19aEGFP. 86.1 % of pig myoblasts expressed EGFP at the highest Ad5EGFP vector dose used, versus 17.8 % with Ad19aEGFP. Corresponding pictures of fluorescing EGFP-expressing cells transduced with 12500 vg/cell are shown in figure 18B.



**Fig.18 Transduction of myoblasts by Ad5EGFP and Ad19aEGFP.** A panel of myoblasts, including primary human, ape, pig, mouse myoblasts and rat L6 cells, were transduced with 1250 vg/cell (white bars), 2500 vg/cell (gray bars) and 12500 vg/cell (black bars), and EGFP expression quantified at 48h. Each value represents the means of three independent experiments  $\pm$  SD (A). Pictures of fluorescent cells transduced with 12500 vg/cell were recorded 48h post transduction with a Leica DMRBE epifluorescence microscope equipped with AxioCam HRC and analyzed with AxioVision 3.1 software (Zeiss, Jena, Germany). Recording time was generally 5s, except for strongly expressing ape myoblast (Ad5 panel), and human myoblasts (Ad19a panel), where the recording time was limited to 1s (B).

### *3.3.4 Differential muscle cell transduction efficiencies of Ad5EGFP and Ad19aEGFP evaluated by quantitative real time PCR*

In order to find out whether the observed variable gene expression was due to differentially regulated gene expression or due to a more efficient delivery of viral genomes, adenovirus genomes were quantified by real time PCR in transduced cells 48h post transduction (Fig.19). Care was taken to eliminate residual surface-bound viral particles before DNA extraction by applying several washing steps. Adenovirus DNA was isolated as previously described and equal amounts of DNA used in each PCR reaction. The determined genomic EGFP copy number (equivalent to virus genome number) correlated well with transgene expression in cells for both vectors (fig.19 and table 5). It may be concluded, that differences in transgene expression are attributed to differences occurring during virus uptake and intracellular transport. Two additional parameters, addressing the transduction efficiency (% of initially applied viral genomes detected at 48h), and EGFP expression activity (particles required per relative fluorescence unit [RFU]) were considered. Most of the values were in accordance with the expected results, though derivations occurred especially for the highest Ad19aEGFP vector dose used. Those derivations are highlighted in red in table 5. First parameter analyzed: In theory, the percentage of vector genomes detected 48h post transduction reflects the transduction efficiency and should be constant for all titers used, assuming vector binding and uptake under non-saturating conditions. In agreement with low EGFP expression, low amounts of vector genomes were found in primary mouse myoblasts and L6 cells. The amount of detected vector genomes increased proportionally to EGFP expression in pig, ape, and human myoblasts. However, it should be emphasized that very high amounts of initial Ad19aEGFP vector genomes ranging from 3.94% to 6.59% were detected in human myoblasts, whereas only 0.096% to 0.132% of the initial vector genomes could be detected in FHMs transduced with Ad5EGFP. This result reflects the extremely efficient uptake of Ad19aEGFP virus by primary human myoblasts. Two prominent derivations were observed in ape and pig myoblasts transduced with 12500 vg/cell Ad19aEGFP. Here, a disproportionate increase of cell-associated vector genomes was observed, which did not correlate with transgene expression. This disproportionate increase in vector genomes may be attributed to either inefficient downstream events occurring after vector endocytosis (*e.g.* mislocalization of the vector), or to species-dependent differential promoter regulation.

**A****Correlation between Ad5EGFP viral genomes and EGFP expression****B****Correlation between Ad19aEGFP viral genomes and EGFP expression**

**Fig.19 Correlation of intracellular vector genomes and transgene expression.** Myoblasts were transduced with 12500 vg/cell and the total EGFP copy-number per  $5 \times 10^4$  transduced cells determined by real time PCR. A serial dilution of linearized plasmid pEGFP-N1 ( $10^1$  to  $10^6$  copies) was used to obtain a standard calibration curve. The virus genome copy numbers were adjusted by factor  $10^{-2}$  (Ad5EGFP genome copy number), and  $10^{-3}$  (Ad19aEGFP genome copy number), respectively, to fit the relative fluorescence unit scale. Values represent the means of three independent experiments.

Table 5:

Cell line	Virus	Vg/cell	[RFU]	Total vg by real time PCR	% vg detected	Particle/ RFU	Vg/cell*
FHM MB	Ad5	1250	148	59962	0,096	405	1,2
	Ad5	2500	457	131737	0,106	240	2,6
	Ad5	12500	3997	818603	0,132	205	16,4
	Ad19a	1250	11594	4120312	6,59	355	82,4
	Ad19a	2500	20139	5198988	4,16	258	103,9
	Ad19a	12500	30542	24640027	3,94	807	492,8
Ape MB	Ad5	1250	1738	208963	0,330	120	4,2
	Ad5	2500	3538	363869	0,291	103	7,3
	Ad5	12500	16960	1896097	0,303	112	37,9
	Ad19a	1250	0	123802	0,199	-	2,5
	Ad19a	2500	83	224492	0,180	2705	4,5
	Ad19a	12500	2557	5573543	0,892	2180	111,5
Pig MB	Ad5	1250	772	64439	0,103	83	1,3
	Ad5	2500	1475	106556	0,085	72	2,1
	Ad5	12500	6857	436480	0,070	64	8,7
	Ad19a	1250	0	18881	0,030	-	0,38
	Ad19a	2500	37	21043	0,016	569	0,42
	Ad19a	12500	419	1212229	0,194	2893	24
Mouse MB	Ad5	1250	0	9649	0,015	-	0,19
	Ad5	2500	0	22760	0,018	-	0,46
	Ad5	12500	0	81540	0,013	-	1,6
	Ad19a	1250	0	9409	0,015	-	0,19
	Ad19a	2500	0	20863	0,017	-	0,42
	Ad19a	12500	0	18126	0,003	-	0,36
Rat L6	Ad5	1250	0	15978	0,026	-	0,32
	Ad5	2500	0	ND	ND	-	ND
	Ad5	12500	0	94428	0,076	-	1,9
	Ad19a	1250	0	8053	0,013	-	0,16
	Ad19a	2500	0	ND	ND	-	ND
	Ad19a	12500	0	25454	0,004	-	0,51

\* In order to allow for optimal transgene expression, cells were kept in growth medium supplemented with 10% fetal bovine serum during the entire experiment (48h).

The particle per RFU ratio describes the activity of the EGFP-expression cassette per cell-associated viral particle. In theory, the intracellular localization of viral particles, the uncoating efficiency, nuclear import of adenoviral DNA, vector-related toxicity, and species-dependent regulation of CMV / adenovirus ITR enhancer elements may affect the

transcriptional activity of the virus-encoded EGFP expression cassette. Remarkably, the particle/RLU ratios were several times higher for Ad19aEGFP (12500 vg/cell) than for Ad5EGFP in human (3.9-fold), ape (19.5-fold), and pig myoblasts pig (45-fold).

### 3.3.5 Lack of maturation-dependent decrease for transfection of myotubes

We next tested the ability of both vectors (Ad5EGFP and Ad19aEGFP) to transduce fully differentiated myotubes derived from human and ape myoblasts. Consistent with previously reported data<sup>252</sup>, Ad5EGFP transduced human myotubes several times less efficient than myoblasts. On the other hand no differentiation-dependent decrease of transduction was observed with Ad19aEGFP. Gene expression in human myotubes transduced with Ad19aEGFP was 20-fold, as compared to Ad5EGFP (Fig.20A).

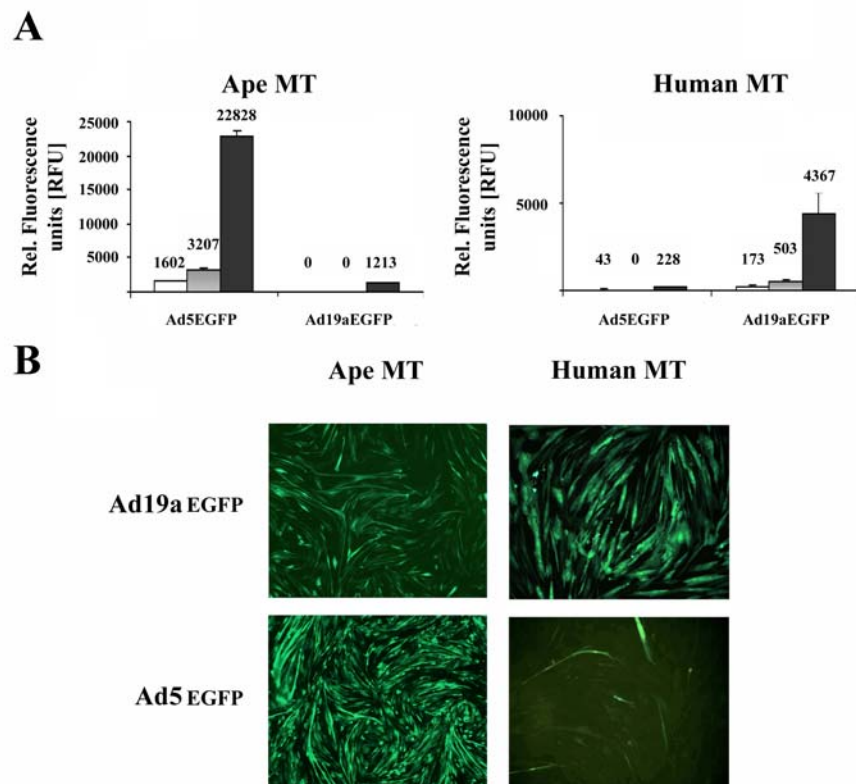


**Fig.20 Transduction of ape and human myotubes by Ad5EGFP and Ad19aEGFP.** Myotubes derived from primary human and ape myoblasts were transduced with 1250 vg/cell (white bars), 2500 vg/cell (gray bars) and 12500 vg/cell (black bars), and EGFP expression measured at 48h. Each value represents the means of three independent infections  $\pm$  SD (A). Pictures of fluorescent cells transduced with 12500vg/cell were recorded 48h post transduction with a Leica DMRBE epi fluorescence microscope equipped with AxioCam HRC and analyzed with AxioVision 3.1 software (Zeiss, Jena, Germany). Recording time was 5s, except for strongly expressing ape myotubes (Ad5 panel), where the recording time was reduced to 1s (B).

In contrast to human muscle cells, gene transfer efficiency in ape myoblasts and myotubes was higher for Ad5EGFP (12500vg/cell), resulting in 19-fold and 5-fold increase, respectively, of transgene expression as compared to Ad19aEGFP. Surprisingly, no maturation-dependent decrease in gene transfer efficiency was observed with ape myotubes transduced by Ad5EGFP.

### *3.3.6 Transduction of primary human cells by Ad19aEGFP.*

Next, we compared the ability of Ad5EGFP and Ad19aEGFP to transduce primary human cells of potential interest for gene therapy. Primary human monocyte-derived immature dendritic cells (DC), epithelial cells (HUVEC) and smooth muscle cells (SMC), were transduced with 1250 vg/cell, 2500 vg/cell, and 12500 vg/cell Ad5EGFP and Ad19aEGFP, respectively, and transgene expression quantified after 48h. Smooth muscle cells were preferentially transduced by Ad19aEGFP whereas HUVEC cells were better transduced by Ad5EGFP (Fig. 21A). Monocyte-derived immature human dendritic cells are target cells in many immunization protocols and unwanted transduction of tissue DCs after gene transfer was reported to trigger the anti-adenovirus immune response. Peripheral blood monocyte cells (PBMCs) were isolated from healthy donor blood and monocytes differentiated in medium containing GM-SCF and IL4. Surface expression of DC-specific markers was characterized at day 7. 46% of differentiated monocytes expressed DC-specific markers CD11c and DC-SIGN (data not shown). Surprisingly, the percentage of EGFP-expressing DCs, transduced with Ad5EGFP or Ad19aEGFP, respectively, was equal for both vectors (Fig.21B), but levels of transgene expression were 10- to 25-fold higher in Ad19aEGFP-transduced DCs (Fig.21A). Since both vectors use  $\alpha_v$  integrins for internalization, one explanation may be, that both vectors transduced the same subset of cells. Moreover, the transduction efficiency may be higher for DCs transduced by Ad19aEGFP vector as compared to Ad5EGFP, and thus explain the observed higher transgene expression.

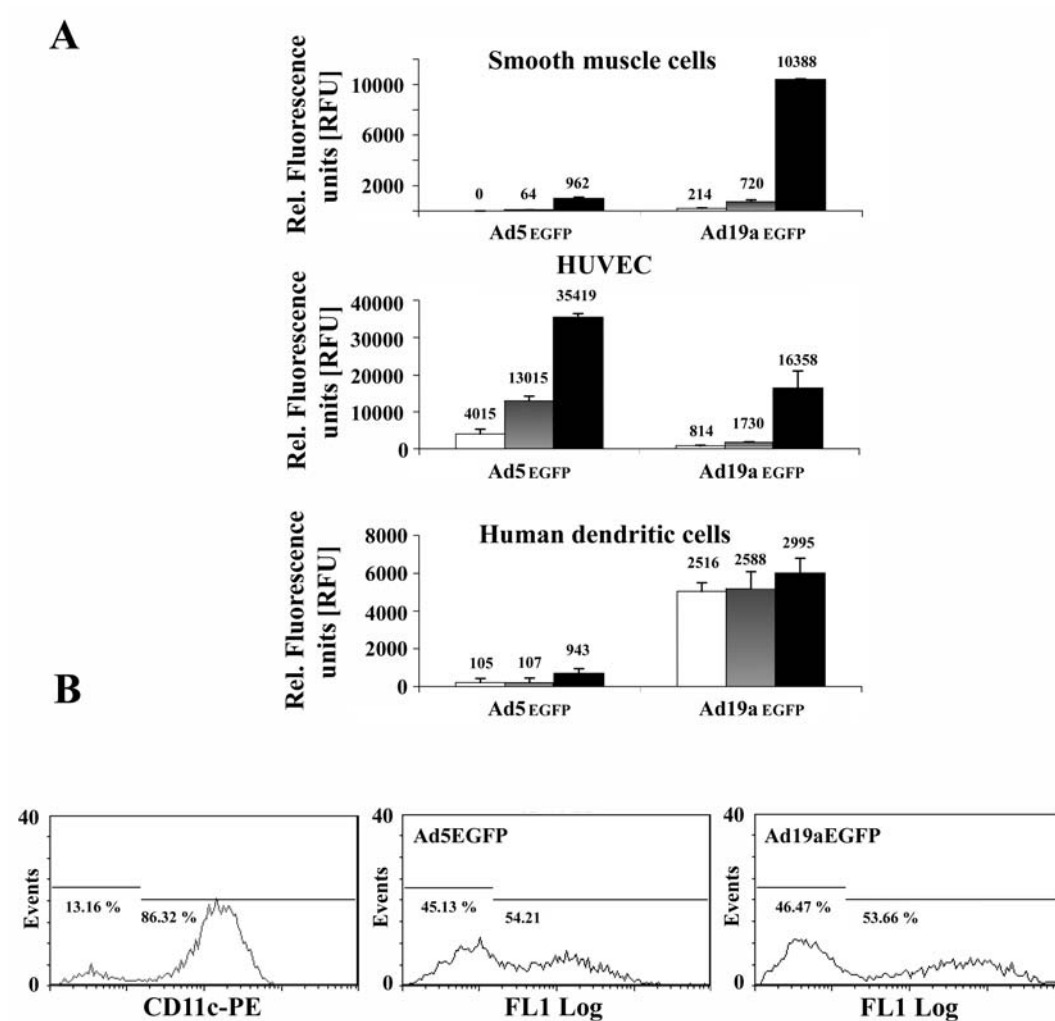


**Fig.21 Transduction of target cells for gene therapy with Ad5EGFP and Ad19aEGFP.** Primary human cells, including primary smooth muscle cells, human umbilical vein endothelial cells (HUVEC), and immature monocyte-derived dendritic cells were transduced with 1250 vg/cell (white bars), 2500 vg/cell (gray bars), and 12500 vg/cell (black bars), and EGFP expression quantified after 48h. Each value represents the means of three independent infections  $\pm$  SD (A). FACS analysis of CD11c-positive DCs transduced with 12500vg/cell reveals equal numbers of EGFP-expressing cells for DCs transduced with Ad5EGFP and Ad19aEGFP, respectively, but a marked increase in the fluorescence intensity with cells transduced by Ad19aEGFP, as compared to Ad5EGFP(B).

## 4. Discussion

### 4.1 Overcoming the hurdles in adenovirus-mediated gene delivery *in vivo*

An ideal viral vector for gene therapy should have the following attributes: it should take advantage of the cellular uptake and intracellular transport machinery and efficiently deliver a gene of interest to the nucleus, it should be non-immunogenic, show persistent and stable gene expression, it should be able to package large cDNA constructs, and it should infect only the tissue of choice. In order to achieve this, great effort must be undertaken to find solutions for each of the above-mentioned goals. Since differentiated human muscle cells express insufficient levels of primary adenovirus attachment receptor, CAR, and hence are relatively resistant to transduction by adenovirus serotype 5, we focussed on the development of virus retargeting to alternative muscle-specific receptors with the aim of simultaneously increasing specificity and transduction efficiency of human muscle cells. Milestones achieved in the development of low-immunogenic and long-term gene expression with adenovirus gene therapy vectors will be discussed first.

#### 4.1.1 Development of low-immunogenic adenovirus gene therapy vectors

Seropositivity for Ad5 and Ad2 in European populations is highly prevalent, and may severely impair vector administration or readministration in gene therapy applications<sup>140</sup>. Although clearance of adenovirus by neutralizing antibodies is an important factor, other components, *e.g.* cells of the reticular endothelial system (RES) and opsonizing serum factors, interact with Ads as well, and have to be taken into consideration as potential inhibiting factors, especially when gene transfer is done via blood circulation. Development of “stealth” adenoviruses by means of chemical modification of the capsid with polymers may be a promising way to shield viral particles from those factors and increase stability and blood circulation properties<sup>253</sup>. Recently, two polymer-modifications, based on polyethylene glycol (PEG) and hydrophilic poly-N-(2-hydroxypropyl)-methacrylate (pHPMA), respectively, have been used to coat adenoviral vectors<sup>139,254</sup>. Targeting ligands like the basic fibroblast growth factor (bFGF) can be incorporated into the pHPMA polymer coat and mediate transduction to bFGFR-positive cells. Vector shielding may also be advantageous for blunting the unspecific uptake of adenoviral particles by liver macrophages (Kupffer cells), since at least opsonizing

serum components do not bind to hydrophilic polymer coats and PEGylation reduces blood clearance rates, which normally lead to clearance of >99% of adenoviral particles within 1h<sup>176,177</sup>. Reduced uptake of Ad by Kupffer cells (and other tissue macrophages) may also reduce the generation of a humoral immune response against virus-encoded transgenes. Expression of AAT under the control of a liver-specific promoter resulted in absence of anti-AAT-1 antibodies after hepatic gene transfer<sup>136</sup>.

#### *4.1.2 Long-term transgene expression and site-specific gene integration into human chromosomes*

Stable integration of genes into a defined chromosomal locus can be achieved with homologous recombination, but occurs with a low frequency of approximately  $10^{-6}$  in multicellular organisms<sup>255</sup>. Several microorganisms, however, provide enzymes that mediate integration and excision of genes at specific target sites in eukaryotic cells without the need for bacterial co-factors. Cre, and Flp recombinases perform both integration and excision of genes at target sites, though the excision reaction predominates and net-integration frequency is 0.03% for Cre recombinase<sup>256,257</sup>. If exclusive integration is required, other types of recombinases, like the integrase from *Streptomyces* phage  $\Phi$ C31 may be better suited, since  $\Phi$ C31 recombinase catalyzes unidirectional integration of genes between phage attachment sites (*attP*) and bacterial attachment sites (*attB*)<sup>258</sup>. Site-specific integration of genes in eukaryotic cells following recombination between *attB* and *attP* sites has been achieved, and used to express therapeutic levels of factor IX (FIX), resulting from stable integration of the FIX gene in chromosomal pseudo-*attP* sites<sup>259,260</sup>. A study, aimed to investigate site-specific integration of *attB*-containing plasmids into chromosomal pseudo *attP* sites, revealed 31 different chromosomal pseudo *attP* sites in 293A cells with high prevalence of integration to a particular site, termed pseudo *attP* site A<sup>261</sup>. It is thus conceivable to direct gene integration into such sites, which may reduce the risk of insertional mutagenesis, as occurring with randomly integrating retroviral vectors. A similar strategy was recently employed to stabilize gene expression *in vivo* with a high-capacity adenovirus-transposon vector<sup>262</sup>. In another attempt to stabilize transgene expression after adenovirus gene transfer, episomal maintenance of circularized adenoviral genomes containing Epstein-Barr virus OriP/EBNA-1 locus was demonstrated<sup>263</sup>.

#### 4.1.3 Retargeting or detargeting?

The K417I, K420I double point mutation within the CAR-binding AB loop, which was characterized in the present work, led to almost complete loss of CAR-binding. The K417I, K420I point mutations lead to CAR-detargeting with comparable efficiency to the most potent mutations previously described, *e.g.*, Y477A, and S408E<sup>174</sup>. However, Alemany *et al.* demonstrated that ablation of the CAR-binding activity alone did not change the biodistribution pattern when Ad5 was injected intravenously<sup>176</sup>. Removal of the natural tropism of Ad5 was shown to require combined removal of CAR and integrin  $\alpha_v$ -binding within the penton base<sup>182</sup>. Maximal removal of the CAR-binding activity through introduction of multiple point mutations within the AB loop (R421S, A415G, E416G, and K417G) only marginally affected transgene expression in skeletal muscle, whereas administration of CAR and integrin double-ablated mutant vectors decreased luciferase expression by about 100-fold and the number of delivered genomes by 15-fold<sup>182</sup>. Similar results were obtained after intravenous administration of CAR-ablated vector mutants to other organs. Double-ablated viruses transduced all tissues lower by up to 700-fold. CAR-ablation alone led to decreased transgene expression in liver only. Hepatocytes express high levels of CAR, which may be accessible, in contrast to CAR in heart tissue, where CAR may be confined to cell-cell junctions. Based on these results one can conclude that reducing the native tropism is synonymous with complete loss of integrin  $\alpha_v$ -binding ability. Introduction of a new targeting moiety thus not only has to provide cell attachment, but also has to target internalization for effective transduction. This strategy may limit the choice of a targeting ligand and confine retargeting of double-ablated vectors to internalization-promoting receptors and pathways.

#### 4.1.4 Genetic retargeting of adenovirus using the protein A-derived antibody-binding domain Z33

In this work, a versatile strategy for retargeting of Ad-vectors, based on the incorporation of an IgG-binding peptide into the capsid and allowing for the use of unmodified monoclonal antibodies to redirect the vector to specific cell surface molecules, was developed. The Z33-domain was incorporated into the HI-loop of the fiber knob where it retained high-affinity IgG-binding activity.

Using surface plasmon resonance measurements, the binding affinity of KnobZ33 protein to a mouse MAb was determined to be  $K_D = 2.4$  nM, suggesting that the binding affinity of Z33 in

the context of the knob domain was in the same range than the affinity of Z33 and the full-length Z-domain polypeptides to IgG1 immunoglobulins, which are  $K_D(\text{Z33}) = 43 \text{ nM}$  and  $K_D(\text{Z}) = 10 \text{ nM}$ , respectively<sup>243</sup>. However, our measurements were performed with a BIAcore sensor chip carrying immobilized mouse IgG<sub>2a</sub> in contrast to the human IgG<sub>1</sub> that was used in the original experiment. The Z33-domain, which is a 33-aa-long double-helix version of the 59-aa long triple-helix Z-module derived from staphylococcal protein A<sup>243,264,265</sup>, may potentially have been stabilized by either flanking aa residues or the tertiary structure of the knob domain. In addition, the homotrimeric nature of the fiber knob carrying three Z33-domains per molecule most probably accounts for the higher overall affinity to IgG<sub>2a</sub> in the BIAcore experiments, as opposed to the monomeric peptide. Insertion of Z33 into the knob domain did not significantly affect CAR binding. BIAcore affinity measurements using a soluble CAR protein as analyte for binding to immobilized Knob and KnobZ33, respectively, yielded similar binding rate constants ( $k_a$  and  $k_d$ ). In accordance to this result, the modified vector AdFZ33 $\beta$ Gal could be readily propagated on CAR-expressing producer cells. The dissociation constants obtained for interaction between sCAR (extracellular part of CAR, containing both extracellular domains D1 and D2) and the knob proteins were high as compared to values previously reported by others for association of the CAR D1-domain alone with wild-type knob protein ( $K_D = 25 \text{ nM}$ )<sup>266</sup>, and binding of full-length fiber protein to CAR-expressing cells *in vitro* ( $K_D = 2 \text{ nM}$ )<sup>9</sup>. This could potentially be due to a modifying or masking effect of the D2-domain in our recombinant sCAR protein on the knob binding site in the D1-domain which might not be exerted if D1 is expressed alone or the full-length CAR protein is anchored to the cellular membrane. True retargeting of Z33-modified AdFZ33 $\beta$ Gal to non-CAR receptors was demonstrated, since recombinant knob protein failed to compete with NCAM-retargeted viruses for binding receptors (Fig.15). Experiments with EGFR-retargeted AdFZ33 $\beta$ Gal confirmed this result and demonstrated that only protein A was able to compete for antibody binding and to ablate the enhanced retargeting efficiency of AdFZ33 $\beta$ Gal<sup>242</sup>. Knob protein (KnobWT) was not able to inhibit transduction of FHMs with NCAM-retargeted AdFZ33 $\beta$ Gal. These results raise the question of whether introduction of CAR-detargeting mutations are necessary to increase specificity of antibody-retargeted AdFZ33 $\beta$ Gal. The gene transfer efficiency was enhanced 2-fold in an unspecific way upon preincubation of AdFZ33 $\beta$ Gal with high concentrations (up to 40 $\mu$ g/ml) of p53 control antibody. This result may be explained by some weak residual binding activity of p53 to cell

surface proteins, but remained moderate if compared to the specific increase (up to 37-fold) with integrin  $\alpha_7$  and NCAM-retargeted AdFZ $\beta$ Gal33<sup>242</sup>. We tried to enhance the gene transfer efficiency to Jurkat and HeLa cells using CD3-, and MHCI-retargeted AdFZ33 $\beta$ Gal, but achieved only minor effects. Similarly, ligand screening with metabolically biotinylated adenoviral vectors for enhanced transduction of bone-marrow-derived dendritic cells yielded variable transduction efficiencies that were strongly dependant on the targeted receptor<sup>281</sup>. In contrast to our results, highly efficient and specific transduction of primary resting T-cells was achieved with CD3-retargeted adenovirus. In this study a bispecific antibody consisting of an anti-FLAG MAb chemically crosslinked to anti-CD3 MAb (different from the anti-CD3 MAb used in this work) was used to retarget a penton-base-modified adenovirus to the CD3 receptor<sup>209</sup>. This result demonstrates that the choice of the retargeting antibody is essential for successful retargeting of adenovirus vectors.

A general concern related to the use of antibody-retargeted viruses is that there could be unwanted activation of the complement system, which may occur if free antibodies are co-injected with the virus, or if antibodies dissociate from the virus during prolonged circulation times. To minimize unwanted side effects, it may therefore be necessary to remove unbound antibodies prior to vector application *in vivo*, or to attach the targeting antibodies covalently to the virus.

#### *4.1.5 Genetic retargeting of adenoviral vectors and the choice of the targeting ligand and insertion site*

This work demonstrates that the insertion capacity of the HI loop can be expanded to larger ligands. In a recent study, the insertion capacity of the HI loop was systematically analysed and the entire RGD-loop from adenovirus penton base (83aa) inserted<sup>267</sup>. Interestingly, the insert size only moderately affected titres of recombinant vectors, though functionality of the inserted RGD sequence was size-dependent. The adenovirus structural proteins are synthesized in the cytosol and thereafter translocated into the nucleus, where adenoviral particles are assembled<sup>268</sup>. The cytoplasmic expression of fiber molecules narrows the choice of targeting ligands to ligands that do not need disulfide bonds for correct folding and solubility. A strict correlation between solubility of chimeric fiber proteins and viability of virus was observed with genetically retargeted knobless adenoviral particles. Rescue of fiber-modified adenovirus vectors with a single-chain antibody fragment (scFv) and fibroblast growth factor (FGF), respectively, was not achieved<sup>269</sup>. Based on these findings, the method

of producing retargeted knobless Ads was improved by fusing cytoplasmically stable antibodies, termed “affibodies” to the fiber protein C-terminus consisting of 7 adenovirus shaft repeats followed by a spacing trimerization domain from lung surfactant protein<sup>200</sup>. One disadvantage of using knobless affibody-targeted vectors is the high genome-to-infectious virus ratio, which is in the range of 1:118 to 1:421, and may be disadvantageous for the use of these vectors *in vivo*<sup>200</sup>. Insertion of the Z33 ligand into the HI loop, which functionality did not rely on expression via the secretory pathway or disulfide bond formation, resulted in expression of soluble Z33-, and Z34C-modified fiber proteins, respectively, and rescue of viable Z33-modified vector. We were unfortunately not able to rescue the corresponding adenovirus with Z34C HI-loop insertion, though Z34C-modified fiber protein (FZ34C) was soluble and trimerized, as shown by Western blot analysis of CV-1 cells transduced with FZ34C-producing vaccinia virus (Fig.8A). Due to the required formation of a disulfide bond, degradation of partially folded Z34C fiber protein may be a likely explanation for the failed virus rescue. An adenovirus vector with functional extension of the fiber protein C-terminus with an engineered 70 aa biotin acceptor protein (BAP) was rescued. When the same ligand was introduced into the HI loop, no viable virus could be obtained<sup>281</sup>. This example demonstrates the importance of a careful ligand design and choice of the appropriate insertion site in order to obtain viable vectors.

Apart from the HI-loop, targeting ligands were successfully inserted into adenovirus protein IX and penton base protein<sup>204,205,206</sup>. Extension of the C-terminus of pIX with the large heterologous proteins EGFP and long targeting ligands have been reported and make this protein very attractive for adenovirus retargeting<sup>206</sup>.

#### *4.1.6 Methods to increase high-affinity binding of targeting ligands to targeted molecules*

Phage display is a powerful tool for screening large populations of targeting ligands. Tissue-specific binding ligands were identified by panning a complex bacteriophage library and successfully used for vector retargeting<sup>191,270</sup>. One major disadvantage of small targeting peptides is their often-weak affinity to target structures and their lack of structural rigidity. One of the most potent ligands ever selected was the ACDCRGDCFCG (RGD-4C) peptide, which has a strong affinity to  $\alpha_v$  integrins<sup>271</sup>. Originally isolated from a phage-displayed peptide library screened for specificity for  $\alpha_v\beta_5$  integrin, RGD-4C was shown to be a potent binder (affinity constant of ~100 nM) of  $\alpha_v\beta_3$  and  $\alpha_v\beta_5$  integrins. Both integrins are

selectively expressed in angiogenic vasculature and direct RGD-4C-retargeted adenoviruses to tumor cells<sup>272,190</sup>. Improvement of avidity and structural rigidity of selected ligands has been achieved using a constrained combinatorial library of 20-residue peptides displayed by the active site loop of *E. coli* thioredoxin. The selected peptide aptamers were able to bind their target with high affinity in the nanomolar range<sup>273</sup>.

In another approach, context-specific peptide-presenting phage libraries have been generated using an adenovirus HI-loop phage display system to mimic the expression of peptides in the viral context. The context-specific peptide library approach is an attractive system to screen even large peptide inserts, circumventing toxicity-related problems with knob-expression libraries or the low complexity of viral libraries<sup>274</sup>. Since modifications of viral capsid proteins can affect the viability of a virus, creating an infectious retargeted virus vector library may allow for efficient screening of tissue-specific viruses *in vivo* and bypass *in vitro* selection. A surface-exposed loop structure was chosen as the site of incorporation for a complex peptide library and used to create an AAV-based virus library<sup>275,276</sup>. Similarly, other virus-based libraries have been generated and used to identify retargeted virus vectors<sup>277,278</sup>.

A high affinity linkage is required if virus vectors are retargeted by means of adaptor molecules or antibodies. Several very high affinity ligand-receptor interactions, like barnase-barnstar complex with  $K_D = 10^{-14}$  M, and biotin streptavidin complex ( $K_D = 10^{-15}$  M), have been described<sup>279,280</sup>. The latter concept was recently used for adenovirus and AAV retargeting by incorporating a small biotin-binding peptide to the C-terminus of fiber protein capsid allowing for metabolic biotinylation in 293 cells<sup>281</sup>.

#### 4.1.7 Perspective for muscle-specific targeting of adenoviral vectors

Though the use of a genetically engineered AdV with a C-terminal poly-lysine moiety enhanced gene transfer into mouse skeletal muscle *in vivo*, these vectors still transduce many other cell types as well. The development of retargeted and muscle-specific AdV is highly desirable for therapeutic use. Potential ligands, *i.e.*, muscle-specific peptides, have been selected by different methods such as phage-display<sup>270,282</sup>. Their ability to enhance AdV-mediated gene transfer upon genetic engineering of Ad shall be evaluated in the future.

Low CAR and  $\alpha_v\beta_3$  integrin expression levels limit adenovirus-mediated gene transfer to adult skeletal muscle<sup>151,155</sup>. To date, only a few muscle-specific and sufficiently expressed surface markers have been characterized that could be used for genetic retargeting of viral vectors<sup>282</sup>. One example is the Fe-transferrin receptor that is overexpressed in regenerating

muscle fibers<sup>283</sup>. Integrin  $\alpha_7\beta_1$  is an excellent candidate for muscle-specific vector targeting, since the integrin  $\alpha_7$  subunit is almost exclusively expressed in skeletal, smooth and cardiac muscle, and is increased on the surface of muscle fibers in DMD patients and *mdx* mice<sup>248,284,285</sup>. Another promising target receptor is NCAM, which is expressed in activated satellite cells and myogenic precursor cells during regeneration<sup>247,286</sup>. The concept of targeting regenerating and newly forming myofibers and muscle satellite cells ("targeting the next generation") may prove particularly useful for young patients with limited fibrosis. In this study it was demonstrated that both integrin  $\alpha_7\beta_1$  and NCAM could serve as attachment receptors for retargeted adenovirus vectors and promoted their internalization in myoblasts as well as in differentiated myotubes. Augmentation of the transduction efficiency of myotubes by integrin  $\alpha_7\beta_1$ - and NCAM-targeted AdFZ33 $\beta$ Gal up to 77-fold is of particular interest for further development of an Ad-vector-based gene therapy of muscular dystrophies. Since myotubes cultivated *in vitro* have a rudimentary extracellular matrix<sup>287</sup> and are difficult to transduce with adenovirus, they may well reflect the behaviour of muscle fibers *in vivo*<sup>252</sup>. One hallmark of dystrophic muscles of DMD patients is the high prevalence of regenerating fibers, in conjunction with an altered expression profile of several muscle-specific proteins<sup>288</sup>. At birth, ~30% of the sublamellar mouse muscle nuclei are satellite cells, decreasing to less than 5% in a 2-month-old adult mouse<sup>289</sup>. Alternative "targetable" receptors in quiescent satellite cells may be the *c-Met* receptor<sup>290</sup> (receptor for hepatocyte growth factor) as well as M-cadherin<sup>286</sup>, which are activated in response to stimuli such as stretching, exercise, injury, and electrical stimulation (reviewed in<sup>289</sup>).

## 4.2 Exploiting the natural adenovirus serotype pool.

### 4.2.1 Infectious pathway of adenovirus serotypes 5 and 19a in primary human muscle cells

A combination of heparin, knob, and soluble GRGDS peptide was necessary to efficiently inhibit binding of Ad5EGFP to primary human myoblasts. Soluble GRGDS peptide, an inhibitor of  $\alpha_v\beta_3$  integrin function, had no effect on vector binding but affected transduction at 37°C, confirming that  $\alpha_v\beta_3$  is involved in virus internalization rather than in virus binding<sup>9</sup>. In agreement with the proposed two-step model for Ad5 cell transduction, additive inhibitory effects of GRGDS peptide and Ad5 knob, and GRGDS and heparin, respectively, occurred at 37°C, at which point virus internalization is promoted, but not at 4°C, which is a non-permissive temperature for virus internalization<sup>7,9</sup>. Taken together these results agree with

previous findings, while also demonstrating the importance of alternative receptors like heparansulfate proteoglycans for Ad5 binding and transduction<sup>23,24,25</sup>. Binding of Ad5 to CAR is crucial for transduction of fetal muscle *in vivo*<sup>291</sup>, and the maturation-dependent decrease in transduction efficiency may be a consequence of the accompanying reduction of CAR and alpha v integrins in mature versus newborn muscles<sup>151</sup>. In contrast, support for the relevance of non-CAR-mediated liver transduction came from experiments with detargeting mutations in the putative HSG-binding motif within the Ad5 shaft, which reduced hepatic gene transfer *in vivo*<sup>175</sup>. Moreover, additional HSG-binding sites, that did not overlap with the CAR-binding region were mapped within the Ad5 knob<sup>292</sup>. The current understanding of subgroup C adenovirus endocytosis involves initial clathrin-mediated endocytosis induced by interaction of penton base with integrin  $\alpha_v\beta_3$  followed by  $\alpha_v\beta_5$ -integrin-mediated endosomal membrane permeabilization and endosome escape. The Ad2 penton base has a propensity to bind to nonionic detergents at low pH, suggesting that membrane-reactive hydrophobic regions may be exposed in acidified early endosomes<sup>293</sup>. Since Ad2 penton base alone did not increase membrane permeabilization, which is a prerequisite for virus escape, it was proposed that other viral/host factors could be involved<sup>294</sup>.

Interestingly, adenovirus protein IIIa exhibits a basic sequence located near the C-terminus with homology to vitronectin and HIV Tat basic region, which were shown to bind to integrin  $\alpha_v\beta_5$  in an RGD-independent way (figure 23)<sup>295</sup>.

Vitronectin (VN) basic region:

Protein IIIa VN-homologue region:

HIV-Tat basic  $\alpha_v\beta_5$  binding region :

C	K	K	Q	R	--	F	R	H	R
T	R	R	Q	R	H	D	R	Q	R
K	R	R	Q	R	--	R	R	--	--

Figure 23: Alignment of the basic  $\alpha_v\beta_5$ -binding sequences from vitronectin, Ad5 protein IIIa, and HIV-1 Tat. Conserved homologous amino acids are highlighted in yellow.

Moreover, analysis of the primary amino acid sequence from Ad5 fiber gene reveals the presence of a functional N-terminal NPXY sequence. The <sup>11</sup>NPVY<sup>14</sup> motif together with the N-terminal Ad5 fiber nuclear localization signal <sup>1</sup>AKRARLSTSF<sup>10</sup> promoted nuclear transduction of plasmid DNA condensed by a poly-lysine moiety<sup>296</sup>. The NPVY motif enhanced transfection up to 30-fold. A conserved NPXY motif is found in many  $\beta$  integrin subunits and was shown to function as a coated pit localization signal<sup>297, 298</sup>. In addition to the

functional RGD motif, the Ad5 penton base contains 6 conserved NXXΦ sequences that may also be involved in endocytosis<sup>299</sup>. Indeed, adenovirus-like particles termed adenovirus dodecahedron, composed solely of Ad3 penton base protein or Ad3 penton base protein and fiber protein enter cells efficiently via endocytosis and accumulate at the nuclear membrane<sup>300</sup>.

#### *The infectious pathway of adenovirus serotype 19a*

Soluble GRGDS peptide had no effect on Ad5EGFP and Ad19aEGFP vector binding, but reduced the transfection efficiency at 37°C, suggesting that  $\alpha_v$ -integrins are involved in virus uptake of both serotypes. Attachment of Ad19aEGFP vector to FHM at 4°C was completely blocked by WGA or neuraminidase. Therefore, Ad19aEGFP may specifically recognize a carbohydrate epitope containing  $\alpha(2,3)$ -linked sialic acid and N-acetyl- $\beta$ -(1,4)-D-glucosamine. Heparin and GRGDS peptide did not interfere with the binding of Ad19aEGFP to muscle cells at 4°C, but reduced the gene transfer efficiency at 37 °C. A two-step model for Ad19aEGFP, similar to Ad5, with separate receptors involved in virus binding and uptake, may therefore be conceivable. Furthermore, heparin and GRGDS may be competing for binding sites on a putative internalized co-receptor. Indeed, the presence of a conserved putative integrin-binding RGD motif within Ad19a penton base protein may explain the sensitivity of virus internalization to soluble GRGDS peptide<sup>6</sup>. A role for heparin-binding receptors in Ad19a internalization has not been reported prior to this study.

#### *4.2.2 Tropism of Ad19a-based recombinant vector*

Subgroup D adenovirus serotypes Ad37, Ad19, and Ad8 have ocular tropism and infect conjunctival cells via sialic acid containing receptors but not CAR-expressing lung epithelial A549 cells<sup>5,6,301</sup>. The natural occurring complexity of adenovirus receptors, as reflected by association of different subclinical symptoms with different adenovirus serotypes, could be well exploited for vector development. A previously reported Ad35-based vector transduced monocyte-derived immature dendritic cells, smooth muscle cells and synoviocytes more efficiently than did Ad5<sup>140</sup>. Similarly, the novel subgroup D adenovirus type 19a vector transduced primary human cells, including dendritic cells, smooth muscle cells, primary human myoblasts, and otherwise difficult-to-transduce myotubes better than did the corresponding Ad5-based vector. Ad19a seems to be particularly well adapted to human

muscle cells because even at low vector doses (1250 vg/cell) more than 90% of myoblasts expressed the transgene. Moreover, immature monocyte-derived dendritic cells (positive for CD11c marker) that were transduced by Ad19aEGFP expressed several-fold-higher levels of EGFP than did DCs transduced with Ad5EGFP. Accordingly, Ad19a-based vectors may be suited for vaccination.

The tropism of one adenoviral serotype can be transferred to another by swapping the entire fiber molecules or the distal fiber knob domains<sup>195,302</sup>. Systematic analysis of fiber-chimeric Ad5-based vectors led to the identification of 3 chimeric vectors (Ad5.Fib16; Ad5.Fib35, and Ad5.Fib50) that showed enhanced transduction of human primary cells and established cancer cell lines<sup>302, 303, 304</sup>. Similar to these chimeric vectors, an Ad5.Fib19a vector may display the same tropism as the Ad19a-based vector. Sequestration of CAR in basolateral membrane adherens junctions of polarized airway epithelial cells is thought to preclude Ad5-mediated gene transfer and successful delivery of CFTR cDNA in well-differentiated airway epithelium cells<sup>305</sup>. Unlike with Ad5 and AAV-2, the airway epithelium can be efficiently transduced with AAV-5, which binds to apically-expressed receptors containing  $\alpha(2-3)$ -linked sialic acid<sup>306,307</sup>. Similarly, Ad19a-derived vectors may be suited for gene transfer to the airway epithelium and prove useful in studies aimed to investigate whether extracellular barriers or a shortage of viral receptors on the apical surface are limiting transduction of airway epithelium. In a very recent publication CD46 was identified as primary attachment receptor for Ad37 on human cervical carcinoma and conjunctival cells<sup>308</sup>. Since Ad19a and Ad37 fiber have identical primary protein sequences, and since the Ad5 vector pseudotyped with Ad37 fiber protein (Ad5.F37) also bound CD46, it is likely that Ad19a also uses CD46 as primary receptor<sup>308</sup>.

#### *4.2.3 Inter-species differences for viral transduction*

One surprising finding was the strong transduction of undifferentiated as well as differentiated ape skeletal muscle cells by Ad5 without a noticeable differentiation-dependent decrease in gene transfer efficiency, which is in contrast to observations in human cells. Moreover, both serotypes showed significantly lower transduction of rat L6 and primary mouse myoblasts. The low transduction efficiency of rat L6 cells and primary mouse myoblasts reflects the poor performance of Ad5 *in vivo* after direct intramuscular injection in adult mice<sup>147</sup>. Similar species-dependent variations in gene transfer and expression were observed in a dose-response study with SMCs derived from carotid arteries of different species. As opposed to

monkey and rabbit, the mouse, pig, and human SMCs were less susceptible to Ad5. Differences in attachment, internalization and intracellular trafficking of Ad5 may occur among other species. A vector displaying the Ad16 fiber molecule on an Ad5 backbone (Ad5.Fib16) preferentially transduced monkey and human SMCs, but only poorly transduced SMCs of pig, rat, rabbit, and mouse origin<sup>302</sup>. Strikingly, Ad5 transduced primate-derived cells the best in both studies, demonstrating that Ad5 may be well adapted to this species. Determination of the viral particle number by real-time PCR in transduced myoblasts of different species revealed two putative barriers. A post-internalization block may occur in pig and ape myoblasts, where high numbers of intracellular particles accumulated without expressing EGFP. In primary mouse and rat L6 myoblasts however, an early block may be present at the level of vector attachment and internalization, where low amounts of intracellular Ad5 and Ad19a particles were detected.

The poor transducibility of non-human myoblasts by Ad19a may be explained by subtle changes in the glycosylation pattern of membrane proteins. In mammals, sialic acid (N-acetylneuramic acid (Neu5Ac) terminates glycoconjugated sugars. Sialic acid is either linked  $\alpha$ 2-3 or  $\alpha$ 2-6 to  $\beta$ -D-galactopyranosyl (Gal),  $\beta$ -D-N-acetyl-galactosaminyl (GalNAc) or  $\beta$ -D-N-acetylglucosaminyl (GlcNAc) residues. Sialic acids are further attached  $\alpha$ 2-8 to sialyl- $\alpha$ 2-3 residues, and form polysialic  $\alpha$ 2-8 homopolymers occurring on glycoproteins (e.g., on NCAM)<sup>309</sup>. Except for humans, all mammals share an enzyme that oxidizes N-acetylneuraminic acid to N-glycolylneuraminic acid (Neu5Gc)<sup>310</sup>. Indeed, N-glycolylneuraminic acid can act as host-range determination factor for neuraminidase-sensitive pathogens like influenza A virus and rotavirus<sup>311,312,313</sup>. Viral mutants of influenza A virus with HA genes recognizing Neu5Gc $\alpha$ 2-3Gal and Neu5Ac $\alpha$ 2-3Gal replicate in horses, where the content of glycolylated sialic acid in erythrocytes and trachea exceeds 90%, whereas a virus strain that recognized preferentially Neu5Ac $\alpha$ 2-6Gal was unable to replicate<sup>311</sup>. Whether similar effects determine the host range of adenovirus type 19a remains to be investigated. Interestingly, small amounts of Neu5Gc have been detected in fetal tissue and tumors, though humans are unable to synthesize Neu5Gc due to a deletion in the corresponding CMP-Neu5Ac-specific hydroxylase gene<sup>310</sup>. It was further shown that Neu5Gc was incorporated into human glycoproteins through a Neu5Gc-rich diet<sup>314</sup>.

The obtained results warrant additional investigations into gene transfer efficiency and the elucidation of host-range determination factors for Ad5 and Ad19a. In order to translate the

results obtained from Ad5-mediated gene-transfer efficiency from the animal model to a human model, a similar evaluation of gene delivery efficiency by real time PCR to muscle tissue and other organs from different species may be useful. Results from Ad19a transduction experiments with non-human skeletal muscle cells, which were only poorly transduced, may suggest the development of a human explant model to study Ad19a-mediated gene transfer *in vivo*.

#### **4.3 Outlook - Finding new molecular targets to treat muscular dystrophy**

The current model of the molecular pathology of dystrophy deficiency includes several mechanisms in addition to mechanical membrane destabilization<sup>78</sup>. Deregulation of ion-channel activity leading to abnormal Ca<sup>2+</sup> homeostasis and protease activation, as well as absence of nNOS signaling to reverse muscle-contraction-induced vasoconstriction, may contribute to muscle pathology. In support of this theory, studies with *C. elegans* double mutant *dys-1:hlh-1 dys-1* (dystrophin ortholog and *hlh-1* MyoD homolog) identified *dyc-1* as the suppressor of the locomotion impaired phenotype<sup>315</sup>. *Dyc-1* encodes the *C. elegans* homolog of CAPON, a protein that regulates interaction of PSD-95 and nNOS in neurons. Though *C. elegans* lacks an obvious nNOS homolog, the ancestral role of the *dyc-1* gene could be the regulation of PDZ domain-mediated complex formation. Reestablishment of a functional DGC-like signaling complex through upregulation of compensatory molecules or ectopic expression of synaptic scaffolding molecules (*e.g.*, utrophin, alpha7 integrin) may partially compensate for dystrophin-deficiency. The interesting finding, that mitigation of the dystrophic phenotype in *mdx* mice overexpressing CT-GalNAc transferase was related to ectopic expression of CT-modified  $\alpha$ -DG and extrasynaptic utrophin localization, underscores the importance of glycosylation for regulation of protein localization and function<sup>84</sup>. In a subset of LGMD-2I patients, an exceptionally mild phenotype was observed<sup>64,316</sup>. It has been suggested that a reduced but still-functional  $\alpha$ -DG glycosylation in satellite cells may allow for correct  $\alpha$ -DG-laminin association in regenerating, but not in mature fibers where hypoglycosylation of  $\alpha$ -DG and loss of  $\alpha$ -DG-laminin connection occurs<sup>63</sup>.

The temporary clinical benefit for some patients of corticosteroids, which increases the muscle strength, is well accepted. Inflammatory cytokines may be linked to NF- $\kappa$ B-regulated muscle wasting through nuclear translocation of NF- $\kappa$ B and subsequent loss of MyoD

mRNA<sup>317</sup>. Proinflammatory cytokines are released upon muscle fiber injury from mast cells in dystrophic muscles and may provide the cytokine source that initiates inflammation<sup>318</sup>. In addition, microarray analysis of *mdx* muscle revealed enhanced activity of inflammation-related molecules including cytokines and cytokine receptors (*e.g.*, TNF $\alpha$  receptor, IL1, and IL4) upregulation of the endothelial leukocyte adhesion molecule Vcam1, upregulation of complement system genes (C1q, C3) and chemokine receptors<sup>318</sup>. Chronic inflammation in dystrophic muscle may thus induce downregulation of MyoD and contractile dysfunction, which may be implicated in non-functional muscle regeneration through NF- $\kappa$ B-mediated inhibition of cell-cycle exit. Targeting the regulatory pathway that involves cytokine-dependent nuclear translocation of NF- $\kappa$ B may therefore release myoblast differentiation block and complement corticosteroid treatment. Whether the regenerative capacity of myoblast precursor cells (satellite cells) becomes exhausted during disease progression of muscular dystrophy or whether it can be restored is a matter of debate. In a recent study by Conboy *et al.*, loss of regenerative potential in aged skeletal muscle was shown to be due to inadequate activation of Notch-1 by its ligand Delta<sup>319</sup>. Impaired regeneration in aged muscle may therefore be linked to insufficient activation and differentiation of satellite cells, rather than to their depletion. The underlying molecular mechanisms for impaired regenerative capacity of satellite cells in dystrophic muscles may be similar to those in aged muscle, and therefore Notch-1-defective activation of regeneration would also need to be addressed. Targeting positive and negative regulators of muscle growth has already proved useful in animal models of muscle dystrophy. Increasing the muscle mass in *mdx* mice by inhibiting myostatin, a negative regulator of muscle growth and satellite cell proliferation, led to functional improvement of dystrophic muscles<sup>320</sup>. Similarly, muscle-specific expression of insulin-like growth factor-1 (IGF-1) activated myogenesis and prevented muscle-fiber loss in *mdx* mice<sup>321,322</sup>. IGF-1 acts through activation of Ca<sup>2+</sup>-calmodulin dependent kinase (CaMK), leading to nuclear translocation of transcription factor NFAT and histone deacetylase-5 (HDAC5) phosphorylation<sup>323,324</sup>. The recent advances in the field of vector development and the further elucidation of the molecular pathology underlying DMD are stimulating clinical and pharmaceutical research. A safe vector for therapeutic gene delivery should be non-immunogenic, non-toxic and able to deliver the transgene exclusively to the tissue of interest. With this work adenovirus-mediated gene transfer was rendered muscle-specific. Though this may only be a small contribution towards the development of safe vectors for gene therapy,

all the efforts combined may ultimately bring vectors for gene therapy into the clinic and relief patients with hereditary diseases from their suffering.

## References

- <sup>1</sup> De Jong JC, Wermenbol AG, Verweij-Uiterwaal MW, *et al.* Adenoviruses from human immunodeficiency virus-transduced individuals, including two strains that represent new candidate serotypes Ad50 and Ad51 of species B1 and D, respectively. *J. Clin. Microbiol* 1999; 37:3940-3945.
- <sup>2</sup> Gaggar A, Shayakhmetov DM, Lieber A. CD46 is a cellular receptor for group B adenoviruses. *Nat. Med.* 2003; 9:1408-1412.
- <sup>3</sup> Segerman A, Atkinson JP, Marttila M, Dennerquist V, Wadell G, Arnberg N. Adenovirus type 11 uses CD46 as a cellular receptor. *J. Virol.* 2003; 77:9183-9191.
- <sup>4</sup> Stevenson SC, Rollence M, White B, Weaver L, McClelland A. Human adenovirus serotypes 3 and 5 bind to two different cellular receptors via the fiber head domain. *J. Virol* 1995; 69:2850-2857.
- <sup>5</sup> Arnberg N, Edlund K, Kidd AH, Wadell G. Adenovirus type 37 uses sialic acid as a cellular receptor. *J. Virol.* 2000; 74:42-48.
- <sup>6</sup> Arnberg N, Kidd AH, Edlund K, Olfat F, Wadell G. Initial interactions of subgenus D adenoviruses with A549 cellular receptors: sialic acid versus alpha(v) integrins. *J. Virol.* 2000; 74:7691-3.
- <sup>7</sup> Bergelson JM, Cunningham JA, Droguett G. *et al.* Isolation of a common receptor for Coxsackie B viruses and adenoviruses 2 and 5. *Science* 1997; 275:1320-1323.
- <sup>8</sup> Tomko RP, Xu R, Philipson L. HCAR and MCAR: the human and mouse cellular receptors for subgroup C adenoviruses and group B coxsackieviruses. *Proc. Natl. Acad. Sci. U S A* 1997; 94:3352-3356.
- <sup>9</sup> Wickham TJ, Mathias P, Cheresch DA, Nemerow GR. Integrins alpha v beta 3 and alpha v beta 5 promote adenovirus internalization but not virus attachment. *Cell* 1993; 73:309-319.
- <sup>10</sup> Li E, Brown SL, Stupack DG, Puente XS, Cheresch DA, Nemerow GR. Integrin alpha(v)beta1 is an adenovirus coreceptor. *J. Virol.* 2001; 75:5405-5409.
- <sup>11</sup> Roelvink PW, Lizonova A, Lee JG, *et al.* The coxsackievirus-adenovirus receptor protein can function as a cellular attachment protein for adenovirus serotypes from subgroups A, C, D, E, and F. *J. Virol.* 1998; 72:7909-7915.

- <sup>12</sup> Tan PK, Michou AI, Bergelson JM, Cotten M. Defining CAR as a cellular receptor for the avian adenovirus CELO using a genetic analysis of the two viral fibre proteins. *J. Gen. Virol.* 2001; 82:1465-1472.
- <sup>13</sup> Cohen CJ, Xiang ZQ, Gao GP, Ertl HC, Wilson JM, Bergelson JM. Chimpanzee adenovirus CV-68 adapted as a gene delivery vector interacts with the coxsackievirus and adenovirus receptor. *J. Gen. Virol.* 2002; 83:151-155.
- <sup>14</sup> Van Raaij MJ, Chouin E, van der Zandt H, Bergelson JM, Cusack S. Dimeric structure of the coxsackievirus and adenovirus receptor D1 domain at 1.7 Å resolution. *Struct. Fold. Res.* 2000; 8: 1147-1155.
- <sup>15</sup> Honda T, Saitoh H, Masuko M, *et al.* The coxsackievirus-adenovirus receptor protein as a cell adhesion molecule in the developing mouse brain. *Brain Res. Mol. Brain Res.* 2000; 77: 19-28.
- <sup>16</sup> Cohen CJ, Shieh JT, Pickles RJ, Okegawa T, Hsieh JT, Bergelson JM. The coxsackievirus and adenovirus receptor is a transmembrane component of the tight junction. *Proc. Natl. Acad. Sci. U S A.* 2001; 98:15191-15196.
- <sup>17</sup> Cohen CJ, Gaetz J, Ohman T, Bergelson JM. Multiple regions within the coxsackievirus and adenovirus receptor cytoplasmic domain are required for basolateral sorting. *J. Biol. Chem.* 2001; 276:25392-25398.
- <sup>18</sup> Walters RW, Freimuth P, Moninger TO, Ganske I, Zabner J, Welsh MJ. Adenovirus fiber disrupts CAR-mediated intercellular adhesion allowing virus escape. *Cell* 2002; 110: 789-799.
- <sup>19</sup> Bewley MC, Springer K, Zhang YB, Freimuth P, Flanagan JM. Structural analysis of the mechanism of adenovirus binding to its human cellular receptor, CAR. *Science* 1999; 286: 1579-1583.
- <sup>20</sup> Freimuth P, Springer K, Berard C, Hainfeld J, Bewley M, Flanagan J. Coxsackievirus and adenovirus receptor aminoterminal immunoglobulin V-related domain binds adenovirus type 2 and fiber knob from adenovirus type 12. *J. Virol.* 1999; 73: 1392-1398.
- <sup>21</sup> Boulanger PA, Puvion F. Large-scale preparation of soluble adenovirus hexon, penton and fiber antigens in highly purified form. *Eur. J. Biochem.* 1973; 39: 37-42.
- <sup>22</sup> Horwitz M. 2001. Adenoviruses, p2301-2326. *In* D.M. Knipe and P.M. Howley (ed.), *Fields' Virology* 4<sup>th</sup> ed. vol.2. Raven Press, New York, N.Y.

- <sup>23</sup> Dehecchi MC, Melotti P, Bonizzato A, Santacatterina M, Chilosi M, Cabrini G. Heparan sulfate glycosaminoglycans are receptors sufficient to mediate the initial binding of adenovirus types 2 and 5. *J. Virol.* 2001; 75:8772-8780.
- <sup>24</sup> Dehecchi MC, Tamanini A, Bonizzato A, Cabrini G. Heparan sulfate glycosaminoglycans are involved in adenovirus type 5 and 2-host cell interactions. *Virology* 2000; 268:382-390.
- <sup>25</sup> Hong SS, Karayan L, Tournier J, Curiel DT, Boulanger PA. Adenovirus type 5 fiber knob binds to MHC class I alpha2 domain at the surface of human epithelial and B lymphoblastoid cells. *EMBO J.* 1997; 16:2294-2306.
- <sup>26</sup> Salone B, Martina Y, Piersanti S, *et al.* Integrin alpha3beta1 Is an alternative cellular receptor for adenovirus serotype 5. *J. Virol.* 2003; 77:13448-13454.
- <sup>27</sup> Roelvink PW, Kovesdi I, Wickham TJ. Comparative analysis of adenovirus fiber-cell interaction: adenovirus type 2 (Ad2) and Ad9 utilize the same cellular fiber receptor but use different binding strategies for attachment. *J. Virol.* 1996; 70:7614-7621.
- <sup>28</sup> Huang S, Kamata T, Takada Y, Ruggeri ZM, Nemerow GR. Adenovirus interaction with distinct integrins mediates separate events in cell entry and gene delivery to hematopoietic cells. *J. Virol.* 1996; 70:4502-4508.
- <sup>29</sup> Meier O, Boucke K, Hammer SV, *et al.* Adenovirus triggers macropinocytosis and endosomal leakage together with its clathrin-mediated uptake. *J. Cell Biol.* 2002; 158:1119-1131.
- <sup>30</sup> Meier O, Greber UF. Adenovirus endocytosis. *J. Gene Med.* 2003; 5:451-462.
- <sup>31</sup> Nemerow GR, Stewart PL. Role of alpha(v) integrins in adenovirus cell entry and gene delivery. *Microbiol. Mol. Biol. Rev.* 1999; 63:725-734.
- <sup>32</sup> Huang S, Endo RI, Nemerow GR. Upregulation of integrins alpha v beta 3 and alpha v beta 5 on human monocytes and T lymphocytes facilitates adenovirus-mediated gene delivery. *J. Virol.* 1995; 69:2257-2263.
- <sup>33</sup> Conner SD, Schmid SL. Regulated portals of entry into the cell. *Nature.* 2003; 422:37-44.
- <sup>34</sup> McNiven MA, Cao H, Pitts KR, Yoon Y. The dynamin family of mechanoenzymes: pinching in new places. *Trends Biochem. Sci.* 2000; 25:115-120.
- <sup>35</sup> Cremona O, De Camilli P. Phosphoinositides in membrane traffic at the synapse. *J. Cell Sci.* 2001; 114:1041-1052.

- <sup>36</sup> Cremona O, Di Paolo G, Wenk MR, *et al.* Essential role of phosphoinositide metabolism in synaptic vesicle recycling. *Cell* 1999; 99:179-188.
- <sup>37</sup> Li E, Stupack D, Klemke R, Cheresch DA, Nemerow GR. Adenovirus endocytosis via alpha(v) integrins requires phosphoinositide-3-OH kinase. *J. Virol.* 1998; 72:2055-2061.
- <sup>38</sup> Li E, Stupack D, Bokoch GM, Nemerow GR. Adenovirus endocytosis requires actin cytoskeleton reorganization mediated by Rho family GTPases. *J. Virol.* 1998; 72:8806-8812.
- <sup>39</sup> Clark EA, Brugge JS. Integrins and signal transduction pathways: the road taken. *Science.* 1995; 268:233-239.
- <sup>40</sup> Greber UF, Willetts M, Webster P, Helenius A. Stepwise dismantling of adenovirus 2 during entry into cells. *Cell* 1993; 75:477-486.
- <sup>41</sup> Greber UF, Webster P, Weber J, Helenius A. The role of the adenovirus protease on virus entry into cells. *EMBO J.* 1996; 15:1766-1777.
- <sup>42</sup> Wang K, Guan T, Cheresch DA, Nemerow GR. Regulation of adenovirus membrane penetration by the cytoplasmic tail of integrin beta5. *J. Virol.* 2000; 74:2731-2739.
- <sup>43</sup> Wickham TJ, Filardo EJ, Cheresch DA, Nemerow GR. Integrin alpha v beta 5 selectively promotes adenovirus mediated cell membrane permeabilization. *J. Cell Biol.* 1994; 127:257-264.
- <sup>44</sup> Loftus JC, O'Toole TE, Plow EF, Glass A, Frelinger AL 3<sup>rd</sup>, Ginsberg MH. A beta 3 integrin mutation abolishes ligand binding and alters divalent cation-dependent conformation. *Science* 1990; 249:915-918.
- <sup>45</sup> Leopold PL, Kreitzer G, Miyazawa N, *et al.* Dynein- and microtubule-mediated translocation of adenovirus serotype 5 occurs after endosomal lysis. *Hum. Gene Ther.* 2000; 11:151-165.
- <sup>46</sup> Bailey CJ, Crystal RG, Leopold PL. Association of adenovirus with the microtubule organizing center. *J. Virol.* 2003; 77:13275-13287.
- <sup>47</sup> Trotman LC, Mosberger N, Fornerod M, Stidwill RP, Greber UF. Import of adenovirus DNA involves the nuclear pore complex receptor CAN/Nup214 and histone H1. *Nat. Cell Biol.* 2001; 3:1092-1100.
- <sup>48</sup> Emery AEH. *Neuromuscular disorders: clinical and molecular genetics.* 1998, England, John Wiley & sons.

- <sup>49</sup> Engel AG, Franzini-Armstrong C (eds): Myology, Chapter 41, McGraw-Hill Book Company, New York, 2<sup>nd</sup> ed. pp 1133-1187, 1994.
- <sup>50</sup> Ervasti JM, Ohlendieck K, Kahl SD, Gaver MG, Campbell KP. Deficiency of a glycoprotein component of the dystrophin complex in dystrophic muscle. *Nature* 1990; 345:315-319.
- <sup>51</sup> Sicinski P, Geng Y, Ryder-Cook AS, Barnard EA, Darlison MG, Barnard PJ. The molecular basis of muscular dystrophy in the *mdx* mouse: a point mutation. *Science*. 1989; 244:1578-1580.
- <sup>52</sup> Petrof BJ, Shrager JB, Stedman HH, Kelly AM, Sweeney HL. Dystrophin protects the sarcolemma from stresses developed during muscle contraction. *Proc. Natl. Acad. Sci. U S A*. 1993; 90:3710-3714.
- <sup>53</sup> Fong PY, Turner PR, Denetclaw WF, Steinhardt RA. Increased activity of calcium leak channels in myotubes of Duchenne human and *mdx* mouse origin. *Science* 1990; 250: 673-676.
- <sup>54</sup> McCarter GC, Steinhardt RA. Increased activity of calcium leak channels caused by proteolysis near sarcolemmal ruptures. *J. Membr. Biol.* 2000; 176:169-174.
- <sup>55</sup> Alderton JM, Steinhardt RA. Calcium influx through calcium leak channels is responsible for the elevated levels of calcium-dependent proteolysis in dystrophic myotubes. *J. Biol. Chem.* 2000; 275:9452-9460.
- <sup>56</sup> Adams ME, Mueller HA, Froehner SC. *In vivo* requirement of the alpha-syntrophin PDZ domain for the sarcolemmal localization of nNOS and aquaporin-4. *J. Cell Biol.* 2001; 155:113-122.
- <sup>57</sup> Thomas GD, Sander M, Lau KS, Huang PL, Stull JT, Victor RG. Impaired metabolic modulation of alpha-adrenergic vasoconstriction in dystrophin-deficient skeletal muscle. *Proc. Natl. Acad. Sci. U S A* 1998; 95:15090-15095.
- <sup>58</sup> Sander M, Chavoshan B, Harris SA, *et al.* Functional muscle ischemia in neuronal nitric oxide synthase-deficient skeletal muscle of children with Duchenne muscular dystrophy. *Proc. Natl. Acad. Sci. U S A* 2000; 97:13818-13823.
- <sup>59</sup> Wehling M, Spencer MJ, Tidball JG. A nitric oxide synthase transgene ameliorates muscular dystrophy in *mdx* mice. *J. Cell Biol.* 2001; 155:123-131.

- <sup>60</sup> Morrison J, Lu QL, Pastoret C, Partridge T, Bou-Gharios G. T-cell-dependent fibrosis in the *mdx* dystrophic mouse. *Lab. Invest.* 2000; 80:881-891.
- <sup>61</sup> Irintchev A, Zweyer M, Wernig A. Impaired functional and structural recovery after muscle injury in dystrophic *mdx* mice. *Neuromuscul. Disord.* 1997; 7:117-125.
- <sup>62</sup> Zacharias JM, Anderson JE. Muscle regeneration after imposed injury is better in younger than older *mdx* dystrophic mice. *J. Neurol. Sci.* 1991; 104:190-196.
- <sup>63</sup> Cohn RD, Henry MD, Michele DE, *et al.* Disruption of DAG1 in differentiated skeletal muscle reveals a role for dystroglycan in muscle regeneration. *Cell.* 2002; 110:639-48.
- <sup>64</sup> Brockington M, Yuva Y, Prandini P, *et al.* Fukutin-related protein gene (FKRP) identify limb girdle muscular dystrophy 2I as a milder allelic variant of congenital muscular dystrophy MDC1C. *Hum. Mol. Genet.* 2001; 10:2851-2859.
- <sup>65</sup> Ibraghimov-Beskrovnaya O, Ervasti JM, Leveille CJ, Slaughter CA, Sernett SW, Campbell KP. Primary structure of dystrophin-associated glycoproteins linking dystrophin to the extracellular matrix. *Nature* 1992; 355:696-702.
- <sup>66</sup> Wizemann H, Garbe JH, Friedrich MV, Timpl R, Sasaki T, Hohenester E. Distinct requirements for heparin and alpha-dystroglycan binding revealed by structure-based mutagenesis of the laminin alpha2 LG4-LG5 domain pair. *J. Mol. Biol.* 2003; 332:635-642.
- <sup>67</sup> Michele DE, Barresi R, Kanagawa M, *et al.* Post-translational disruption of dystroglycan-ligand interactions in congenital muscular dystrophies. *Nature* 2002; 418:417-422.
- <sup>68</sup> Kobayashi K, Nakahori Y, Miyake M, *et al.* An ancient retrotransposal insertion causes Fukuyama-type congenital muscular dystrophy. *Nature* 1998; 394:388-392.
- <sup>69</sup> Longman C, Brockington M, Torelli S, *et al.* Mutations in the human LARGE gene cause MDC1D, a novel form of congenital muscular dystrophy with severe mental retardation and abnormal glycosylation of alpha-dystroglycan. *Hum. Mol. Genet.* 2003; 12:2853-2861.
- <sup>70</sup> Yosjida A, Kobayashi K, Manya H, *et al.* Muscular dystrophy and neuronal migration disorder caused by mutations in a glycosyltransferase, POMGnT1. *Dev. Cell.* 2001; 1:717-724.
- <sup>71</sup> von der Mark HJ., Durr J, Sonnenberg A, von der Mark K, Deutzmann R, and Goodman, SI. Skeletal myoblasts utilize a novel  $\alpha$ 1-series integrin and not  $\alpha$ 6 $\beta$ 1 for binding to the E8 and T8 fragments of laminin. *J. Biol. Chem.* 1991; 266:23593-23601.

- <sup>72</sup> Hayashi YK, Chou FL, Engvall E, *et al.* Mutations in the integrin alpha7 gene cause congenital myopathy. *Nat. Genet.* 1998; 19:94-97.
- <sup>73</sup> Wheeler MT, Zarnegar S, McNally EM. Zeta-sarcoglycan, a novel component of the sarcoglycan complex, is reduced in muscular dystrophy. *Hum. Mol. Genet.* 2002; 11:2147-2154.
- <sup>74</sup> Straub V, Ettinger AJ, Durbeej M, *et al.* Epsilon-sarcoglycan replaces alpha-sarcoglycan in smooth muscle to form a unique dystrophin-glycoprotein complex. *J. Biol. Chem.* 1999; 274:27989-27996.
- <sup>75</sup> Coral-Vazquez R, Cohn RD, *et al.* Disruption of the sarcoglycan-sarcospan complex in vascular smooth muscle: a novel mechanism for cardiomyopathy and muscular dystrophy. *Cell* 1999; 98:465-74.
- <sup>76</sup> Durbeej M, Cohn RD, Hrstka RF, *et al.* Disruption of the beta-sarcoglycan gene reveals pathogenetic complexity of limb-girdle muscular dystrophy type 2E. *Mol. Cell.* 2000; 5:141-151.
- <sup>77</sup> Rando TA. The dystrophin-glycoprotein complex, cellular signaling, and the regulation of cell survival in the muscular dystrophies. *Muscle Nerve* 2001; 24:1575-1594.
- <sup>78</sup> Blake DJ, Weir A, Newey SE, Davies KE. Function and genetics of dystrophin and dystrophin-related proteins in muscle. *Physiol. Rev.* 2002; 82:291-329.
- <sup>79</sup> Tinsley J, Deconinck N, Fisher R, *et al.* Expression of full-length utrophin prevents muscular dystrophy in *mdx* mice. *Nat. Med.* 1998; 4: 1441-1444.
- <sup>80</sup> Deconinck N, Tinsley J, De Backer F, *et al.* Expression of truncated utrophin leads to major functional improvements in dystrophin-deficient muscles of mice. *Nat. Med.* 1997; 3: 1216-1221.
- <sup>81</sup> Dudley RW, Lu Y, Gilbert R, *et al.* Sustained improvement of muscle function one year after full-length dystrophin gene transfer into *mdx* mice by a gutted helper-dependent adenoviral vector. *Hum. Gene Ther.* 2004; 15:145-156.
- <sup>82</sup> Gilbert R, Dudley RW, Liu AB, Petrof BJ, Nalbantoglu J, Karpatis G. Prolonged dystrophin expression and functional correction of *mdx* mouse muscle following gene transfer with a helper-dependent (gutted) adenovirus-encoding murine dystrophin. *Hum. Mol. Genet.* 2003; 12:1287-1299.

- <sup>83</sup> Gilbert R, Nalbantoglu J, Petrof BJ, *et al.* Adenovirus-mediated utrophin gene transfer mitigates the dystrophic phenotype of *mdx* mouse muscles. *Hum. Gene Ther.* 1999; 10:1299-1310.
- <sup>84</sup> Nguyen HH, Jayasinha V, Xia B, Hoyte K, Martin PT. Overexpression of the cytotoxic T cell GalNAc transferase in skeletal muscle inhibits muscular dystrophy in *mdx* mice. *Proc. Natl. Acad. Sci. U S A.* 2002; 99:5616-5621.
- <sup>85</sup> Jayasinha V, Hoyte K, Xia B, Martin PT. Overexpression of the CT GalNAc transferase inhibits muscular dystrophy in a cleavage-resistant dystroglycan mutant mouse. *Biochem. Biophys. Res. Commun.* 2003; 302:831-836.
- <sup>86</sup> Burkin DJ, Wallace GQ, Nicol KJ, Kaufman DJ, Kaufman SJ. Enhanced expression of the alpha 7 beta 1 integrin reduces muscular dystrophy and restores viability in dystrophic mice. *J. Cell Biol.* 2001; 152:1207-1218.
- <sup>87</sup> Hoffman EP, Fischbeck KH, Brown RH, *et al.* Characterization of dystrophin in muscle-biopsy specimens from patients with Duchenne's or Becker's muscular dystrophy. *N. Engl. J. Med.* 1988; 318:1363-1368.
- <sup>88</sup> Hayase Y, Inoue H, Ohtsuka E. Secondary structure in formylmethionine tRNA influences the site-directed cleavage of ribonuclease H using chimeric 2'-O-methyl oligodeoxyribonucleotides. *Biochemistry* 1990; 29:8793-8797.
- <sup>89</sup> van Deutekom JC, Bremmer-Bout M, *et al.* Antisense-induced exon skipping restores dystrophin expression in DMD patient derived muscle cells. *Hum. Mol. Genet.* 2001; 10:1547-1554.
- <sup>90</sup> De Angelis FG, Sthandier O, Berarducci B, *et al.* Chimeric snRNA molecules carrying antisense sequences against the splice junctions of exon 51 of the dystrophin pre-mRNA induce exon skipping and restoration of a dystrophin synthesis in Delta 48-50 DMD cells. *Proc. Natl. Acad. Sci. U S A.* 2002; 99:9456-9461.
- <sup>91</sup> Lu QL, Mann CJ, Lou F, *et al.* Functional amounts of dystrophin produced by skipping the mutated exon in the *mdx* dystrophic mouse. *Nat. Med.* 2003; 9:1009-1014.
- <sup>92</sup> Brun C, Suter D, Pauli C, *et al.* U7 snRNAs induce correction of mutated dystrophin pre-mRNA by exon skipping. *Cell. Mol. Life Sci.* 2003; 60:557-566.

- <sup>93</sup> Barton-Davis ER, Cordier L, Shoturma DI, Leland SE, Sweeney HL. Aminoglycoside antibiotics restore dystrophin function to skeletal muscles of *mdx* mice. *J. Clin. Invest.* 1999; 104:375-381.
- <sup>94</sup> Howard M, Frizzell RA, Bedwell DM. Aminoglycoside antibiotics restore CFTR function by overcoming premature stop mutations. *Nat. Med.* 1996; 2:467-469.
- <sup>95</sup> Dunant P, Walter MC, Karpati G, Lochmüller H. Gentamicin fails to increase dystrophin expression in dystrophin-deficient muscle. *Muscle Nerve* 2003; 27:624-627.
- <sup>96</sup> Wagner KR, Hamed S, Hadley DW, *et al.* Gentamicin treatment of Duchenne and Becker muscular dystrophy due to nonsense mutations. *Ann. Neurol.* 2001; 49:706-711.
- <sup>97</sup> Drachman DB, Toyka KV, Myer E. Prednisone in Duchenne muscular dystrophy. *Lancet* 1974; II:1409–1412.
- <sup>98</sup> Mesa LE, Dubrovsky AL, Corderi J, Marco P, Flores D. Steroids in Duchenne muscular dystrophy--deflazacort trial. *Neuromuscul. Disord.* 1991; 1: 261-266.
- <sup>99</sup> Partridge TA, Beauchamp JR, Morgan JE. Conversion of *mdx* myofibers from dystrophin-negative to -positive by injection of normal myoblasts. *Nature* 1989; 337:176-179.
- <sup>100</sup> Ohtsuka Y, Udaka K, Yamashiro Y, Yagita H, Okumura K. Dystrophin acts as a transplantation rejection antigen in dystrophin-deficient mice: implication for gene therapy. *J. Immunol.* 1998; 160:4635-4640.
- <sup>101</sup> Decary S, Mouly V, Hamida CB, Sautet A, Barbet JP, Butler-Browne GS. Replicative potential and telomere length in human skeletal muscle: implication for myogenic cell-mediated gene therapy. *Hum. Gene Ther.* 1997; 4:713-723.
- <sup>102</sup> Gussoni E, Soneoka Y, Strickland CD, *et al.* Dystrophin expression in the *mdx* mouse restored by stem cell transplantation. *Nature* 1999; 401:390-394.
- <sup>103</sup> Sampaolesi M, Torrente Y, Innocenzi A, *et al.* Cell therapy of alpha-sarcoglycan null dystrophic mice through intra-arterial delivery of mesoangioblasts. *Science* 2003; 301: 487-92.
- <sup>104</sup> Tachibana R, Harashima H, Ide N, *et al.* Quantitative analysis of correlation between number of nuclear plasmids and gene expression activity after transfection with cationic liposomes. *Pharm. Res.* 2002; 19:377-81.

- <sup>105</sup> Molly BJ, Todd DG. Nuclear-Associated Plasmid, but Not Cell-Associated Plasmid, Is Correlated with Transgene Expression in Cultured Mammalian Cells. *Mol. Ther.* 2000; 1 :339-346.
- <sup>106</sup> Acsadi G, Dickson G, Love DR, *et al.* Human dystrophin expression in *mdx* mice after intramuscular injection of DNA constructs. *Nature* 1991; 352:815-818.
- <sup>107</sup> Wiethoff CM, Middaugh CR. Barriers to nonviral gene delivery. *J. Pharm. Sci.* 2003 ; 92:203-217.
- <sup>108</sup> Niidome T, Huang L. Gene therapy progress and prospects: nonviral vectors. *Gene Ther.* 2002; 9:1647-1652.
- <sup>109</sup> Zhang G, Budker V, Williams P, Subbotin V, Wolff JA. Efficient expression of naked DNA delivered intraarterially to limb muscles of nonhuman primates. *Hum. Gene Ther.* 2001; 12:427-438.
- <sup>110</sup> Wagner E. Strategies to improve DNA polyplexes for *in vivo* gene transfer: Will “artificial viruses” be the answer? *Pharm. Res.* 2004; 21:8-14.
- <sup>111</sup> Cavazzana-Calvo M, Hacein-Bey S, de Saint Basile G, *et al.* Gene therapy of human severe combined immunodeficiency (SCID)-X1 disease. *Science* 2000; 288:669-672.
- <sup>112</sup> Hacein-Bey-Abina S, Von Kalle C, Schmidt M, *et al.* LMO2-associated clonal T cell proliferation in two patients after gene therapy for SCID-X1. *Science* 2003; 302:415-419.
- <sup>113</sup> Kordower JH, Emborg ME, Bloch J, *et al.* Neurodegeneration prevented by lentiviral vector delivery of GDNF in primate models of Parkinson's disease. *Science* 2000; 290:767-773.
- <sup>114</sup> Consiglio A, Quattrini A, Martino S, *et al.* *In vivo* gene therapy of metachromatic leukodystrophy by lentiviral vectors: correction of neuropathology and protection against learning impairments in affected mice. *Nat. Med.* 2001; 7:310-316.
- <sup>115</sup> Kotin RM, Linden RM, Berns KI. Characterization of a preferred site on human chromosome 19q for integration of adeno-associated virus DNA by non-homologous recombination. *EMBO J.* 1992; 11:5071-5078.
- <sup>116</sup> Nakai H, Montini E, Fuess S, Storm TA, Grompe M, Kay MA. AAV serotype 2 vectors preferentially integrate into active genes in mice. *Nat. Genet.* 2003; 34:297-302.
- <sup>117</sup> Fisher KJ, Jooss K, Alston J, *et al.* Recombinant adeno-associated virus for muscle directed gene therapy. *Nat. Med.* 1997; 3:306-312.

- <sup>118</sup> Greelish JP, Su LT, Lankford EB, *et al.* Stable restoration of the sarcoglycan complex in dystrophic muscle perfused with histamine and a recombinant adeno-associated viral vector. *Nat. Med.* 1999; 5:439-443.
- <sup>119</sup> McCarty DM, Monahan PE, Samulski RJ. Self-complementary recombinant adeno-associated virus (scAAV) vectors promote efficient transduction independently of DNA synthesis. *Gene Ther.* 2001; 8:1248-1254.
- <sup>120</sup> Nakai H, Storm TA, Kay MA. Increasing the size of rAAV-mediated expression cassettes *in vivo* by intermolecular joining of two complementary vectors. *Nat. Biotechnol.* 2000; 18:527-532.
- <sup>121</sup> Assessment of adenoviral safety and toxicity: report of the National Institute of health recombinant DNA Advisory Committee. *Hum. Gene Ther.* 2002; 13:3-13.
- <sup>122</sup> Adenoviral Vector Safety and Toxicity. *Hum. Gene Ther.* 2002; 13:1-163.
- <sup>123</sup> Schnell MA, Zhang Y, Tazelaar J, *et al.* Activation of innate immunity in nonhuman primates following intraportal administration of adenoviral vectors. *Mol. Ther.* 2001; 3:708-722.
- <sup>124</sup> Higginbotham JN, Seth P, Blaese RM, Ramsey WJ. The release of inflammatory cytokines from human peripheral blood mononuclear cells *in vitro* following exposure to adenovirus variants and capsid. *Hum. Gene Ther.* 2002; 13:129-141.
- <sup>125</sup> Kafri T, Morgan D, Krahl T, Sarvetnick N, Sherman L, Verma I. Cellular immune response to adenoviral vector transduced cells does not require *de novo* viral gene expression: implications for gene therapy. *Proc. Natl. Acad. Sci U S A.* 1998; 95:11377-11382.
- <sup>126</sup> Kochanek S, Clemens PR, Mitani K, Chen K-H, Chan S, Caskey CT. 1996. A new adenoviral vector: Replacement of all viral coding sequences with 28 kb of DNA independently expressing both full-length dystrophin and  $\beta$ -galactosidase. *Proc. Natl. Acad. Sci. USA* 1996; 93:5731-5736.
- <sup>127</sup> Morral N, Parks R, Zhou H, Langston C, *et al.* High doses of a helper-dependent adenoviral vector yield supraphysiological levels of  $\alpha_1$ -antitrypsin with negligible toxicity. *Hum. Gene Ther.* 1998; 9:2709-2716.
- <sup>128</sup> Schiedner G, Morral N, Parks RJ, Wu Y, *et al.* Genomic DNA transfer with a high-capacity adenovirus vector results in improved *in vivo* gene expression and decreased toxicity. *Nat. Genet.* 1998; 18:180-183.

- <sup>129</sup> O'Neal WK, Zhou H, Morral N, *et al.* Toxicity associated with repeated administration of first-generation adenovirus vectors does not occur with a helper-dependent vector. *Mol. Med.* 2000; 6:179-195.
- <sup>130</sup> Thomas CE, Schiedner G, Kochanek S, Castro MG, Lowenstein PR. Peripheral infection with adenovirus causes unexpected long-term brain inflammation in animals injected intracranially with first-generation, but not with high-capacity, adenovirus vectors: toward realistic long-term neurological gene therapy for chronic diseases. *Proc. Natl. Acad. Sci. U S A.* 2000; 97:7482-7487.
- <sup>131</sup> Byrnes AP, MacLaren RE, Charlton HM. Immunological instability of persistent adenovirus vectors in the brain: peripheral exposure to vector leads to renewed inflammation, reduced gene expression, and demyelination. *J. Neurosci.* 1996; 16:3045-3055.
- <sup>132</sup> Dai Y, Schwarz EM, Gu D, Zhang WW, Sarvetnick N, Verma IM. Cellular and humoral immune responses to adenoviral vectors containing factor IX gene: tolerization of factor IX and vector antigens allows for long-term expression. *Proc. Natl. Acad. Sci. U S A.* 1995; 92:1401-1405.
- <sup>133</sup> Thomas CE, Birkett D, Anozie I, Castro MG, Lowenstein PR. Acute direct adenoviral vector cytotoxicity and chronic, but not acute, inflammatory responses correlate with decreased vector-mediated transgene expression in the brain. *Mol. Ther.* 2001; 3:36-46.
- <sup>134</sup> Harvey BG, Hackett NR, El-Sawy T, *et al.* Variability of human systemic humoral immune responses to adenovirus gene transfer vectors administered to different organs. *J. Virol.* 1999; 73:6729-6742.
- <sup>135</sup> Chen P, Kovesdi I, Bruder JT. Effective repeat administration with adenovirus vectors to the muscle. *Gene Ther.* 2000; 7:587-595.
- <sup>136</sup> Pastore L, Morral N, Zhou H, *et al.* Use of a liver-specific promoter reduces immune response to the transgene in adenoviral vectors. *Hum. Gene Ther.* 1999; 10:1773-1781.
- <sup>137</sup> De Geest BR, Van Linthout SA, Collen D. Humoral immune response in mice against a circulating antigen induced by adenoviral transfer is strictly dependent on expression in antigen-presenting cells. *Blood.* 2003; 101:2551-2556.
- <sup>138</sup> Blackwell JL, Li H, Gomez-Navarro J, *et al.* Using a tropism-modified adenoviral vector to circumvent inhibitory factors in ascites. *Hum. Gene Ther.* 2000; 11:1657-1669.

- <sup>139</sup> Fisher KD, Stallwood Y, Green NK, Ulbrich K, Mautner V, Seymour LW. Polymer-coated adenovirus permits efficient retargeting and evades neutralizing antibodies. *Gene Ther.* 2001; 8:341-348.
- <sup>140</sup> Vogels R, Zuijdgeest D, van Rijnsoever R, *et al.* Replication-deficient human adenovirus type 35 vectors for gene transfer and vaccination: efficient human cell infection and bypass of preexisting adenovirus immunity. *J Virol.* 2003; 77:8263-8271
- <sup>141</sup> Mastrangeli A, Harvey BG, Yao J, *et al.* "Sero-switch" adenovirus-mediated *in vivo* gene transfer: circumvention of anti-adenovirus humoral immune defenses against repeat adenovirus vector administration by changing the adenovirus serotype. *Hum. Gene Ther.* 1996; 7:79-87.
- <sup>142</sup> Morral N, O'Neal W, Rice K. *et al.* Administration of helper-dependent adenoviral vectors and sequential delivery of different vector serotype for long-term liver-directed gene transfer in baboons. *Proc. Natl. Acad. Sci. U S A* 1999; 96:12816-12821.
- <sup>143</sup> Larochelle N, Lochmüller H, Zhao J, *et al.* Efficient muscle-specific transgene expression after adenovirus-mediated gene transfer in mice using a 1.35 kb muscle creatine kinase promoter/enhancer. *Gene Ther.* 1997; 4:465-472.
- <sup>144</sup> Chen HH, Mack LM, Kelly R, Ontell M, Kochanek S, Clemens PR. Persistence in muscle of an adenoviral vector that lacks all viral genes. *Proc. Natl. Acad. Sci. U S A* 1997; 94:1645-1650.
- <sup>145</sup> Hartigan-O'Connor D, Kirk CJ, Crawford R, Mule JJ, Chamberlain JS. Immune evasion by muscle-specific gene expression in dystrophic muscle. *Mol. Ther.* 2001; 4:525-533.
- <sup>146</sup> Sigal LJ, Crotty S, Andino R, Rock KL. Cytotoxic T-cell immunity to virus-transduced non-hematopoietic cells requires presentation of exogenous antigen. *Nature* 1999; 398:77-80.
- <sup>147</sup> Huard J, Lochmüller H, Acsadi G, *et al.* Differential short-term transduction efficiency of adult versus newborn mouse tissues by adenoviral recombinants. *Exp. Mol. Pathol.* 1995; 62:131-143.
- <sup>148</sup> Guibinga GH, Ebihara S, Nalbantoglu J, Holland P, Karpati G, Petrof BJ. Forced myofiber regeneration promotes dystrophin gene transfer and improved muscle function despite advanced disease in old dystrophic mice. *Mol. Ther.* 2001;4:499-507.

- <sup>149</sup> van Deutekom JC, Cao B, Pruchnic R, Wickham TJ, Kovesdi I, Huard J. Extended tropism of an adenoviral vector does not circumvent the maturation-dependent transducibility of mouse skeletal muscle. *J Gene Med.* 1999; 1:393-399.
- <sup>150</sup> Feero WG, Rosenblatt JD, Huard J, *et al.* Viral gene delivery to skeletal muscle: insights on maturation-dependent loss of fiber infectivity for adenovirus and herpes simplex type 1 viral vectors. *Hum. Gene Ther.* 1997; 8:371-380.
- <sup>151</sup> Nalbantoglu J, Pari G, Karpati G, Holland PC. Expression of the primary coxsackie and adenovirus receptor is downregulated during skeletal muscle maturation and limits the efficacy of adenovirus-mediated gene delivery to muscle cells. *Hum. Gene Ther.* 1999; 10:1009-1019.
- <sup>152</sup> Bergelson JM, Krithivas A, Celi L, *et al.* The murine CAR homolog is a receptor for coxsackie B viruses and adenoviruses. *J. Virol.* 1998; 72:415-419.
- <sup>153</sup> Pari G, Nalbantoglu J, Holland PC, Karpati G. Immunohistochemical characterization of the coxsackie-adenovirus receptor (CAR) in normal and pathological muscle biopsies. *Neurology* 2001; 56 (Suppl.3):A327.
- <sup>154</sup> Kimura E, Maeda Y, Arima T. *et al.* Efficient repetitive gene delivery to skeletal muscle using recombinant adenovirus vector containing the Coxsackievirus and adenovirus receptor cDNA. *Gene Ther.* 2001; 8:20-27.
- <sup>155</sup> Nalbantoglu J, Larochelle N, Wolf E, Karpati G, Lochmüller H, Holland PC. Muscle-specific overexpression of the adenovirus primary receptor CAR overcomes low efficiency of gene transfer to mature skeletal muscle. *J. Virol.* 2001; 75:4276-4282.
- <sup>156</sup> Kitazono M, Rao VK, Robey R, *et al.* Histone deacetylase inhibitor FR901228 enhances adenovirus infection of hematopoietic cells. *Blood* 2002; 99:2248-2251.
- <sup>157</sup> Yurchenco PD. Assembly of basement membranes. *Ann. NY Acad. Sci.* 1990; 580:195-213.
- <sup>158</sup> Huard J, Feero WG, Watkins SC, Hoffman EP, Rosenblatt DJ, Glorioso JC. The basal lamina is a physical barrier to herpes simplex virus-mediated gene delivery to mature muscle fibers. *J. Virol.* 1996; 70:8117-8123.
- <sup>159</sup> Hoffman EP, Arahata K, Minetti C, Bonilla E, Rowland LP. Dystrophinopathy in isolated cases of myopathy in females. *Neurology* 1992; 42:967-975.

- <sup>160</sup> Watkins SC, Hoffman EP, Slayter HS, Kunkel LM. Dystrophin distribution in heterozygote *mdx* mice. *Muscle Nerve* 1989; 12:861-868.
- <sup>161</sup> Huard J, Lochmüller H, Acsadi G, Jani A, Massie B, Karpati G. The route of administration is a major determinant of the transduction efficiency of rat tissues by adenoviral recombinants. *Gene Ther.* 1995; 2:107-115.
- <sup>162</sup> O'Hara AJ, Howell JM, Taplin RH, *et al.* The spread of transgene expression at the site of gene construct injection. *Muscle Nerve* 2001; 24:488-495.
- <sup>163</sup> Karpati G, Pouliot Y, Zubrzycka-Gaarn E. *et al.* Dystrophin is expressed in *mdx* skeletal muscle fibers after normal myoblast implantation. *Am. J. Pathol.* 1989; 135:27-32.
- <sup>164</sup> Zhang G, Budker V, Williams P, Subbotin V, Wolff JA. Efficient expression of naked DNA delivered intraarterially to limb muscles of nonhuman primates. *Hum. Gene Ther.* 2001; 12:427-438.
- <sup>165</sup> Cho WK, Ebihara S, Nalbantoglu J. *et al.* Modulation of Starling forces and muscle fiber maturity permits adenovirus-mediated gene transfer to adult dystrophic (*mdx*) mice by the intravascular route. *Hum. Gene Ther.* 2000; 11:701-714.
- <sup>166</sup> Buchholz CJ, Stitz J, Cichutek K. Retroviral cell targeting vectors. *Curr. Opin. Mol. Ther.* 1999; 1:613-621.
- <sup>167</sup> Curiel DT. Strategies to adapt adenoviral vectors for targeted delivery. *Ann. NY Acad. Sci.* 1999; 886:158-171.
- <sup>168</sup> Wickham TJ. Targeting adenovirus. *Gene Ther.* 2000; 7:110-114.
- <sup>169</sup> Girod A, Ried M, Wobus C, *et al.* Genetic capsid modifications allow efficient re-targeting of adeno-associated virus type 2. *Nat. Med.* 1999; 5:1052-1056.
- <sup>170</sup> Bewley MC, Springer K, Zhang YB, Freimuth P, Flanagan JM. Structural analysis of the mechanism of adenovirus binding to its human cellular receptor, CAR. *Science* 1999; 286:1579-1583.
- <sup>171</sup> Roelvink PW, Mi Lee G, Einfeld DA, Kovesdi I, Wickham TJ. Identification of a conserved receptor-binding site on the fiber proteins of CAR-recognizing adenoviridae. *Science* 1999; 286:1568-1571
- <sup>172</sup> Kirby I, Davison E, Beavil AJ, *et al.* Mutations in the DG loop of adenovirus type 5 fiber knob protein abolish high-affinity binding to its cellular receptor CAR. *J. Virol.* 1999; 73:9508-9514.

- <sup>173</sup> Leissner P. Influence of adenoviral fiber mutations on viral encapsidation, infectivity and *in vivo* tropism. *Gene Ther.* 2001; 8:49-57
- <sup>174</sup> Thirion C, Larochelle N, Volpers C, *et al.* Strategies for muscle-specific targeting of adenoviral gene transfer vectors. *Neuromuscul. Disord.* 2002; 12:S30-S39.
- <sup>175</sup> Smith TA, Idamakanti N, Rollence ML, *et al.* Adenovirus serotype 5 fiber shaft influences *in vivo* gene transfer in mice. *Hum. Gene Ther.* 2003; 14:777-787.
- <sup>176</sup> Alemany R, Curiel DT. CAR-binding ablation does not change biodistribution and toxicity of adenoviral vectors. *Gene Ther.* 2001; 8:1347-1353.
- <sup>177</sup> Alemany R, Suzuki K, Curiel DT. Blood clearance rates of adenovirus type 5 in mice. *J. Gen. Virol.* 2000; 81:2605-2609.
- <sup>178</sup> Huang S, Kamata T, Takada Y, Ruggeri ZM, Nemerow GR. Adenovirus interaction with distinct integrins mediates separate events in cell entry and gene delivery to hematopoietic cells. *J. Virol.* 1996; 70:4502-4508.
- <sup>179</sup> Tao N, Gao GP, Parr M, *et al.* Sequestration of adenoviral vector by Kupffer cells leads to a nonlinear dose response of transduction in liver. *Mol. Ther.* 2001; 3:28-35.
- <sup>180</sup> Schiedner G, Hertel S, Johnston M, Dries V, van Rooijen N, Kochanek S. Selective depletion or blockade of Kupffer cells leads to enhanced and prolonged hepatic transgene expression using high-capacity adenoviral vectors. *Mol. Ther.* 2003; 7:35-43.
- <sup>181</sup> Tillman BW, de Gruijl TD, Luykx-de Bakker SA, *et al.* Maturation of dendritic cells accompanies high-efficiency gene transfer by a CD40-targeted adenoviral vector. *J. Immunol.* 1999; 162:6378-6383.
- <sup>182</sup> Einfeld DA, Schroeder R, Roelvink PW, *et al.* Reducing the native tropism of adenovirus vectors requires removal of both CAR and integrin interactions. *J. Virol.* 2001; 75:11284-11291.
- <sup>183</sup> Wickham TJ, Roelvink PW, Brough DE, Kovesdi I. Adenovirus targeted to heparan-containing receptors increases its gene delivery efficiency to multiple cell types. *Nat. Biotech.* 1996; 14:1570-1573.
- <sup>184</sup> Wickham TJ, Tzeng E, Shears LL 2<sup>nd</sup>, *et al.* Increased *in vitro* and *in vivo* gene transfer by adenovirus vectors containing chimeric fiber proteins. *J. Virol.* 1997; 71:8221-8229.
- <sup>185</sup> Michael SI, Hong JS, Curiel DT, Engler JA. Addition of a short peptide ligand to the adenovirus fiber protein. *Gene Ther.* 1995; 2:660-668.

- <sup>186</sup> Yoshida Y, Sadata A, Zhang W, Saito K, Shinoura N, Hamada H. Generation of fiber-mutant recombinant adenoviruses for gene therapy of malignant glioma. *Hum. Gene Ther.* 1998; 9:2503-2515.
- <sup>187</sup> Bouri K, Feero WG, Myerburg MM, *et al.* Polylysine modification of adenoviral fiber protein enhances muscle cell transduction. *Hum. Gene Ther.* 1999; 10:1633-1640.
- <sup>188</sup> Hong JS, Engler JA. Domains required for assembly of adenovirus type 2 fiber trimers. *J. Virol.* 1996; 70:7071-7078.
- <sup>189</sup> Krasnykh V, Dmitriev I, Mikheeva G, Miller CR, Belousova N, Curiel DT. Characterization of an adenovirus vector containing a heterologous peptide epitope in the HI loop of the fiber knob. *J. Virol.* 1998; 72:1844-1852.
- <sup>190</sup> Dmitriev I, Krasnykh V, Miller CR, *et al.* An adenovirus vector with genetically modified fibers demonstrates expanded tropism via utilization of a coxsackievirus and adenovirus receptor-independent cell entry mechanism. *J. Virol.* 1998; 72:9706-9713.
- <sup>191</sup> Nicklin SA, Von Seggern DJ, Work LM, *et al.* Ablating adenovirus type 5 fiber-CAR binding and HI loop insertion of the SIGYPLP peptide generate an endothelial cell-selective adenovirus. *Mol. Ther.* 2001; 4:534-542.
- <sup>192</sup> Biermann V, Volpers C, Hussmann S, *et al.* Targeting of high-capacity adenoviral vectors. *Hum. Gene Ther.* 2001; 12:1757-69.
- <sup>193</sup> Krasnykh VN, Douglas JT, van Beusechem VW. Genetic targeting of adenoviral vectors. *Mol. Ther.* 2000; 1:391-405.
- <sup>194</sup> Krasnykh VN, Mikheeva GV, Douglas JT, Curiel DT. Generation of recombinant adenovirus vectors with modified fibers for altering viral tropism. *J. Virol.* 1996; 70:6839-6846.
- <sup>195</sup> Gall J, Kass-Eisler A, Leinwand L, Falck-Pedersen E. Adenovirus type 5 and 7 capsid chimera: fiber replacement alters receptor tropism without affecting primary immunoneutralization epitopes. *J. Virol.* 1996; 70:2116-2123
- <sup>196</sup> Shayakhmetov DM, Papayannopoulou T, Stamatoyannopoulos G, Lieber A. Efficient gene transfer into human CD34(+) cells by a retargeted adenovirus vector. *J. Virol.* 2000; 74:2567-2583.

- <sup>197</sup> Krasnykh V, Belousova N, Korokhov N, Mikheeva G, Curiel DT. Genetic targeting of an adenovirus vector via replacement of the fiber protein with the phage T4 fibritin. *J. Virol.* 2001; 75:4176-4183.
- <sup>198</sup> Magnusson MK, Hong SS, Boulanger P, Lindholm L. Genetic retargeting of adenovirus: novel strategy employing "deknobbing" of the fiber. *J. Virol.* 2001; 75:7280-7289.
- <sup>199</sup> Van Beusechem VW, van Rijswijk AL, van Es HH, Haisma HJ, Pinedo HM, Gerritsen WR. Recombinant adenovirus vectors with knobless fibers for targeted gene transfer. *Gene Ther.* 2000; 7:1940-1946.
- <sup>200</sup> Henning P, Magnusson MK, Gunneriusson E, *et al.* Genetic modification of adenovirus 5 tropism by a novel class of ligands based on a three-helix bundle scaffold derived from staphylococcal protein A. *Hum. Gene Ther.* 2002; 13:1427-39.
- <sup>201</sup> Lindholm L. Cold spring harbour meeting 2003 on "Vector targeting strategies for gene therapy". Cold spring harbour laboratory, NY, 2003; abstract book, p67.
- <sup>202</sup> Hong SS, Magnusson MK, Henning P, Lindholm L, Boulanger PA. Adenovirus stripping: a versatile method to generate adenovirus vectors with new cell target specificity. *Mol. Ther.* 2003; 7:692-699.
- <sup>203</sup> Vigne E, Mahfouz I, Dedieu JF, Brie A, Perricaudet M, Yeh P. RGD inclusion in the hexon monomer provides adenovirus type 5-based vectors with a fiber knob-independent pathway for infection. *J. Virol.* 1999; 73:5156-5161.
- <sup>204</sup> Wickham TJ, Carrion ME, Kovesdi I. Targeting of adenovirus penton base to new receptors through replacement of its RGD motif with other receptor-specific peptide motifs. *Gene Ther.* 1995; 2:750-756.
- <sup>205</sup> Dmitriev IP, Kashentseva EA, Curiel DT. Engineering of adenovirus vectors containing heterologous peptide sequences in the C terminus of capsid protein IX. *J. Virol.* 2002; 76:6893-6899.
- <sup>206</sup> Meulenbroek RA, Sargent KL, Lunde J, Jasmin B, Parks RJ. Use of adenovirus protein IX (pIX) to display polypeptides on the virion – generation of fluorescent virus through the incorporation of pIX-GFP. *Mol. Ther.* 2004; 9:617-624.
- <sup>207</sup> Douglas JT, Rogers BE, Rosenfeld ME, Michael SI, Feng M, Curiel DT. Targeted gene delivery by tropism-modified adenoviral vectors. *Nat. Biotech.* 1996; 14:1574-1578.

- <sup>208</sup> Wickham TJ, Segal DM, Roelvink PW, *et al.* Targeted adenovirus gene transfer to endothelial and smooth muscle cells by using bispecific antibodies. *J. Virol.* 1996; 70:6831-6838.
- <sup>209</sup> Wickham TJ, Lee GM, Titus JA, *et al.* Targeted adenovirus-mediated gene delivery to T cells via CD3. *J. Virol.* 1997; 71:7663-7669.
- <sup>210</sup> Harari OA, Wickham TJ, Stocker CJ, *et al.* Targeting an adenoviral gene vector to cytokine-activated vascular endothelium via E-selectin. *Gene Ther.* 1999; 6:801-807.
- <sup>211</sup> Watkins SJ, Mesyanzhinov VV, Kurochkina LP, Hawkins RE. The 'adenobody' approach to viral targeting: specific and enhanced adenoviral gene delivery. *Gene Ther.* 1997; 4:1004-1012.
- <sup>212</sup> Rogers BE, Douglas JT, Ahlem C, Buchsbaum DJ, Frincke J, Curiel DT. Use of a novel cross-linking method to modify adenovirus tropism. *Gene Ther.* 1997; 4:1387-1392.
- <sup>213</sup> Nettelbeck DM, Miller DW, Jerome V, *et al.* Targeting of adenovirus to endothelial cells by a bispecific single-chain diabody directed against the adenovirus fiber knob domain and human endoglin (CD105). *Mol. Ther.* 2001; 3:882-891.
- <sup>214</sup> Li E, Brown SL, Von Seggern DJ, Brown GB, Nemerow GR. Signaling antibodies complexed with adenovirus circumvent CAR and integrin interactions and improve gene delivery. *Gene Ther.* 2000; 7:1593-1599.
- <sup>215</sup> Gu DL, Gonzalez AM, Printz MA, *et al.* Fibroblast growth factor 2 retargeted adenovirus has redirected cellular tropism: evidence for reduced toxicity and enhanced antitumor activity in mice. *Cancer Res.* 1999; 59:2608-2614.
- <sup>216</sup> Gu DL *et al.* Fibroblast growth factor 2 retargeted adenovirus has redirected cellular tropism: evidence for reduced toxicity and enhanced antitumor activity in mice. *Cancer Res.* 1999; 59:2608-2614.
- <sup>217</sup> Printz MA, Gonzalez AM, Cunningham M. *et al.* Fibroblast growth factor 2-retargeted adenoviral vectors exhibit a modified biolocalization pattern and display reduced toxicity relative to native adenoviral vectors. *Hum. Gene Ther.* 2000; 11:191-204.
- <sup>218</sup> Reynolds PN, Zinn KR, Gavrilyuk VD. *et al.* A targetable, injectable adenoviral vector for selective gene delivery to pulmonary endothelium *in vivo*. *Mol. Ther.* 2000; 2:562-578.

- <sup>219</sup> Reynolds PN, Nicklin SA, Kaliberova L. *et al.* Combined transductional and transcriptional targeting improves the specificity of transgene expression *in vivo*. *Nat. Biotech.* 2001; 19:838-842.
- <sup>220</sup> Braun M, Pietsch P, Zepp A, Schror K, Baumann G, Felix SB. Regulation of tumor necrosis factor alpha- and interleukin-1-beta-induced adhesion molecule expression in human vascular smooth muscle cells by cAMP. *Arterioscler. Thromb. Vasc. Biol.* 1997; 17:2568-2575.
- <sup>221</sup> Schiedner G, Hertel S, Kochanek S. Efficient transformation of primary human amniocytes by E1 functions of Ad5: generation of new cell lines for adenoviral vector production. *Hum. Gene Ther.* 2000; 11:2105-16.
- <sup>222</sup> Hitt M, Bett A, Prevec L, Graham FL. Construction and propagation of human adenovirus vectors. *Cell Biology: A laboratory handbook*, pp 500-512. Second edition Vol.1, Academic Press 1998.
- <sup>223</sup> Mittereder N, March KL, Trapnell BC. Evaluation of the concentration and bioactivity of adenovirus vectors for gene therapy. *J. Virol.* 1996; 70:7498-7509.
- <sup>224</sup> Ma L, Bluysen HA, De Raeymaeker M, *et al.* Rapid determination of adenoviral vector titers by quantitative real-time PCR. *J. Virol. Methods.* 2001; 93:181-188.
- <sup>225</sup> Mayer U, Saher G, Fassler R, *et al.* Absence of integrin alpha7 causes a novel form of muscular dystrophy. *Nat. Genet.* 1997; 17:318-323.
- <sup>226</sup> Schober S, Mielenz D, Echtermeyer F, *et al.* The role of extracellular and cytoplasmic splice domains of alpha7-integrin in cell adhesion and migration on laminins. *Exp. Cell Res.* 2000; 255:303-313.
- <sup>227</sup> Patel K, Moore SE, Dickson G, *et al.* Neural cell adhesion molecule (NCAM) is the antigen recognized by monoclonal antibodies of similar specificity in small-cell lung carcinoma and neuroblastoma. *Int. J. Cancer* 1989; 44:573-578.
- <sup>228</sup> Walsh FS, Ritter MA. Surface antigen differentiation during human myogenesis in culture. *Nature* 1981; 289:60-64.
- <sup>229</sup> Sambrook J, Fritsch EF, Maniatis T. (eds.) 1989. "Molecular Cloning: A Laboratory Manual." 2<sup>nd</sup> ed., Cold Spring Harbor Laboratory, Cold Spring Harbor, New York.
- <sup>230</sup> Romeo C, Seed B. Cellular immunity to HIV activated by CD4 fused to T cell or Fc receptor polypeptides. *Cell* 1991; 64:1037-1046.

- <sup>231</sup> Janknecht R, de Martynoff G, Lou J, Hipskind RA, Nordheim A, Stunnenberg HG. Rapid and efficient purification of native histidine-tagged protein expressed by recombinant vaccinia virus. *Proc. Natl. Acad. Sci. USA* 1991; 88:8972-8976.
- <sup>232</sup> Laemmli U K. Cleavage of structural proteins during the assembly of the head of bacteriophage T4. *Nature* 1970; 227:680-685.
- <sup>233</sup> Thomas CE, Birkett D, Anozie I, Castro MG, Lowenstein PR. Acute direct adenoviral vector cytotoxicity and chronic, but not acute, inflammatory responses correlate with decreased vector-mediated transgene expression in the brain. *Mol. Ther.* 2001; 3:36-46.
- <sup>234</sup> Cedergren L, Andersson R, Jansson B, Uhlen M, Nilsson B. Mutational analysis of the interaction between staphylococcal protein A and human IgG1. *Protein Eng.* 1993; 6:441-448.
- <sup>235</sup> Surolia A, Pain D, Khan MI. Protein A: nature's universal anti-antibody. *Trends Biochem. Sci.* 1982; 7:74-76.
- <sup>236</sup> Nilsson B, Moks T, Jansson B, *et al.* A synthetic IgG-binding domain based on staphylococcal protein A. *Protein Eng.* 1987; 1:107-113.
- <sup>237</sup> Ojala K, Mottershead DG, Suokko A, Oker-Blom C. Specific binding of baculoviruses displaying gp64 fusion proteins to mammalian cells. *Biochem. Biophys. Res. Commun.* 2001; 284:777-784.
- <sup>238</sup> Mottershead DG, Alfthan K, Ojala K, Takkinen K, Oker-Blom C. Baculoviral display of functional scFv and synthetic IgG-binding domains. *Biochem. Biophys. Res. Commun.* 2000; 275:84-90.
- <sup>239</sup> Iijima Y, Ohno K, Ikeda H, Sawai K, Levin B, Meruelo D. Cell-specific targeting of a thymidine kinase/ganciclovir gene therapy system using a recombinant Sindbis virus vector. *Int. J. Cancer* 1999; 80:110-118.
- <sup>240</sup> Ohno K, Sawai K, Iijima Y, Levin B, Meruelo D. Cell-specific targeting of Sindbis virus vectors displaying IgG-binding domains of protein A. *Nat. Biotech.* 1997; 15:763-767.
- <sup>241</sup> Ried MU, Girod A, Leike K, Buning H, Hallek M. Adeno-associated virus capsids displaying immunoglobulin-binding domains permit antibody-mediated vector retargeting to specific cell surface receptors. *J. Virol.* 2002; 76:4559-4566.
- <sup>242</sup> Thirion C, Volpers C, Biermann V, *et al.* Antibody-mediated targeting of an adenovirus vector modified to contain a synthetic immunoglobulin G-binding domain in the capsid. *J. Virol.* 2003; 77:2093-2104.

- <sup>243</sup> Braisted AC, Wells JA. Minimizing a binding domain from protein A. Proc. Natl. Acad. Sci. USA 1996; 93:5688-5692.
- <sup>244</sup> Starovasnik MA, Braisted AC, Wells JA. Structural mimicry of a native protein by a minimized binding domain. Proc. Natl. Acad. Sci. USA 1997; 94: 10080-10085
- <sup>245</sup> Hong JS, Engler JA. Domains required for assembly of adenovirus type 2 fiber trimers J. Virol. 1996; 70:7071-7080.
- <sup>246</sup> Schiedner G, Hertel S, Kochanek S. Efficient transformation of primary human amniocytes by E1 functions of Ad5: Generation of new cell lines for adenoviral vector production. Hum. Gene Ther. 2000; 11:2105-2116.
- <sup>247</sup> Hodges BL, Hayashi YK, Nonaka I, Wang W, Arahata K, Kaufman SJ. Altered expression of the alpha7beta1 integrin in human and murine muscular dystrophies. J. Cell Sci. 1997; 110:2873-2881.
- <sup>248</sup> Hurko O, Walsh FS. Human fetal muscle-specific antigen is restricted to regenerating myofibers in diseased adult muscle. Neurology 1983; 33:737-743.
- <sup>249</sup> Goridis C, Brunet J-F. NCAM: structural diversity, function and regulation of expression. Sem. Cell Biol. 1992; 3:189-197.
- <sup>250</sup> Blum H, Beier H, Gross HJ. Improved silver staining of plant proteins, RNA, and DNA in polyacrylamide gels. Electrophoresis 1987; 8:93-99.
- <sup>251</sup> Klein D, Bugl B, Gunzburg WH, Salmons B. Accurate estimation of transduction efficiency necessitates a multiplex real-time PCR. Gene Ther. 2000; 7:458-463.
- <sup>252</sup> Acsadi G, Jani A, Huard J, *et al.* Cultured human myoblasts and myotubes show markedly different transducibility by replication-defective adenovirus recombinants. Gene Ther. 1994; 1:338-340.
- <sup>253</sup> Alemany R, Suzuki K, Curiel DT. Blood clearance rates of adenovirus type 5 in mice. J. Gen. Virol. 2000; 81:2605-2609.
- <sup>254</sup> O'Riordan CR, Lachapelle A, Delgado C, *et al.* PEGylation of adenovirus with retention of infectivity and protection from neutralizing antibodies *in vitro* and *in vivo*. Hum. Gene Ther. 1999; 10:1349-1358.
- <sup>255</sup> Vega MA. Prospects for homologous recombination in human gene therapy. Hum. Genet. 1991; 87:245-253.

- <sup>256</sup> Sauer B, Henderson N. Targeted insertion of exogenous DNA into the eukaryotic genome by the Cre recombinase. *New Biol.* 1990; 2:441-449.
- <sup>257</sup> O'Gorman S, Fox DT, Wahl GM. Recombinase-mediated gene activation and site-specific integration in mammalian cells. *Science* 1991; 251:1351-1355.
- <sup>258</sup> Thorpe HM, Smith MC. In vitro site-specific integration of bacteriophage DNA catalyzed by a recombinase of the resolvase/invertase family. *Proc. Natl. Acad. Sci. U S A.* 1998; 95:5505-5510.
- <sup>259</sup> Groth AC, Olivares EC, Thyagarajan B, Calos MP. A phage integrase directs efficient site-specific integration in human cells. *Proc. Natl. Acad. Sci. USA* 2000; 97:5995-6000.
- <sup>260</sup> Olivares EC, Hollis RP, Chalberg TW, Meuse L, Kay MA, Calos MP. Site-specific genomic integration produces therapeutic factor IX levels in mice. *Nat. Biotech.* 2002; 20:1124-1128.
- <sup>261</sup> Thyagarajan B, Olivares EC, Ginsburg DS, Calos MP. Site-specific genomic integration in mammalian cells mediated by phage  $\Phi$ C31 integrase. *Mol. Cell. Biol.* 2001; 21:3926-3934.
- <sup>262</sup> Yant SR, Erhardt A, Mikkelsen JG, Meuse L, Pham T, Kay MA. Transposition from a gutless adeno-transposon vector stabilizes transgene expression *in vivo*. *Nat. Biotech.* 2002; 20:999-1005.
- <sup>263</sup> Kreppel F, Kochnaek S. Long-term expression in proliferating cells mediated episomally maintained high-capacity adenovirus vectors. *J. Virol.* 2004; 78:9-22.
- <sup>264</sup> Cedergren L, Andersson R, Jansson B, Uhlen M, Nilsson B. Mutational analysis of the interaction between staphylococcal protein A and human IgG1. *Protein Eng.* 1993; 6:441-448.
- <sup>265</sup> Nilsson B, Moks T, Jansson B, *et al.* A synthetic IgG-binding domain based on staphylococcal protein A. *Protein Eng.* 1987; 1:107-113.
- <sup>266</sup> Lortat-Jacob H, Chouin E, Cusack S, van Raaij MJ. Kinetic analysis of adenovirus fiber binding to its receptor reveals an avidity mechanism for trimeric receptor-ligand interactions. *J. Biol. Chem.* 2001; 276:9009-9015.
- <sup>267</sup> Belousova N, Krendelichtchikova V, Curiel DT, Krasnykh V. Modulation of adenovirus vector tropism via incorporation of polypeptide ligands into the fiber protein. *J. Virol.* 2002; 76:8621-8631.

- <sup>268</sup> Shenk T. Adenoviridae: the viruses and their replication. *Fields Virology*, Third edition. 1996. Edited by B.N. Fields, D.M. Knipe, P.M. Howley *et al.* Lippincott-Raven publishers, Philadelphia. 1996; pp 2111-2148.
- <sup>269</sup> Magnusson MK, Hong SS, Henning P, Boulanger P, Lindholm L. Genetic retargeting of adenovirus vectors: functionality of targeting ligands and their influence on virus viability. *J. Gene Med.* 2002; 4:356-70.
- <sup>270</sup> Barry MA, Dower WJ, Johnston SA. Towards cell-targeting gene therapy vectors: selection of cell-binding peptides from random peptide-presenting phage libraries. *Nat. Med.* 1996; 2:299-305.
- <sup>271</sup> Pasqualini R, Koivunen E, Ruoslahti E. Alpha v integrins as receptors for tumor targeting by circulating ligands. *Nat. Biotechnol.* 1997; 15:542-546.
- <sup>272</sup> Arap W, Pasqualini R, Ruoslahti E. Cancer Treatment by Targeted Drug Delivery to Tumor Vasculature in a Mouse Model. *Science* 1998; 279:377-380.
- <sup>273</sup> Colas P, Cohen B, Jessen T, Grishina I, McCoy J, Brent R. Genetic selection of peptide aptamers that recognize and inhibit cyclin-dependent kinase 2. *Nature* 1996; 380: 548-550.
- <sup>274</sup> Ghosh D, Barry MA. Context-specific peptide-presenting phage libraries. Abstract of papers presented at the 2003 meeting on vector targeting strategies for gene therapy. Cold Spring Harbor, New York.
- <sup>275</sup> Perabo L, Büning H, Kofler DM, *et al.* *In vitro* selection of viral vectors with modified tropism: the adeno-associated virus display. *Mol. Ther.* 2003; 8: 151-157.
- <sup>276</sup> Müller OJ, Kaul F, Weitzman MD, Pasqualini R, Arap W, Kleinschmidt JA, Trepel M. Random peptide libraries displayed on adeno-associated virus to select for targeted gene therapy vectors. *Nat. Biotechnol.* 2003; 21:1040-1046.
- <sup>277</sup> Khare PD, Rosales AG, Bailey KR, Russell SJ, Federspiel MJ. Epitope selection from an uncensored peptide library displayed on avian leukosis virus. *Virology* 2003; 315:313-21.
- <sup>278</sup> Soong NW, Nomura L, Pekrun K, *et al.* Molecular breeding of viruses. *Nat. Genet.* 2000; 25:436-9.
- <sup>279</sup> Deyev SM, Waibel R, Lebedenko EN, Schubiger AP, Pluckthun A. Design of multivalent complexes using the barnase\*barstar module. *Nat. Biotechnol.* 2003; 21:1486-92.
- <sup>280</sup> Green NM. Avidin and streptavidin. *Methods Enzymol.* 1990; 184:51-67.

- <sup>281</sup> Parrott MB, Adams KE, Mercier GT, Mok H, Campos SK, Barry MA. Metabolically biotinylated adenovirus for cell targeting, ligand screening, and vector purification. *Mol. Ther.* 2003; 8:688-700.
- <sup>282</sup> Samoylova TI, Smith BF. Elucidation of muscle-binding peptides by phage display screening. *Muscle Nerve* 1999; 22:460-466.
- <sup>283</sup> Feero WG, Li S, Rosenblatt JD. *et al.* Selection and use of ligands for receptor-mediated gene delivery to myogenic cells. *Gene Ther.* 1997; 4:664-674.
- <sup>284</sup> Yao CC, Breuss J, Pytela R, Kramer RH. Functional expression of the alpha7 integrin receptor in differentiated smooth muscle cells. *J. Cell Sci.* 1997; 110:1477-1487.
- <sup>285</sup> Burkin DJ, Kaufman SJ. The  $\alpha 7\beta 1$  integrin in muscle development and disease. *Cell Tissue Res.* 1999; 296:183-190.
- <sup>286</sup> Irintchev A, Zeschnigk M, Starzinski-Powitz A, Wernig A. Expression pattern of M-cadherin in normal, denervated, and regenerating mouse muscles. *Dev. Dyn.* 1994; 199:326-337.
- <sup>287</sup> Sanes JR. 1994. The extracellular matrix, p. 242-260. *In* A. G. Engel and C. Franzini-Armstrong (eds.), *Myogenesis*, McGraw-Hill, New York.
- <sup>288</sup> Chen YW, Zhao P, Borup R, Hoffman EP. Expression profiling in the muscular dystrophies: identification of novel aspects of molecular pathophysiology. *J. Cell. Biol.* 2000; 151:1321-1336.
- <sup>289</sup> Bischoff R. The satellite cell and muscle regeneration. *In*: Engel A.G and Franzini-Armstrong eds., *Myogenesis*, New York: McGraw-Hill, 1994:97-118.
- <sup>290</sup> Cornelison DD, and Wold BJ. Single-cell analysis of regulatory gene expression in quiescent and activated mouse skeletal muscle satellite cells. *Dev. Biol.* 1997; 191:270-283.
- <sup>291</sup> Bilbao R, Srinivasan S, Reay D, *et al.* Binding of adenoviral fiber knob to the coxsackievirus-adenovirus receptor is crucial for transduction of fetal muscle. *Hum. Gene Ther.* 2003; 14:645-649.
- <sup>292</sup> Rosa-Calatrava M. Point mutations in the fiber knob domain of Ad5 impair the heparan sulfate proteoglycan (HSG) – mediated entry pathway of adenovirus. Cold spring harbour meeting 2003 on “Vector targeting strategies for gene therapy”. Cold spring harbour laboratory, NY, 2003; abstract book, p73.

- <sup>293</sup> Seth P, Willingham MC, Pastan I. Binding of adenovirus and its external proteins to Triton X-114. Dependence on pH. *J. Biol. Chem.* 1985; 260:14431-14434.
- <sup>294</sup> Wickham TJ, Filardo EJ, Cheresch DA, Nemerow GR. Integrin alpha v beta 5 selectively promotes adenovirus mediated cell membrane permeabilization. *J. Cell Biol.* 1994; 127:257-64.
- <sup>295</sup> Vogel BE, Lee SJ, Hildebrand A, *et al.* A novel integrin specificity exemplified by binding of the alpha v beta 5 integrin to the basic domain of the HIV Tat protein and vitronectin. *J. Cell Biol.* 1993; 121:461-468.
- <sup>296</sup> Zhang F, Andreassen P, fender P, Geissler E, Hernandez JF, Chroboczek J. A transfecting peptide derived from adenovirus fiber protein. *Gene Ther.* 1999; 6:171-181.
- <sup>297</sup> Kibbey RG, Rizo J, Gierasch LM, Anderson RG. The LDL clustering motif interacts with the clathrin terminal domain in a reverse turn conformation. *J. Cell Biol.* 1998; 142:59-67.
- <sup>298</sup> Brown D, Breton S. Sorting proteins and their target membranes. *Kidney Int.* 2000; 57:816-24.
- <sup>299</sup> Li Y, Marzolo MP, van Kerkhof P, Strous GJ, Bu G. The YXXL motif, but not the two NPXY motifs serves as the dominant endocytosis signal for low density lipoprotein receptor-related protein. *J. Biol. Chem.* 2000; 275:17187-17194.
- <sup>300</sup> Fender P, Ruigrok RW, Gout E, Buffet S, Chroboczek J. Adenovirus dodecahedron a new vector for human gene therapy. *Nat. Biotechnol.* 1997; 15:52-56.
- <sup>301</sup> Huang S, Reddy V, Dasgupta N, Nemerow GR. A single amino acid in the adenovirus type 37 fiber confers binding to human conjunctival cells. *J. Virol.* 1999; 73:2798-2802.
- <sup>302</sup> Havenga MJ, Lemckert AA, Ophorst OJ, *et al.* Exploiting the natural diversity in adenovirus tropism for therapy and prevention of disease. *J. Virol.* 2002; 76:4612-4620.
- <sup>303</sup> Rea D, Havenga MJ, van Den Assem M, *et al.* Highly efficient transduction of human monocyte-derived dendritic cells with subgroup B fiber-modified adenovirus vectors enhances transgene-encoded antigen presentation to cytotoxic T cells. *J. Immunol.* 2001; 166:5236-5244.
- <sup>304</sup> Knaan-Shanzer S, Van Der Velde I, Havenga MJ, Lemckert AA, De Vries AA, Valerio D. Highly efficient targeted transduction of undifferentiated human hematopoietic cells by adenoviral vectors displaying fiber knobs of subgroup B. *Hum. Gene Ther.* 2001; 12:1989-2005.

- <sup>305</sup> Pickles RJ, McCarty D, Matsui H, Hart PJ, Randell SH, Boucher RC. Limited entry of adenovirus vectors into well-differentiated airway epithelium is responsible for inefficient gene transfer. *J. Virol.* 1998; 72:6014-6023.
- <sup>306</sup> Walters RW, Yi SM, Keshavjee S, *et al.* Binding of adeno-associated virus type 5 to 2,3-linked sialic acid is required for gene transfer. *J. Biol. Chem.* 2001; 276:20610-20616.
- <sup>307</sup> Zabner J, Seiler M, Walters R, *et al.* Adeno-associated virus type 5 (AAV5) but not AAV2 binds to the apical surfaces of airway epithelia and facilitates gene transfer. *J. Virol.* 2000; 74:3852-3858.
- <sup>308</sup> Wu E, Trauger SA, Pache L, *et al.* Membrane cofactor protein is a receptor for adenoviruses associated with epidemic keratoconjunctivitis. *J. Virol.* 2004; 78:3897-3905.
- <sup>309</sup> Harduin-Lepers A, Vallejo-Ruiz V, Krzewinski-Recchi MA, Samyn-Petit B, Julien S, Delannoy P. The human sialyltransferase family. *Biochimie* 2001; 83:727-737.
- <sup>310</sup> Varki A. N-glycolylneuraminic acid deficiency in humans. *Biochimie.*2001; 83:615-622.
- <sup>311</sup> Suzuki Y, Ito T, Suzuki T, Holland RE Jr, *et al.* Sialic acid species as a determinant of the host range of influenza A viruses. *J. Virol.* 2000; 74:11825-11831.
- <sup>312</sup> Suzuki T, Horiike G, Yamazaki Y, *et al.* Swine influenza virus strains recognize sialylsugar chains containing the molecular species of sialic acid predominantly present in the swine tracheal epithelium. *FEBS Lett.* 1997; 404:192-196.
- <sup>313</sup> Delorme C, Brussow H, Sidoti J, *et al.* Glycosphingolipid binding specificities of rotavirus: identification of a sialic acid-binding epitope. *J. Virol.* 2001; 75:2276-2287.
- <sup>314</sup> Tangvoranuntakul P, Gagneux P, Diaz S, *et al.* Human uptake and incorporation of an immunogenic nonhuman dietary sialic acid. *Proc. Natl. Acad. Sci. U S A.* 2003; 100:12045-12050.
- <sup>315</sup> Gieseler K, Grisoni K, Segalat L. Genetic suppression of phenotypes arising from mutations in dystrophin-related genes in *Caenorhabditis elegans*. *Curr. Biol.* 2000; 10:1092-1097.
- <sup>316</sup> Walter M, Petersen JA, Stucka R, *et al.* FKR<sub>P</sub> (826C>A) frequently causes limb-girdle muscular dystrophy in German patients. *J. Med. Genet.* 2004; 41:e50.
- <sup>317</sup> Guttridge DC, Mayo MW, Madrid LV, Wang CY, Balswin AS Jr. NF-κB-induced loss of MyoD mRNA : Possible role in muscle decay and cachexia. *Science* 2000; 289:2363-2366.

- <sup>318</sup> Porter JD, Khanna S, Kaminski HJ, *et al.* A chronic inflammatory response dominates the skeletal muscle molecular signature in dystrophin-deficient *mdx* mice. *Hum. Mol. Genet.* 2002; 11:263-272.
- <sup>319</sup> Conboy IM, Conboy MJ, Smythe GM, Rando TA. Notch-mediated restoration of regenerative potential to aged muscle. *Science* 2003; 302: 1575-1577.
- <sup>320</sup> Bogdanovich S, Krag TO, Barton ER, *et al.* Functional improvement of dystrophic muscle by myostatin blockade. *Nature* 2002; 420: 418-421.
- <sup>321</sup> Musaro A, McCullagh K, Paul A, *et al.* Localized Igf-1 transgene expression sustains hypertrophy and regeneration in senescent skeletal muscle. *Nat. Genet.* 2001; 27:195-200.
- <sup>322</sup> Barton ER, Morris L, Musaro A, Rosenthal N, Sweeney HL. Muscle-specific expression of insulin-like growth factor I counters muscle decline in *mdx* mice. *J. Cell Biol.* 2002; 157:137-148.
- <sup>323</sup> Musaro A, McCullagh KJ, Naya FJ, Olson EN, Rosenthal N. IGF-1 induces skeletal myocyte hypertrophy through calcineurin in association with GATA-2 and NF-ATc1. *Nature* 1999; 400:581-585.
- <sup>324</sup> McKinsey TA, Zhang CL, Lu J, Olson EN. Signal-dependent nuclear export of a histone deacetylase regulates muscle differentiation. *Nature* 2000; 408:106-111.

## Curriculum Vitae

### Personal details:

Surname: Thirion  
Forename: Christian Olivier  
Nationalities: French, German  
Date of birth: April 20<sup>th</sup>, 1971  
Place of birth: Konstanz, Germany

### Education:

1981-1990  
Okengymnasium Offenburg, Germany  
May 1990 university entrance qualification, German Abitur

### Military service:

October 1990 – October 1992  
Military training, Offizierschule der Luftwaffe,  
Fürstenfeldbruck, Munich

Appointment to German air force lieutenant in November 1993

### Scientific training:

October 1992 – August 1998,  
Study of Chemistry  
Ludwig-Maximilians-University Munich, Germany

Degree: “Diplom Chemiker”

### Diploma thesis:

February 1998 - August 1998  
Gene Center, Ludwig-Maximilians-University Munich,  
Germany

Title: Molekulare Charakterisierung der  
muskelspezifischen Isoform von Cofilin im menschlichen  
Skelettmuskel.

Supervisor: Prof. Dr. Hanns Lochmüller

### Doctoral thesis:

September 1998 – December 2003  
Gene Center, Ludwig-Maximilians-University Munich,  
Germany

Title: Improving gene transfer into skeletal muscle  
through genetic retargeting of adenoviral vectors

Supervisor: Prof. Dr. Hanns Lochmüller

### Postdoctoral training:

March 2004 - present  
Postdoctoral position at ZKF University of Ulm, Germany  
Department of Gene Therapy  
Head of department: PD Dr. Stefan Kochanek

